Doctoral Dissertation
Doctoral Program in Management, Production and Design (36th Cycle)

Technological Innovations for Sustainable Manufacturing

Concepts, frameworks, and supporting tools

By

Luigi Panza

Supervisor:
Prof. Franco Lombardi

Doctoral Examination Committee:
Prof. Simone Arena , Referee, University of Cagliari
Prof. Alberto De Marco, Commissioner, Polytechnic University of Turin
Prof. Serena Finco , Referee, University of Padova
Prof. Mirco Peron, Commissioner, NEOMA Business School
Prof. Rossella Pozzi, Commissioner, LIUC Business School

Politecnico di Torino
2023

Declaration

I hereby declare that, the contents and organization of this dissertation constitute my own original work and does not compromise in any way the rights of third parties, including those relating to the security of personal data.

Luigi Panza

2023

* This dissertation is presented in partial fulfillment of the requirements for **Ph.D. degree** in the Graduate School of Politecnico di Torino (ScuDo)

Abstract

For 10,000 years the Earth experienced an environmentally stable period, also known as the Holocene epoch, where human civilization have arisen and developed. Throughout the Holocene, natural environmental changes took place, and the Earth's carrying capacity preserved the conditions to enable human development. The Earth's carrying capacity can be represented by nine life support systems, in which each of them is controlled by specific quantitative variables. The threshold values of such variables represent the Planetary Boundaries (PBs) that define a 'safe operating space' for human development. The massive exploitation of resources by human activities over the years has significantly altered the natural functioning of our planet. In fact, to date, six out of the nine PBs have already been transgressed, and the Earth is in a quantifiably different state than before, corresponding to a new geological epoch, known as the Anthropocene. This highlights the urgent need to shift towards responsible and sustainable human development.

In this context, the manufacturing sector plays a critical role. During the second quarter of 2022, it accounted for 23% of the greenhouse gas emissions (GHG), which are a major contributor to climate change, within the European Union. Consequently, there is an increasing need for the generation of sustainable value and, in response to this challenge, the Circular Economy (CE) model has gained significant attention recently. The CE model is considered effective because it seeks to decouple economic growth from its environmental impact through a continuous reintegration of used products, components, and materials into value chains. However, implementing CE principles within the manufacturing context necessitates significant technological innovations across product, process, and system levels. At the same time, it is fundamental to consider the technological lifecycle when these innovations are delivered into the economy. In fact, the lifecycle of a technology is characterized by different phases that require different types of innovations, as affirmed by the Abernathy & Utterback's model.

The aim of this doctoral dissertation is to support sustainability-oriented technological innovation at different levels, i.e., at product, process, and system levels. It starts with the presentation of a sustainability-oriented technological innovation framework that effectively connects the innovation levels - namely, product, process, and system - with distinct phases of a technological lifecycle. The main purpose of this framework is contextualize the different types of sustainability-oriented innovations. In fact, it can serve as a valuable reference to

determine the most appropriate timing for specific sustainability-oriented innovations. Additionally, it enables an evaluation of the suitability of the methods and tools proposed for implementing sustainability-oriented innovations in alignment with the technology lifecycle. Then, three different research activities are developed in line with such framework, which represent the core of the doctorate research.

The first research activity is focused on supporting sustainability-oriented product innovation, primarily applicable during the initial phase of a technology lifecycle, where early product design and development hold greater significance, and the product requirements drive the design process. Specifically, a decision-making tool for the establishment of product requirements for a CE is developed. This is achieved through the creation of a decision-making tool in the form of a decision tree. Such decision tree shows when a CE business model outperforms a linear economy (LE) model considering both economic and environmental criteria. Moreover, if the CE is selected, it further illustrates whether the product's components should be recycled, remanufactured, or reused. The decision tree provides a step-by-step graphical representation of the decision rules that must be followed to adopt a CE. Consequently, the decision rules within the tree can serve as a foundation for establishing product requirements for a CE business model. Moreover, the role of carbon tax on circular economy adoption is investigated. More in detail, carbon tax level curves are developed that show, for each product manufacturing cost and carbon footprint, which is the minimum carbon tax value that make include at least one environmental parameter in the decision tree and, hence, in the product requirements for a CE.

Then, the second research activity is focused on supporting sustainability-oriented system innovation, better suited in the second phase of a technology lifecycle. In fact, this research conveys greater added value when the dominant design of a technology has emerged, and, hence, the value chain configuration is well-established. In this context, the implementation of a digital product passport, meant as a digital information system that fosters value chain transparency, can result in considerable sustainability improvements. Therefore, sustainability-oriented data requirements for the digital product passport are proposed aimed at conducting a comprehensive evaluation of environmental sustainability that aligns with the Earth's ecological limits. These requirements are proposed by referring to the well-established Life Cycle Assessment (LCA) and the Planetary Boundaries (PBs) frameworks. Moreover, technical data to insert in the digital product passport are proposed with the aim of fostering the application of CE principles throughout

the value chain. Furthermore, a framework based on Cyber-Physical Systems (CPSs) is proposed to facilitate the automated collection of both technical and environmental data.

Lastly, the third research activity focuses on supporting sustainability-oriented process innovation and it finds wider applicability in the final phase of a technology lifecycle, when sustainability improvements can be better achieved through process innovations. In this context, a case study is conducted on a manufacturing process that holds great opportunities in terms of sustainability enhancements. Specifically, the Resistance Spot Welding (RSW) process, widely employed in the automotive sector, is investigated. This process serves as the primary joining method in car-body assembly lines. It is characterized by significant uncertainty related to the electrode wear, as the degradation process encompasses several distinct phenomena, including mechanical, thermal, metallurgical, and more. Typically, car manufacturers perform considerable redundant welds (1000-1200 per each car-body) to account for the uncertainty connected with the electrode wear. If these redundant welds could be eliminated, it would result in significant resource savings, encompassing energy, time, and costs. Therefore, an experiment involving more than 1200 resistance spot welds was performed in this research. These welds were performed with the aim of inducing the electrode degradation and investigate its effect on the weld quality. The electrode degradation was induced through the repetition of the same welding cycle throughout the experiment so that the only phenomenon that could systematically alter the weld quality was the electrode degradation. Data recorded from sensors during the experiment are processed and used to feed a neural network (NN) with the aim of quantitatively computing, in real-time, the electrode degradation.

Contents

1. Introduction....1
1.1 Sustainability problem....1
1.2 Sustainable Manufacturing....6
1.3 Thesis objectives and structure....8
2. Technological innovations for sustainable manufacturing....10
2.1 Main definitions....10
2.2 Technology lifecycle and innovation dynamics....12
2.3 Sustainability-oriented technological innovation framework....17
2.4 Research activities and research questions....21
3. Technological innovation at product level for sustainable manufacturing....26
3.1 Theoretical background....26
3.2 Literature analysis....29
3.2.1 Guidelines for circular product design....30
3.2.2 Optimization of disassembly and EoL activities....31
3.3 Methodology....33
3.3.1 Mathematical model....36
3.3.2 Bi-level computer-based factorial experiment....48
3.3.3 Multi-level computer-based factorial experiment....51
3.3.4 Decision tree....52
3.3.5 Carbon tax level curves....53
3.4 Results and discussion....55
3.4.1 Decision-making tool at product level....55
3.4.2 Decision-making tool at component level....63
3.4.3 Carbon tax level curves....68

3.5 Main contributions and limitations....79
4. Technological innovation at system level for sustainable manufacturing....82
4.1 Theoretical background....82
4.2 Literature analysis and current state of DPP....85
4.2.1 Literature analysis....85
4.2.2 Current state of the DPP....87
4.3 Methodology....92
4.4 Results and discussion....99
4.4.1 Sourcing data....99
4.4.2 Transformation and Assembly data....100
4.4.3 Use data....100
4.4.4 End of Life data....101
4.4.5 Reusing, Remanufacturing, Recycling data....101
4.4.6 DPP platform based on CPSs....101
4.5 Main contributions and limitations....105
5. Technological innovation at process level for sustainable manufacturing....108
5.1 Theoretical background....108
5.2 Literature analysis....112
5.3 Methodology....116
5.3.1 Asset monitoring....116
5.3.2 Target variable definition....117
5.3.3 Predictive variables definition....117
5.3.4 Inferential analysis....119
5.3.5 Predictive analysis....120
5.4 Results and discussion....122
5.4.1 Asset monitoring....122
5.4.2 Target variable definition....128
5.4.3 Predictive variables definition....133

5.4.4 Inferential analysis 141
5.4.5 Predictive analysis 144
5.5 Main contributions and limitations 147
6. Conclusions 149
6.1 Summary of the work 149
6.2 Discussion of research questions 151
6.3 Conclusive remarks 154
6.4 Limitations and future developments 156
7. References 157

List of Figures

Figure 1: Diagram depicting the planetary boundaries. Orange areas denoting "overshoot" and green areas denoting a "safe" state within the boundaries (data for September 2023) [6]. 2

Figure 2: The Great Acceleration; a) socio-economic trends; b) Earth's system trends [7]. 3

Figure 3: Operationalization of the circular economy principles at product, process, and system level to achieve sustainable manufacturing, based on [17].....7

Figure 4: Schematization of a technological trajectory. 12

Figure 5: schematization of the technological progress. 13

Figure 6: The Abernathy and Utterback's model [27]. 15

Figure 7: Sustainability-oriented technological innovation framework. 18

Figure 8: Contextualization of the carried out research activities according to the sustainability-oriented technological innovation framework. 24

Figure 9. The decision-making tool developed in this research aims to support the definition of product requirements for a CE during the concept development process. 28

Figure 10. Life cycle model considered in this work. 34

Figure 11: Main effects plot at product level; in the y-axis the class value for the product decision class is reported ('0' stands for CE and '1' for LE). 56

Figure 12: Strongest interaction plot between the model parameters for the business model selection at product level. 57

Figure 13: Decision tree for the selection of the most performing business model. The decision rules to apply represent the product requirements for a CE. 59

Figure 14: Relative importance of the model parameters at product level. 61

Figure 15: Box and whisker plot of the performance provided by each business model when it represents the preferable choice. The horizontal line represents the median value, while the target symbol represents the mean value. 62

Figure 16: Main effects plot at component level; in the y-axis the class value for the CE strategy is reported ('0' stands for Remanufacturing and '1' for Recycling). 63

Figure 17: Strongest interaction plot between model parameters for the CE strategy selection.....64

Figure 18: Decision tree for the selection of the CE strategy between recycling and remanufacturing. The decision rules to apply represent the product requirements for a CE at component level.....66

Figure 19: Relative importance of the model parameters for CE strategy selection. 67

Figure 20: Performance provided by each CE strategy ('REC' stands for recycling and 'REM' for remanufacturing) when it represents the preferable choice. The horizontal line represents the median value, while the target symbol represents the mean value. 68

Figure 21: Carbon tax level curves. The solid red line represents the maximum value currently present.....70

Figure 22: Decision tree for business model selection with the new carbon tax regime. 71

Figure 23: Relative importance of the input parameters for the business model selection with new carbon tax regime.....73

Figure 24: Comparison of each business model performance when it represents the preferable choice under different carbon tax regimes: a) CE comparison; b) LE comparison.....74

Figure 25: Decision tree for CE strategy selection with the new carbon tax regime. 75

Figure 26: Relative importance of model parameters for CE strategy with new carbon tax regime.....76

Figure 27: Comparison of each CE strategy performance when it represents the preferable choice under different carbon tax regimes: a) Remanufacturing comparison; b) Recycling comparison. 78

Figure 28. Relations between EF impact categories and PBs based on [125].96

Figure 29: Use of stakeholder's CPS to fill the DPP.....104

Figure 30: Use of CPSs for filling the DPP throughout the product lifecycle. 105

Figure 31: Schematization of the RSW process.....110

Figure 32: Schematization of a spot weld cycle.....111

Figure 33. Data-driven methodology for the health assessment of industrial assets. 116

Figure 34: Linear position sensor embedded on the machine and structural block diagram. 123

Figure 35: Geometry of the truncated cone electrodes. 124

Figure 36: Schematization of the spot weld cycle used in the experimental campaign. 125

Figure 37: Edge and weld spacing distances used on the panel welds for the endurance test according to the AWS D9.8 M standard. 125

Figure 38: Geometry of the shear tension samples according to JIS Z 3136 standard. 127

Figure 39: Shear tension strength of the welded spots at varying number of welds. 128

Figure 40: Electrode tip shape as obtained from the carbon imprint tests at a) 0 welds, b) 600 welds, c) 1200 welds. 129

Figure 41: Contact area and equivalent diameter vs. number of welds and failure load 130

Figure 42: Major and minor contact length vs. number of welds and failure load. 131

Figure 43: Perimeter and circularity factor vs. number of welds and failure load. 132

Figure 44. The contact area indicator allows to effectively discriminate the instability of RSW process due to electrode wear. 133

Figure 45: A typical (a) electrode displacement curve with (b) the corresponding spot weld cycle. 135

Figure 46: Different electrode displacement curves with associated electrode imprints. 136

Figure 47: Geometrical features extracted from the electrode displacement curve vs. the number of welds. 139

Figure 48: Scatter plots of the electrode wear indicator, i.e., the contact area, vs. the predictive variables.....140

Figure 49: Fitting of the contact area vs. normalized decreasing speed with the polynomial regression model. 143

Figure 50: Graphical residual analysis. 144

Figure 51: Neural Network architecture. 145

Figure 52: Neural Network performances for the prediction of the electrode contact area and relative error. 146

List of Tables

Table 1: Model variables. 36

Table 2: Model parameters. 38

Table 3: Values adopted for the 2-levels computer-based factorial experiment. 49

Table 4: Values adopted for the multi-level computer-based factorial experiment at product level. 58

Table 5: Values adopted for the multi-level computer-based factorial experiment at component level. 65

Table 6. Definition of environmental impact according to the EF method [125]. 92

Table 7. Definition of Planetary Boundaries [6]. 94

Table 8: Planetary Boundaries applied to Environmental Footprint impact categories based on [125]. 97

Table 9*:* Correlation matrix between the predictive and response variables obtained from the welding experiments. 141

Table 10: Coefficient estimates of the regression model displayed in Eq. 68. 142

Table 11: Neural Network performance metrics obtained from the data of Figure 49a. 146

List of Acronyms and Abbreviations

A.U.	Abernathy & Utterback
BC	Blockchain
CE	Circular economy
CPS	Cyber-Physical System
DID	Digital Decentralized Identifier
DPP	Digital Product Passport
EC	European Commission
EF	Environmental Footprint
EoL	End of Life
EU	European Union
GDP	Gross Domestic Product
GHG	Greenhouse Gas Emissions
ICT	Information and Communication Technology
IGBP	International Geosphere-Biosphere Programme
IoT	Internet of Things
KPI	Key Performance Indicator
LCA	Life Cycle Assessment

LE	Linear Economy
ML	Machine Learning
MRMR	Minimum Redundancy Maximum Relevance
NGO	Non-Governmental Organization
NN	Neural Network
PB	Planetary Boundary
PHM	Prognostics and Health Managements
PSILCA	Product Social Impact Life Cycle Assessment
PSS	Product-Service System
R&D	Research and Development
RQ	Research Question
RSW	Resistance Spot Welding
SM	Sustainable Manufacturing
SR	Sustainability Report
UNEP	United Nations Environment Program
US	United States
VC	Verifiable Credentials

Chapter 1

Introduction

1.1 Sustainability problem

For 10,000 years the Earth experienced an environmentally stable period, also known as the Holocene epoch, where human civilization have arisen and developed. Throughout the Holocene, natural environmental changes took place, and the Earth's carrying capacity preserved the conditions to enable human development [1]. As early as 1798, the English professor Thomas Malthus noted that the human population, because of its exponential grow, was inevitably destined to surpass the Earth's carrying capacity [2]. The latter, according to Hauschild [3], can be defined as "*the maximum sustained environmental intervention a natural system can withstand without experiencing negative changes in structure or functioning that are difficult or impossible to revert*". The Earth's carrying capacity can be scientifically represented by nine life support systems, most of them quantitatively monitorable by specific indicators. The threshold values of these quantitative indicators represent the planetary boundaries (PBs) defining a "safe operating space" for human development [4]. Nowadays, six out of nine PBs have already been transgressed leading to a globally recognized environmental crise [5]. Figure 1 depicts the current situation according to the PBs framework.

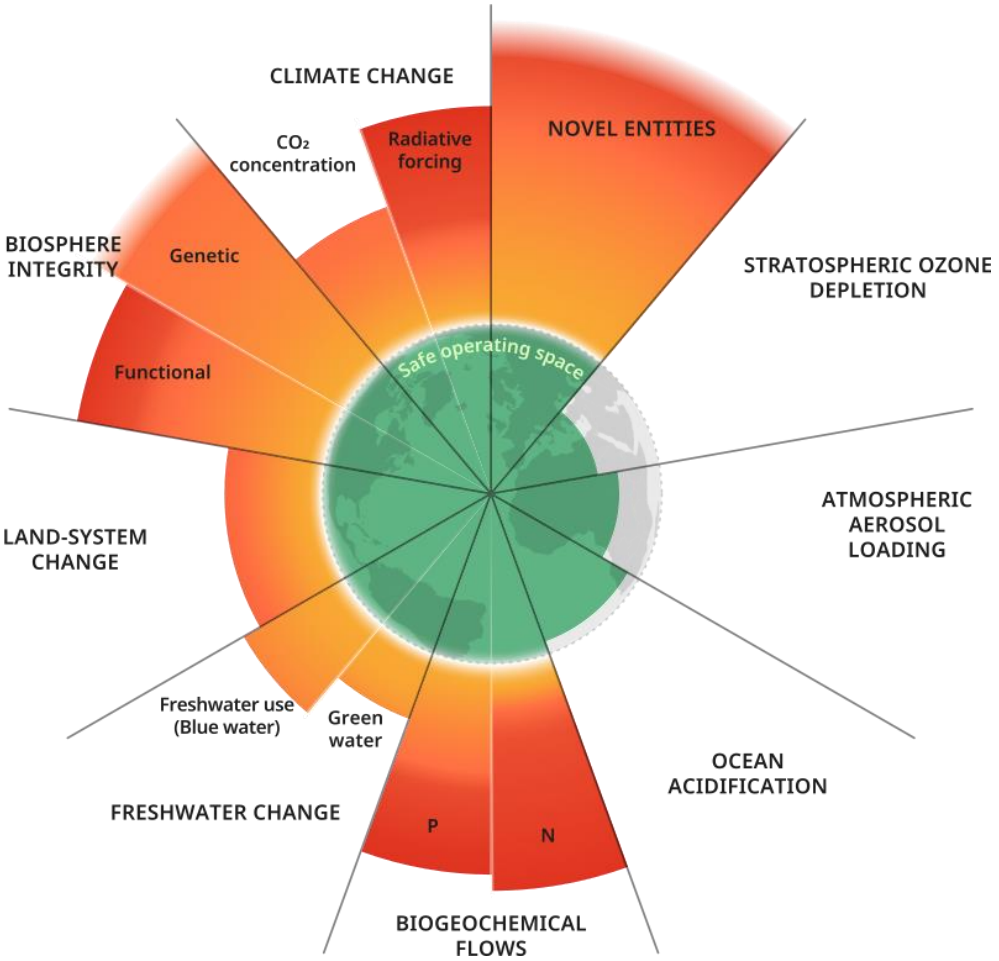


Figure 1: Diagram depicting the planetary boundaries. Orange areas denoting "overshoot" and green areas denoting a "safe" state within the boundaries (data for September 2023) [6].

Human activities are considered the leading cause of this environmental crisis. In fact, already in 2004, the International Geosphere-Biosphere Programme (IGBP) released a study that presented the socio-economic trends spanning the period from 1750 to 2000 driven by human activities, together with the concurrent Earth system trends. The study encompassed a set of 12 indicators for socio-economic trends and 12 indicators for Earth system trends. Subsequently, these results were revisited and updated in 2014, and they are depicted in Figure 2 [7].

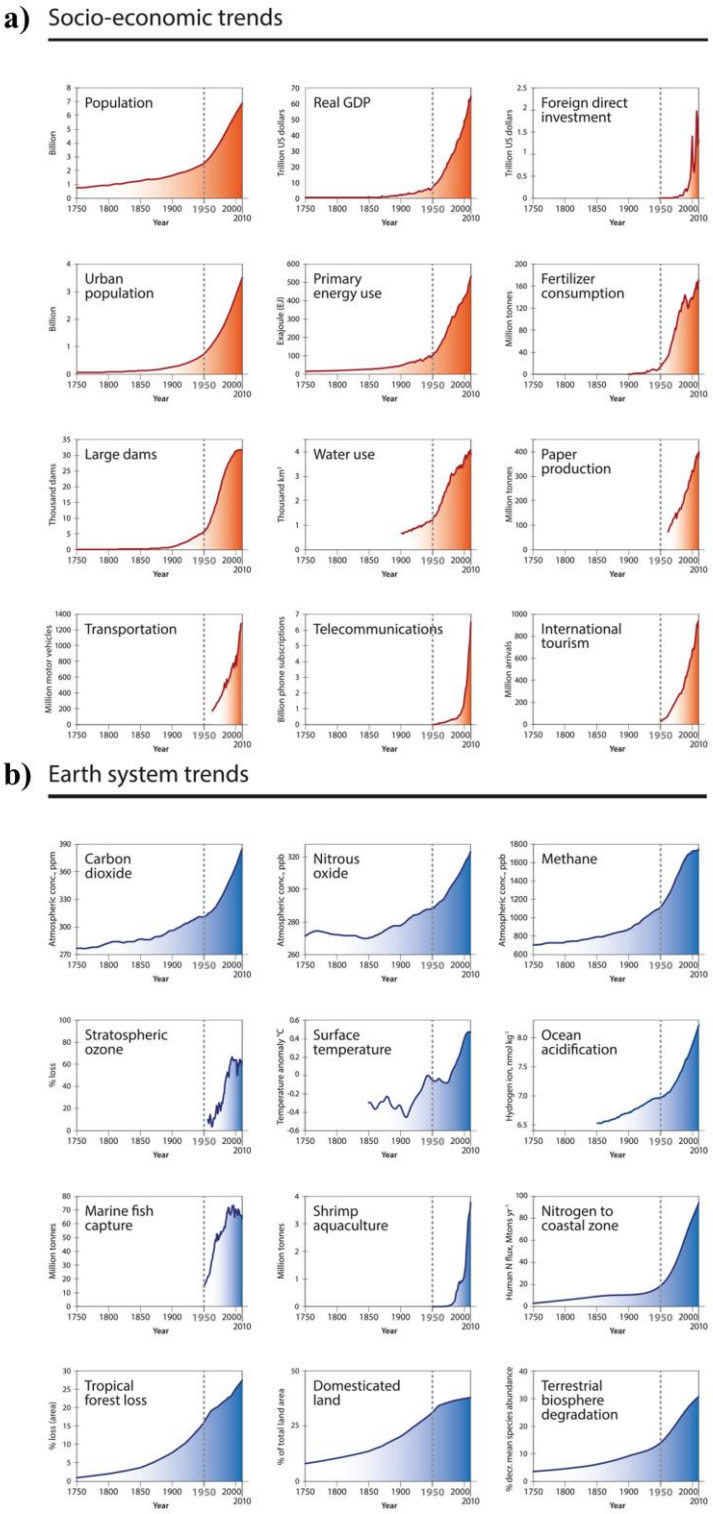


Figure 2: The Great Acceleration; a) socio-economic trends; b) Earth's system trends [7].

The presentation and discussion of each indicator are not within the scope of the present doctoral thesis, but, through the observation of their temporal trends, a key fact stands out. The simultaneous increase in these trends from the 1950s up to the present day clearly shows a correlation between the socio-economic trends and the Earth system trends. These collectively recognized trends are referred to as the "Great Acceleration" [8]. Transformations in human production and consumption, as represented by metrics like Gross Domestic Product (GDP), foreign direct investment, primary energy use, and telecommunications, are mirrored by alterations in the Earth's natural systems. These changes manifest in various ways, such as the climate (carbon dioxide and surface temperature), ocean acidification, terrestrial biosphere degradation, and so forth [8].

Today, many Earth system indicators are beyond their natural variability, and the Earth is in a quantifiably different state than before, corresponding to a new geological epoch, known as the Anthropocene. The beginning of the Anthropocene was considered to be as the Industrial Revolution kicked off around 1800, although there is increasingly evidence nowadays that the beginning of the Great Acceleration marks the start date of the Anthropocene [7].

To understand how these major socioeconomics phenomena, such as population and urbanization expansion, as well as the increasing affluence due to GDP growth and trading of numerous commodities, affect the environmental impact, the IPAT equation can be useful. The latter represents the total environmental impact (I) associated to a specific environmental impact category caused by human activities, as a function of three driving factors: the human population (P), i.e., the number of people; the human affluence (A), i.e., the average number of technologies used by each person; the technology factor (T), i.e., the average environmental impact generated by the technology when providing its functionality.

$$I = f\ (P,\ A,\ T) \tag{1}$$

The inverse of the technology factor (T) is known as the eco-efficiency of a technology, i.e., the functionality provided divided by the average environmental impact. Improving the eco-efficiency of technologies means creating products and services with the same or greater functionality and reduced environmental impact. Although this has been pursued for many years, this is not sufficient to address the current environmental challenge. As explained in [2], the lighting technology represents an outstanding example. Ausubel and Marchetti found that, starting in

the early 19th century, the energy efficiency of lighting systems increased exponentially, rising by more than two orders of magnitude from paraffin candles to contemporary diode lamps [9] Thus, the lighting service can now be obtained with only a tiny portion of the energy required two centuries ago. Higher energy efficiency may be expected to assist a reduction of the environmental impact, but since it also leads to lower lighting costs, it also encourages higher demand and usage of lighting. This phenomenon, known as a *rebound effect* in the market, more than cancels out the efficiency improvements achieved. Magee and Devezas examined 57 cases of technological efficiency improvement spanning various materials and technologies over the past decades; they discovered that it is a general finding that rebound effects neutralize efficiency improvements. They were not able to show that the achieved efficiency improvements resulted in environmental benefits [10].

In order to prevent an increasingly environmental impact (I) caused by the population (P) and wealth growth (A), the eco-efficiency of technology (T) that supports the growing population's wealth must also increase more and more. Furthermore, it is essential to note that a strong interdependency between the three driving factors of the IPAT equation occur, as explained for what concerns the rebound effect phenomenon where technology improvements affects both the population and affluence factors [11].

Thus, it turns out that an exclusive focus on eco-efficiency is not sufficient to achieve sustainability, even though a significant improvement in the eco-efficiency of technologies is definitely required to ensure sustainable development. This means that the required sustainability levels that respect the Earth’s carrying capacity must be set. These targets must be achieved with solutions that allow to weaken the effect of the interdependency between the driving factors of the environmental impact, as well as with solutions that further improve the eco-efficiency of technologies [2].

1.2 Sustainable Manufacturing

In this context, it is crucial to recognize that manufacturing is the primary source of income creation for every country. Both developed and developing countries have demonstrated how important manufacturing is to the growth of their economies, the creations of jobs, and societal well-being. In fact, manufacturing sector has a significant effect on the economy, environment, and society. For instance, regarding the economic aspect, the manufacturing value added (% of GDP) in the European Union (EU) was reported at 14.70% in 2022 [12]. Regarding the environmental impact, then, in the second quarter of 2022 the Manufacturing sector accounted for 23 % of the EU's carbon footprint [13]. Finally, for what concerns the social aspect, in 2021 manufacturing employment shared 14.85% of total employment in EU [14].

This highlights the responsibility of the manufacturing sector in Sustainability, and the urgent need for a rapid and effective shift towards a Sustainable Manufacturing (SM) paradigm. While there is not a universally agreed-upon definition for the concept of "Sustainable Manufacturing", significant efforts have been undertaken in recent times, with ongoing initiatives continuing to develop this definition. For instance, [15] offers the following definition of Sustainable Manufacturing:

"producing products in a way that minimizes environmental impacts and takes social responsibility for employees, the community, and consumers throughout a product's life cycle, while achieving economic benefit".

In recent years, the idea of a circular economy (CE) has gained global attention as the traditional linear economy (LE), characterized by the "take-make-dispose" model, is proving inadequate in addressing the sustainability challenges. The CE is based on the following concepts [16]:

"*reducing wasteful resources through effective design and implementation of products and processes for improved resource-efficiency with circular material flow involving recovery, reuse, recycling and remanufacturing of products*".

SM can be achieved through the application of the CE principles in manufacturing [17]. However, a huge gap regarding the practical implementation of CE principles within the manufacturing context is widely recognised [18], [19], [20]. In fact, only 8.6% of the 100 billion tons of materials needed annually to fuel

our economy in 2020, according to [21], originated from CE business models. This percentage has been on the decline since then, falling to 7.2% in 2022 [22].

In fact, the CE paradigm poses a substantial technological challenge, far beyond being a mere social or political vision. It demands the development for technological innovations at product, process, and system levels towards the creation of sustainable value for humanity [16], [17], [23], [24], as schematically depicted in Figure 3.

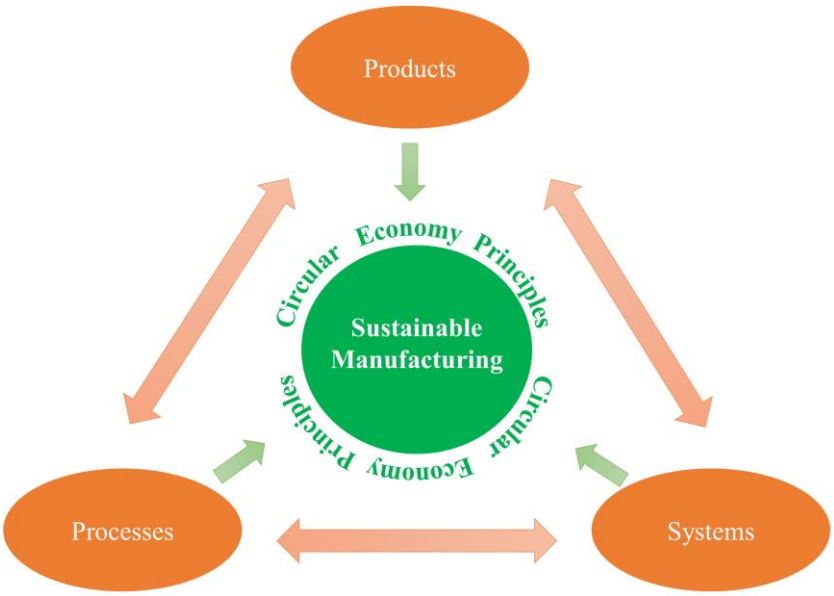


Figure 3: Operationalization of the circular economy principles at product, process, and system level to achieve sustainable manufacturing, based on [17].

This consideration holds significant importance because the product, process, and system are three enabling elements for the integration of CE principles in Manufacturing. For the sake of example, the product must be purposely designed and developed with characteristic suitable for a CE in terms of disassembly, remanufacturing, recycling, and so on. Then, it is necessary to consider that the lifecycle of manufactured products experiences multiple phases, beginning with the extraction and processing of materials, their transformation and assembly to obtain the final product, and the product use and post-use phases. This means that many different processes are involved during a product life cycle, and the sustainability of their operations is a pivotal element for SM. At the same time, this implies the engagement of several stakeholders during a product lifecycle, which requires a proper organization of the value chain system [24], [25], [26].

1.3 Thesis objectives and structure

It turns out that technological innovations at product, process, and system levels are needed to integrate the CE principles in manufacturing and achieve SM. However, in order to effectively deliver sustainability-oriented technological innovations, it is crucial consider that types of innovation activities change based on the technological lifecycle phase. Therefore, in this doctoral thesis will be presented a sustainability-oriented technological innovation framework that links the different types of innovations with the technology lifecycle phases. This framework aims to provide a structured context for stainability-oriented technological innovations by gaining a comprehensive understanding of the suitability of specific methods and tools in addressing sustainability.

After the introduction of such framework, which contextualize the research conducted in this doctoral thesis, three distinct sustainability-oriented technological innovation activities are developed to target a specific innovation level in each technology lifecycle phase. First, an activity focused on sustainability-oriented product innovation will be presented. As it will be explained in the next chapter, this type of innovation conveys greater added value during the initial phase of the technology lifecycle, where early product design and development hold greater significance. Second, an activity focused on sustainability-oriented innovation at system level will be presented. Such activity will provide greater added value if performed during the second phase of technological lifecycle where a value chain needs to be properly configured. Finally, the third sustainability-oriented technological innovation activity of this doctoral thesis focuses on the last phase of a technology lifecycle, during which sustainability improvements can be attained through process innovations. In this context, a case study was undertaken concerning a manufacturing process that hold great opportunities for sustainability enhancements.

These three sustainability-oriented technological innovation activities will address specific research questions (RQs) that will be revealed at the end of the next chapter, after that a solid background on the technological innovation and the dynamics of innovations is provided.

Therefore, the remainder of the doctoral thesis is structured as follows. Chapter 2 will pose the basis for the sustainability-oriented technological innovation framework by providing an overview of definitions and models in the field of technological innovation. In this chapter the reference framework is presented, as

well as the RQs of this doctoral thesis. Then, the following three chapters present the research activities carried out during the doctorate to address the research questions. Each chapter is composed of a theoretical background, literature analysis, methodology, results and discussion, and main contributions and limitations. Finally, chapter 6 summarizes the entire research activity, discusses the RQs, provide the conclusive remarks and outline the limitations of the research.

Chapter 2

Technological innovations for sustainable manufacturing

2.1 Main definitions

Innovation can be defined as "*the act or process of introducing new ideas, devices, or methods*". The primary emphasis of innovation lies in the influence that novel ideas, devices, or methods exert on both the business landscape and society. This definition allows to distinguish *innovation* from related terms such as *discovery* and *invention*. As a first approximation, it is possible to propose the following definitions [27]:

- ***Discovery***. It is the achievement of uncovering something previously unknown. Discovery therefore produces scientific knowledge by building new results on top of prior knowledge of the same kind, and it is the usual result of Science.
- ***Invention***. It is the result of technology, meant as the application of scientific and technological knowledge to create a solution to a problem, i.e., the invention.
- ***Innovation***. It can be defined as the economic exploitation of an invention. In other words, the invention becomes innovation when it is successfully diffused into the market. It is the result of development activities performed by a company to provide customers a utility greater than the production cost.

Among the numerous innovation possibilities, the present thesis specifically focuses on discrete products, i.e., individual, distinct items or goods that are separate and countable entities. Consequently, only the pertinent concepts related to this domain will be presented.

Before to discuss the main features of innovation for discrete products, it is preparatory to discuss the concept of *product architecture*. The product architecture can be defined as "*the relationships between its functional elements, the mapping among functional elements and physical components and the interfaces among physical components*" [28]. The structure of the product architecture can be *integral* or *modular*. The former takes place when each product function is fulfilled by multiple components and each component performs multiple functions. The latter, instead, is characterized by functionally independent components. Each function is fulfilled by a single component, and each component fulfils a single function only. The structure of the product architecture determines the structure of the product supply chain and it has a strong influence on the type of technological innovation. The supply chain bonds of an integral product architecture are very strong, whereas the ones of a modular architecture are easily destroyable [27].

An innovation can be *incremental* if there is a gradual improvement of the performance or functionalities of a product. This type of innovation can be costly to achieve, but it is easier to manage, since the underlying technology and the product architecture do not change [27]. *Radical* innovation, instead, entails to introduce a product with totally new functionalities and/or performance drastically superior to the previous versions of the product. In this type of innovation both the underlying technology and the product architecture change. Undoubtedly, the pursuit of this form of innovation is quite challenging. *Modular* innovation, then, entails to change the technology of one or more functional elements, but without changing the product architecture. Such innovation may be challenging to pursue in the modules in question; however, the issues will be isolated to the impacted modules, and the development of the entire product will be kept relatively easy to manage [27]. In *architectural* innovation, instead, the underlying technology does not change, whereas the functional and/or physical relationships between components do. Managing architectural innovation is typically a complex task because the well-established organizational procedures needed to develop a product will not be readily accessible. In fact, they will require some time and possibly entail costly errors before to emerge [27]. Finally, innovations can be classified as either *sustaining* or *disruptive*, as defined in [29], based on their influence on the industry. A sustaining innovation typically does not bring alterations in competitors' market positions or market shares. In contrast, a disruptive innovation enables significant changes. Market leaders may get left behind or even go out of business as a result of disruption, while startups, new entrants, and companies that played a smaller role in the past may become new leaders.

2.2 Technology lifecycle and innovation dynamics

The technological evolution can be described by observing the behaviour of its representative performance indicator. When a new technology is introduced in the market, usually it exhibits a relatively low performance. In this initial phase innovations push technological progress slowly, and the growth of the corresponding performance is weak. Once a sufficient level of maturity is achieved, innovations push technologies easier, with a notable increase of the technological performance. This sharp increase continues until when the performance approaches its intrinsic superior limits, i.e., a performance level that cannot be overcome due to limitations that are intrinsic to the specific technology. In this last phase, the technological evolution is again slow, and many efforts are needed to achieve small incremental improvements.

It turns out that the evolution of the technological performance does not follow a linear process, but an S-shaped curve, known as *technological trajectory*, as schematically depicted in Figure 4.

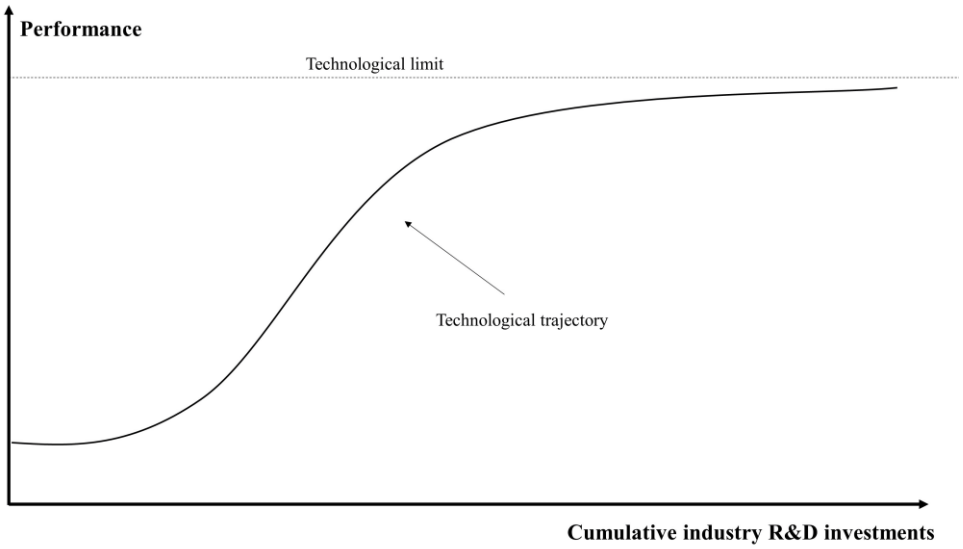


Figure 4: Schematization of a technological trajectory.

It is worth noting that the performance monitored to represent the technological progress should also be representative of the user needs. Moreover, it can be deceptive to use time as the independent variable, as technological advancements are the result of corporate investments and effort rather than just passing time. As a

result, s-curves should actually be drawn as a function of cumulative industry R&D investment rather than time. Since it might be difficult to locate data on R&D spending, industry-level cumulative sales are sometimes used as a stand-in [27].

Upon reaching the technological limit, companies that aspire to enhance their products must explore new technological solutions. They must select from various new candidate technologies, some of which may have originated independently and outside the industry. This *revolutionary phase* will entail substantial experimentation until stakeholders can discern which competing technology can effectively meet the current or evolving customer needs. The revolutionary phase coincides with the establishment of a new technological trajectory, i.e., a new S-shaped curve. Thus, it turns out that the *technological progress* is characterized by two distinct phases, the *evolutionary phase*, i.e., the progress within the technological trajectory referred to a specific technology, and the revolutionary phase, i.e., the shift from one technological trajectory to another, as schematically represented in Figure 5.

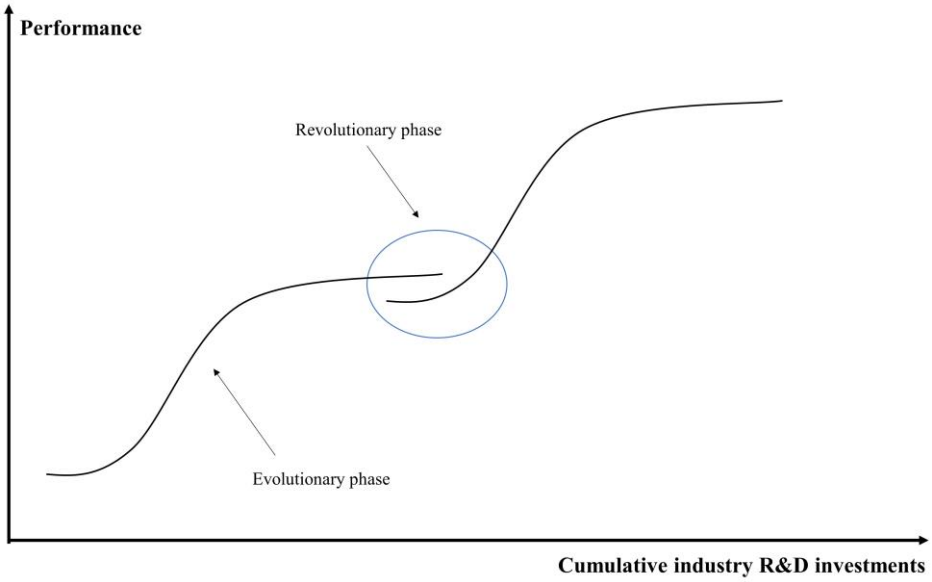


Figure 5: schematization of the technological progress.

In any phase, the advancement of the technological progress is due to innovation. However, within these phases, innovation is influenced by two distinct phenomena. During revolutionary phases, innovation occurs because companies are compelled to explore novel technological solutions that can potentially surpass the existing technological limits. They seek these solutions from developments that

have originated externally to the industry and integrate them to meet a clear or latent need. Thus, the revolutionary phase is usually refers as *technology-push*. Conversely, in evolutionary phases, the technological evolution is guided by innovations that directly meet the explicit market needs. The revolutionary phase is usually refers as *demand-pull* [27].

The innovations that determine a technological evolution and, hence, a technological trajectory, can be explained with the Abernathy and Utterback (A.U.)'s model [30]. The A.U's model represents a valuable contribution to understand the different types of innovation that occur during the technology lifecycle, i.e., during a trajectory technological [31]. Abernathy & Utterback and other authors have suggested that performance, sales, number of firms in the industry, and the rates of product and process innovation should be considered in order to understand the dynamics of innovation, as displayed in Figure 6.

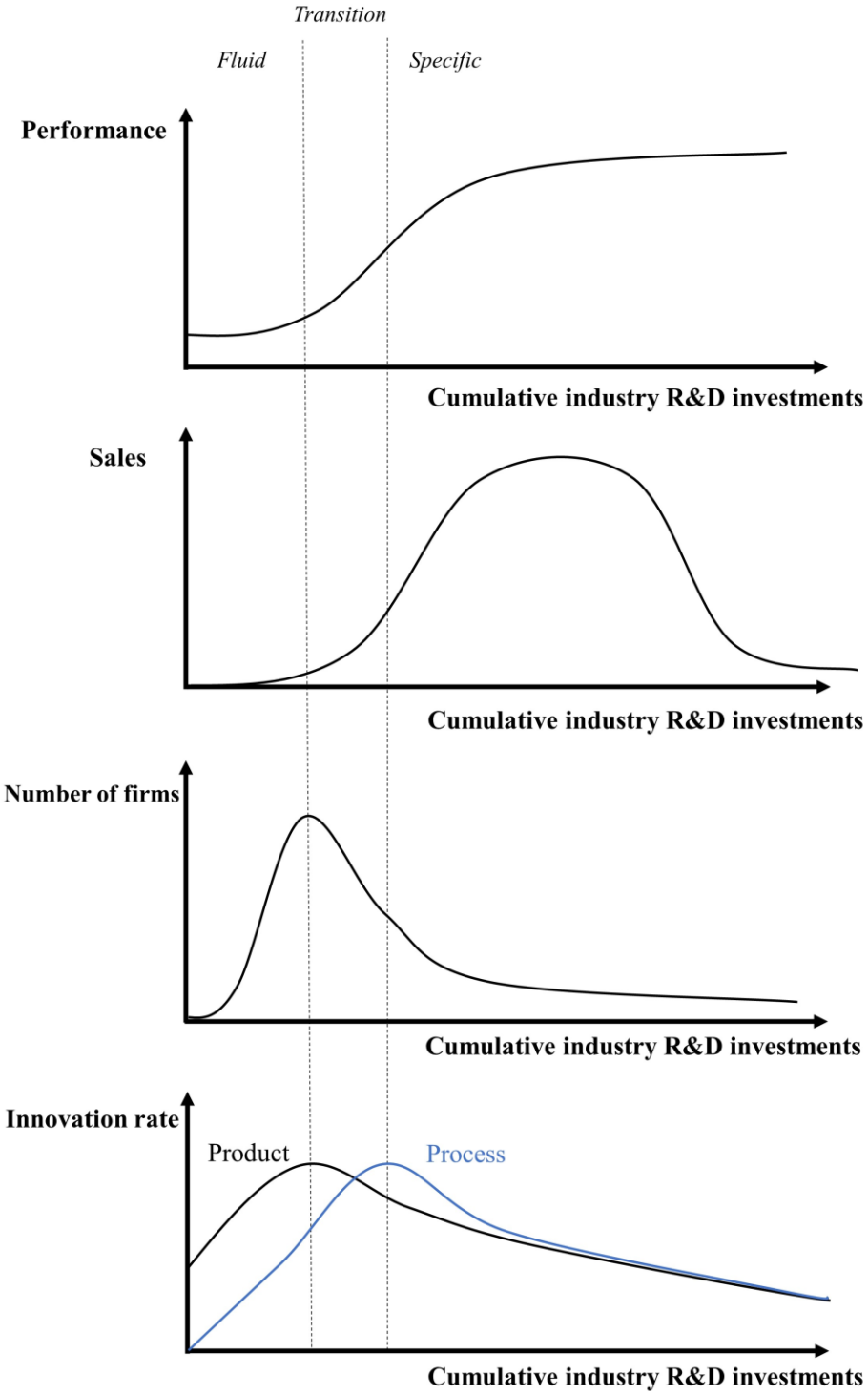


Figure 6: The Abernathy and Utterback's model [27].

A growing number of companies enter the market during the beginning of a technological revolution, i.e., the beginning of a new technological trajectory, drawn by the potential for future growth, similar to a “gold rush”. During this phase, known as *fluid phase*, there is a very wide variety of competing and alternative technical solutions since every company entering the market has a stock of past competencies and assets that it believes will be valuable. Although there is a high rate of product innovation, this does not result in considerable evolution since businesses are not focusing their efforts in the same technical direction, which prevents them from creating cumulative progress through imitating and improving the ideas of their competitors. This increasing number of businesses therefore competes on a persistently low demand and, in turn, low sales.

The industry transitions from its fluid phase to the *transition phase* when a single product architecture establishes itself as the frontrunner and it is recognized to be the *dominant design*. The dominant design encompasses the product concept, the technical solutions, the components, and their relationships that achieve broad acceptance within that industry and market, effectively surpassing other competing designs. The growth of the technological trajectory can now begin, and a sort of avalanche effect is established. Product performance increases as a result of technical knowledge now being concentrated on the dominant design, which permits competitors to imitate it and lead to a technological progress. Product sales begin to increase as well, owing to enhanced product performance. Simultaneously, the number of active firms begins to decline (the industry experiences a "shakeout"). This can be attributed to two reasons: either the assets and competencies of some companies do not match the dominant design, or the required growth rates are too high for the firms with weaker management or finances.

The rising industry sales and the decreasing number of competitors result in even more demand for the firms that remain, intensifying their need to sustain such expansion. At this stage, the technology lifecycle transitions into the phase commonly referred to as *specific phase*. In this phase, companies aim to compete on both cost and quality as demand continues to rise. Since the product architecture is now well-established, companies are focusing more on process innovation than product innovation because it is both strategically and technically feasible to improve the process in order to lower costs and improve quality. As a result, businesses create capital-intensive, optimized processes tailored to the dominant design, enabling considerable economies of scale and improved quality. Consequently, this results in reduced product costs, lower prices, and a continual surge in demand that, in turn, intensify the industry shakeout as the new processes

establish a minimum efficient scale. Such phenomenon continues until when the technological limit is reached, the sales start to decline, and a new technological revolution begins.

During these three distinct phases identified by Abernathy and Utterback, innovations occurs in different ways and it determines how the design activities of the companies are conducted. In the *fluid phase*, a *radical innovation* both at product and system level is usually observed because products are subject to significant change in both the underlying technology and the product architecture.

During the *transition phase*, in some cases, the dominant design may be subject to some further revisions or optimizations, usually without significant change in the underlying technology. This implies *architectural innovation* at product and system level. Instead, once the dominant design is established, innovation typically does not result in substantial alterations to either the underlying technology or product architecture. Consequently, an *incremental innovation* both at product and system level is usually observed.

In the *specific phase*, *incremental innovation* can occur at all the levels product, process, and system level, with a special emphasis on process innovation. However, the integration of radically new technology within the dominant design can occur during the lifetime of the specific phase, which frequently spans decades, as long as such change can be localized within components and seamlessly integrated into the overall product architecture. In such a case, what appears to be a *radical innovation* at component level is considered a *modular innovation* at product and system levels [27], [31].

2.3 Sustainability-oriented technological innovation framework

As described in the first chapter of the present doctoral thesis, the implementation of the CE principles in manufacturing requires innovations at product, process, and system levels. However, different types of innovation occur depending on the current position in the technological lifecycle. Therefore, this section presents a sustainability-oriented technological innovation framework with the aim of contextualizing sustainability practices into the technology lifecycle. This framework facilitates the contextualization of common design and development tasks associated with each type of innovation activity, and assist

evaluate the suitability of methods and supportive tools. The sustainability-oriented technological innovation framework is presented in Figure 7.

Technological innovation level	Technology lifecycle phase: Fluid phase	Transition phase	Specific phase
Product level	Concept design delivers *radical innovations.* Sustainability-oriented requirements guide the design team towards sustainable product concepts.	The key product architecture emerges, and the design space is more constrained. *Incremental innovations* are usual and focused on meeting better-defined user and environmental requirements.	Detailed design delivesr *incremental innovations* with the goal of enhancing technical, economic, and environmental performance.
System level	The systemic feature of sustainability can be addressed by delivering *radical innovation* because the main product architecture, highly linked with the value chain configuration, has not emerged yet.	The sustainability performance of a value chain can be improved with *incremental innovations*. Occasionally, there may be the introduction of *modular innovations* that do not alter the product architecture.	*Incremental innovations* and/or *architectural innovations* can optimize economic and environmental performance of a value chain.
Process level	*Innovation* usually does not occur in this phase, and it cannot provide any contribute to sustainability.	Manufacturing processes can be design to enhanced resource-efficiency, meeting increased demand, and reducing production costs.	*Incremental innovation* can optimize manufacturing operations to enhance their economic and environmental performance.

Figure 7: Sustainability-oriented technological innovation framework.

During the *fluid phase* innovations are usually radical. Previous technology has reached its intrinsic limit and it is unable to address emerging or more demanding environmental and customer needs. *Product innovation* mainly rely on concept design, where product ideas are created and assessed. At this stage, the comprehension of functional and performance requirements are still vague and uncertain, mainly because the market is in its nascent stages. However, sustainability-oriented requirements can be set in order to guide the design team towards the conceptualization of sustainable product ideas. Design guidelines can be employed in this phase. In fact, design guidelines provide valuable recommendations and constraints to guide the creative and innovative process, ensuring that the final design aligns with specific targets, standards, user and environmental requirements. Starting to use design guidelines early in the conceptual design phase can help prevent the need for major design revisions later in the development process, saving time and money. Regarding the *system innovation*, this can experience a radical innovation during the fluid phase, because the main product architecture, which highly affects the value chain configuration, has not emerged yet. An example is represented by the development of Product-Service Systems (PSSs) that fundamentally changes the way products are delivered, used, and maintained. In fact, in this new paradigm, manufacturers retain the

ownership of products and deliver performance for their customers. This new way of delivery value in the economy requires a radical transformation at system-level because requires collaboration with multiple stakeholders, including service providers, logistics and transportation companies, and so on [32]. The implementation of PSSs are regarded to enhance sustainability for different reasons; in fact, manufacturers are economically incentivised to reduce, as much as possible, material, energy and resources consumption needed to provide performance in the market, since they keep the product ownership throughout its lifecycle [33]. *Process innovation*, instead, plays a minor role in this phase due to the low production volumes, the potential for higher customer willingness to pay, and, most importantly, the lack of a stable product architecture. In fact, a dominant design has yet to be firmly established, and design decisions are recognized to be transitional and not fully optimized. Consequently, process innovation usually does not occur in this phase and it cannot provide a useful contribute to sustainability. However, it is worth noting that what might be a process innovation for a company, this might be a product innovation for another company. By the way of example, the same microwave oven could be seen as a product innovation from the perspective of the manufacturer, while serving as a process innovation for the restaurant that adopts it [27].

In the early stages of *transition phase*, then, the key challenge for *product innovation* is the correct understanding of user requirements. Designers must gradually shift their focus from just functional features to technical performance, usability, and user experience. The design space is gradually more constrained until the dominant design emerges and, thus, the key product architecture is frozen [31]. Differently from user requirements, instead, environmental requirements are known since the first phase of technological lifecycle because they represent the sustainability targets to be achieved; in this second phase, such requirements can be tuned and adjusted according to the constrained dictated by the dominant design. For instance, when the product architecture has been established, the product disassembly features can be optimized in order to make the implementation of CE practices more efficient and attractive for manufacturers. In this case, using standardized or easily removable screws, clips, or fasteners to connect components together, facilitate product disassembly by fostering the application of CE. The establishment of a dominant design allow the proper value chain optimization, calling for incremental *system innovation*. Occasionally, there may be the introduction of modular innovations that do not alter the product architecture. By the way of example, once the dominant design is emerged, transportation and

logistic of the supply chain can be efficiently innovated by implementing strategies to optimize transportation routes and reduce emissions. This includes using eco-friendly transportation modes, consolidating shipments, and employing technologies to track and manage logistics more efficiently. In the transition phase, it is easier to develop and improve manufacturing processes that are tailored to a fixed dominant design. Hence, it is the right time for *process innovation*, aiming at minimizing the environmental impact of operations, as well as to accommodate rising demand and lower production costs. For instance, manufacturers can design processes according to the lean manufacturing paradigm, which focuses on reducing waste and increasing efficiency throughout the manufacturing process. By implementing lean manufacturing principles, companies not only reduce operational costs but also enhance their sustainability thanks to resources savings. This approach aligns with environmental goals and contributes to more responsible resource management and waste reduction.

Finally, the *specific phase* leads to an incremental *product innovation*, no longer focused on the product conceptual phases but on the detailed phases, aiming at improving technical, economic, and environmental performance. An outstanding example of gradual product improvement is represented by the subsea power cable, that is an element used to convey electric energy underwater. The layered structure of these cables involves a variety of materials with distinct mechanical properties. From a structural viewpoint, lead sheathing is the critical element and it usually experiences failures. As an incremental improvement, it is possible to enhance the fatigue resistance of the lead sheath by varying the winding angle of the supporting steel tape. This, in turn, extend the durability of the subsea cable. Longer-lasting subsea cables require less frequent maintenance and repair. This can result in reduced maintenance and repair cost by providing significant resource savings for cable operators and owners, as underwater repairs are expensive and time-consuming [34]. Incremental *process innovation* also plays an important role in delivering sustainability enhancements. For instance, data-driven approaches can identify opportunities for energy efficiency improvements. Manufacturers can monitor energy consumption, analyse patterns, and consequently implement strategies to optimize energy use, starting from data collected from sensors embedded in the assets. This not only lowers operational costs but also reduces greenhouse gas emissions by contributing to make the product more sustainable. Regarding the system level, incremental *system innovation* prevails. As an example, innovations in inventory management systems can occur; implementing more advanced inventory management software and algorithms that optimize stock

levels, reduce excess inventory, and lower carrying costs can provide benefits both from an economic and environmental perspective at value chain level. It is worth noting that architectural innovations that do not alter the product architecture can be established, which often results to be radical innovation at sub-system level as previously described. For example, in a product value chain, blockchain technology can revolutionize the way information and assets are tracked, verified, and shared. Blockchain is built upon a distributed ledger architecture, eliminating the need for a high-performance data centre infrastructure to establish a secure and trustworthy network. This decentralized approach enables the involvement of multiple parties, and cryptographic algorithms are employed to ensure the verification and integrity of data-sharing procedures [35]. Well-defined mechanisms for information security and updates allow for the storage of various types of data, such as events, records, and transactions [36]. Blockchain can have key functionalities in boosting the adoption of CE by providing enhanced supply chain traceability, increased cooperation and coordination within business ecosystems, and heightened levels of trust [37]. Thus, it represents a radical innovation at sub-system level that does not alter the product architecture and, hence, the dominant design.

2.4 Research activities and research questions

In line with the presented reference framework, three distinct researches to support sustainability-oriented technological innovations are developed to target a specific innovation level in each technology lifecycle phase.

Therefore, a research activity focused on supporting sustainability-oriented product innovation is presented, primarily applicable during the initial phase of the technology lifecycle, where early product design and development hold greater significance, and the design team efforts are guided by product requirements. As it will be better described in the chapter 3, although there are many works oriented to the product design for a CE, no research has been dedicated to analyse which characteristics a product should have to be functional for a CE. This is a crucial point to address because product requirements represent the targets that the design team need to meet during product design activities [28]. Therefore, this gap lays the foundation for the first set of research questions addressed in this doctoral thesis:

1.1 What are the product requirements for a CE?

1.2 What is the minimum carbon tax value that causes at least one environmental parameter to be included in the product requirements?

To support this analysis, therefore, a decision-making tool for the establishment of product requirements for a CE is developed. This is achieved through the creation of a decision-making tool in the form of a decision tree. This decision tree illustrates when a CE business model outperforms a LE model considering both economic and environmental criteria. Moreover, if the CE is selected, it further illustrates whether the product components should be recycled, remanufactured, or reused. The decision tree provides clear and transparent guidance on the decision rules that must be followed to adopt a CE. Consequently, the decision rules within the tree can serve as a foundation for establishing product requirements for a CE business model. The economic criterion is represented by the economic cost of each phase involved in the business models (LE and CE), while the environmental criterion is quantified by the $CO_{2,eq}$ emissions generated by each phase involved the business models. The environmental criterion is then monetized through the application of a carbon tax, so that both the criteria can be expressed in monetary terms and be integrated into a single metric, called total cost. As it will be demonstrated, the value of the carbon tax alters the importance of the environmental parameter. Therefore, the second RQ (1.2) is addressed by developing carbon tax level curves that show, for each product manufacturing cost and carbon footprint, which is the minimum carbon tax value that make include at least one environmental parameter in the decision tree and, hence, in the product requirements for a CE.

Subsequently, a second research activity focused on supporting sustainability-oriented system innovation is presented, better suited in the second phase of the technology lifecycle. In fact, this research conveys greater added value when the dominant design of a technology has emerged, and its architecture is well-established. In this context, the implementation of a digital product passport, meant as a digital information system that fosters value chain transparency, can result in substantial sustainability improvements. Chapter 4 will show how currently sustainability-oriented data requirements are partially addressed in the literature. As a result, a second set of RQs has been formulated:

2.1 What are the sustainability-oriented data requirements for the digital product passport ?

2.2 How can these data automatically collect and store in the DPP?

Sustainability-oriented data requirements for the digital product passport are proposed aimed at conducting a comprehensive evaluation of absolute environmental sustainability that aligns with the Earth's ecological limits. These

requirements are proposed by referring to the well-established Life Cycle Assessment (LCA) and the Planetary Boundaries (PBs) frameworks. Specifically, the Environmental Footprint (EF) methodology is considered within the LCA framework because it is used as a reference inside the EU. Moreover, general technical data to insert in the digital product passport are proposed with the aim of fostering the application of CE principles throughout the value chain. RQ 2,2, instead, is addressed by proposing a conceptual framework for the establishment of a digital product passport. Specifically, a framework based on Cyber-Physical Systems (CPSs) is proposed to facilitate the automated collection of both technical and environmental data identified in addressing the RQ 2.1.

Lastly, the third research activity focuses on supporting sustainability-oriented process innovation and it finds wider applicability in the final phase of a technology lifecycle, during which sustainability improvements can be better achieved through process innovations. In this context, a case study was conducted on a manufacturing process that hold great opportunities in terms of sustainability enhancements. Specifically, the Resistance Spot Welding (RSW) process, widely employed in the automotive sector, is investigated. This process serves as the primary joining method in car-body assembly lines. It is characterized by significant uncertainty related to the health of the electrodes, as the degradation process encompasses various distinct phenomena, including mechanical, thermal, metallurgical, and more. Typically, car manufacturers perform significant redundant welds to account for the uncertainty connected with the electrode. If these redundant welds could be eliminated, it would result in significant resource savings, encompassing energy, time, and costs. Chapter 5 will show how, to date, electrode degradation is not quantitatively predicted in real-time and, therefore, the third set of research questions, aimed at supporting sustainability-oriented process innovation, has been defined as follows:

3.1 In Resistance Spot Welding, when the electrode starts to produce low-quality quality welds?

3.2 Is it possible to quantitatively predict this condition in real-time?

RQ 3.1 is addressed by conducting a huge experiment involving more than 1200 resistance spot welds. These welds were performed with the aim of inducing the electrode degradation and investigate its effect on the weld quality. The electrode degradation was induced through the repetition of the same welding cycle throughout the experiment so that the only phenomenon that could systematically

alter the weld quality was the electrode degradation. RQ 3.2, finally, is addressed by developing a data-driven electrode health assessment tool, in form of a neural network (NN). The aim is to quantitatively compute, in real-time, the electrode health indicator discovered in addressing RQ 3.1 in order to detect when the electrode starts to produce low-quality welds because of its degradation process.

Figure 8 reassumes the three research activities carried out during the doctorate and their contextualization within the sustainability-oriented technological innovation framework.

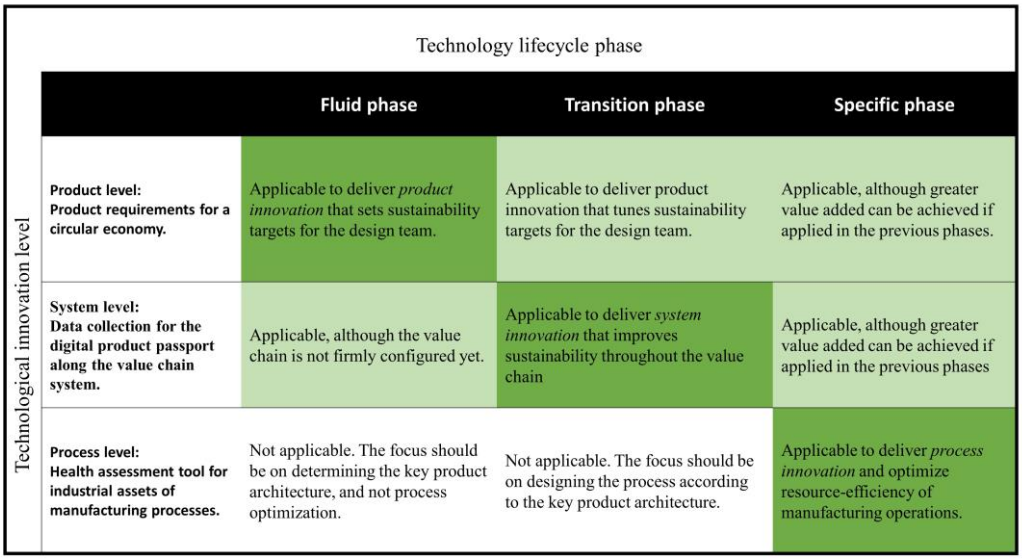


Figure 8: Contextualization of the carried out research activities according to the sustainability-oriented technological innovation framework.

As it is possible to observe, the research carried out to support sustainability oriented product innovation can provide major value added if applied at the onset of a technological trajectory, i.e., during a technological revolution. In fact, in this phase, the early phase of product design (concept design) has greater importance, and product requirements for a CE can represent valuable targets for the development of more resource efficient technologies. However, the developed research activity at product level can be adopted also in the further phases of the technology life cycle.

The research carried out to support sustainability oriented system innovation, instead, finds greater applicability in the second phase of the technology lifecycle, i.e., when the key product architecture emerges and, hence, the corresponding value

chain can be properly optimized. In this phase, the establishment of a digital product passport that enhances value chain transparency can be established. However, the digital product passport can be established also in the other phases, although with reduced benefits: in the first phase, in fact, many different product architectures can arise. In a scenario where product architecture undergoes constant changes, implementing a digital product passport may result in frequent alterations to the stakeholders within the value chain, consequently affecting the participants within the digital product passport. This could result in prohibitively high expenses if the passport is not designed with a flexible structure. Instead, implementing the digital product passport in the last phase of a technology lifecycle can be beneficial, even if implementing it before can provide higher competitive advantage.

Finally, the research carried out to support sustainability oriented process innovation can be applied only in the last phase of a technology lifecycle, because it exclusively provides an incremental improvement of the process resource-efficiency. As explained in the A.U's model, this types of innovation is suitable after that the dominant design has been established, i.e., in the last phase of a technology lifecycle.

Chapter 3

Technological innovation at product level for sustainable manufacturing

3.1 Theoretical background

The previous section highlighted the importance of innovation at product level during the first phases of a technology lifecycle. In fact, more than 80% of a product's environmental impact is determined by the decisions made at the early stages of a product development process [38], and these stages heavily impact the innovation activities at the onset of a technology. Because of this, to address sustainability issues, many research efforts have studied design methods to develop product suitable for a CE [39].

Despite the recognized importance of the CE, its adoption is still quite low, having a significant impact on the environment. Only 8.6% of the 100 billion tons of materials needed annually to fuel our economy in 2020, according to [21], originated from CE business models. This percentage has been on the decline since then, falling to 7.2% in 2022 [22]. This level of circularity is insufficient to achieve the Paris Agreement's climate change goals for reducing $CO_{2,eq}$ emissions [40]. In fact, given these circumstances, an increase in temperature of around 3.2 °C is predicted for this century. However, an increase in circularity adoption to 17% is expected to keep the increase in temperature under 2°C and, hence, satisfy the Paris Agreement's climate change goals [41].

One of the main reasons behind the low CE adoption has been reported to be the lack of suitable tools that support the product design for a CE. Many authors, in fact, have written about its relevance for CE adoption, such as [42] who stated that "*design methods and tools are especially important to support the transition*

towards a CE" or [43] who stressed "*the need to support design decision-making process (also aided by quantitative indicators)*", but the literature is still lacking in this perspective: as recently stated by [44], "*the lack of knowledge on circular product design impedes firms' transition to CE*".

According to [28], the design process of a discrete product can be generally divided into three activities: (i) *conceptual design*, where product ideas are created and assessed, (ii) *system-level design*, where the product architecture is defined by decomposing the product into subsystems and components, (iii) *detailed design*, where the specifications for the geometry, materials, and tolerances of the product's components to be manufactured are defined.

As it will be better detailed in the next section, the literature has tried to support the design process by developing either design guidelines for circular product design or optimization of disassembly and EoL activities to support the design decisions. However, it is worth recognizing that the design process is preceded by two fundamental steps of the product development process: the identification of stakeholders needs and their translation into technical product requirements. A technical requirement consists of a metric and a value. A set of requirements precisely outline measurable details what the product has to do. Thus, the product requirements represent the targets that design team needs to achieve [28]. To date, there has not been any research devoted to quantitatively studying which requirements a product should have to be functional for a CE.

This research aims to overcome these limitations by analysing which requirements a product should have to be suitable for a CE. This is achieved through the creation of a decision-making tool in the form of a decision tree. This decision tree illustrates when a CE business model outperforms a LE model considering both economic and environmental criteria. Moreover, if the CE is the selected model, it further delineates whether the product components should be recycled, remanufactured, or reused. The decision tree provides clear and transparent guidance on the decision rules that must be followed to make the most performing decision. Consequently, the decision rules within the tree can serve as a foundation for establishing product requirements for a CE model.

As shown in Figure 9, the target specifications are commonly set before the concept design process. However, the final specifications are refined and definitely defined once that the product concept is selected. Thus, the decision-making tool,

in a form of a decision tree, aims to support the entire concept development process for the establishment of product requirements for a CE.

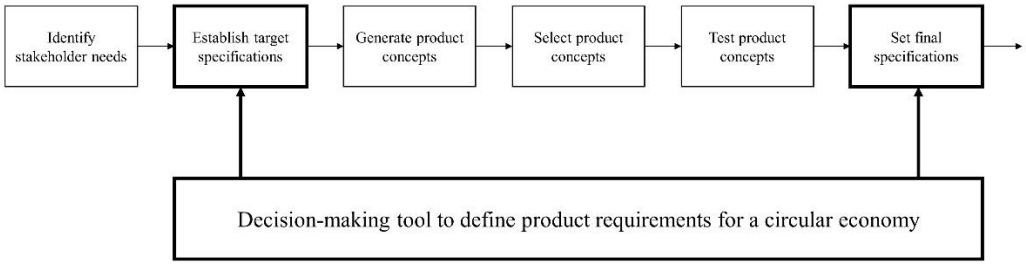


Figure 9. The decision-making tool developed in this research aims to support the definition of product requirements for a CE during the concept development process.

The creation of the decision tree starts with the construction of a mathematical model that encompasses both the LE and CE business models, taking into account their economic and environmental performance. Specifically, the economic performance is quantified by the economic cost involved in the two business models (i.e., LE and CE), while the environmental performance is measured by the $CO_{2,eq}$ emissions connected to the different phases involved in the two business models. Moreover, the $CO_{2,eq}$ emissions are monetized through the application of a carbon tax as already done in other works available in the literature [45]–[47]. In this way, the two performance can be aggregated in a single metric, called total cost, and the mathematical model allows the determination of the business model leading to the minimum total cost. Then, the mathematical model is implemented in MATLAB in order to perform a bi-level computer-based factorial experiment and determine the parameters that mostly affect the response of the mathematical model. This enables the identification of the most important parameters in the selection of the preferable business model and, thus, the parameters that mostly influent the determination of the CE. The most impactful parameters are then used to perform a multi-level computer-based factorial experiment in order to create a multi-scenario dataset. Finally, such dataset is fed to a decision tree algorithm, with the aim of quantitatively defining the decision rules that should be apply to the most important parameters for the determination of the preferable business model. This step allows the identification of product requirements for a CE. It is worth noting that such process is performed both at product level (for the selection between LE and CE)

and at component level (for the selection of recycling, remanufacturing, or reusing strategies, when the CE is the selected business model).

In this way, product requirements for a CE can be identified. They represent the targets that the design team need to meet at the onset of a technological revolution.

Therefore, this research, will allow to answer the following RQ:

1.1 What are the product requirements for a CE?

Furthermore, the impact of the carbon tax on the decision-making process is also investigated, in order to ascertain whether environmental parameters, in addition to economic ones, really influence the choice between a CE or LE business model. This allows to understand when the environmental parameters starts to appear in the decision tree and, thus, become part of the product requirements for a CE. More in detail, carbon tax level curves are created with the aim of identifying the minimum carbon tax value that render the environmental criterion impactful in the decision-making process. This part has the potential to offer quantitative assistance to policy makers as they strive to establish customized carbon tax values tailored to the specific needs of their regions and industries. As it will be shown, these customized values can have a significant impact on achieving substantial reductions in $CO_{2,eq}$ emissions. It offers valuable insights into the influence of carbon tax policies on the product requirements for a CE. Therefore, this research will answer to a second RQ:

1.2 What is the minimum carbon tax value that causes at least one environmental parameter to be included in the product requirements?

As product requirements are primarily addressed in the initial phases of the product development process, this contribution may find greater relevance during the early stages of a technology lifecycle. However, its validity holds true across the entire technology lifecycle.

3.2 Literature analysis

As mentioned above, research on circular product design can be grouped mainly into design guidelines and optimization of disassembly and EoL activities. The literature belonging to these two categories will be described below in two separate Sections.

3.2.1 Guidelines for circular product design

Two remarkable works delve into the foundational principles of circular product design, that are the work of [48] and that of [39]. The former undertook a thorough examination of existing CE terminology and conceived a circular product design model consisting of five key elements: future-proof, disassembly, maintenance, remake, and recycle. Within their analysis, they revised design guidelines associated with each of these elements by providing a valuable support for circular product design. The latter, instead, encompassed the concepts of 'design for product integrity' and 'design for recycling'. While integrating recyclability into product design is important, emphasizing design for maintaining product integrity is even more crucial in safeguarding economic and environmental values. This can be achieved addressing three different design elements: resisting obsolescence (increasing physical durability and emotional durability), postponing obsolescence (enhancing maintenance activity and upgradability opportunities), and reversing obsolescence (increasing repurposing, repairing, refurbishment and remanufacturing activities).

Then, researchers have tried to develop design guidelines to support decisions during the circular product design activity. For example, the work available at [49] formulated design guidelines targeted on recyclability, with the intention of aiding the design team in the creation of more recyclable products. These efforts yielded four key categories of guidelines, addressing concerns like hazardous components, accessibility for removal, recyclable materials, and the facilitation of disconnections. These categories of guidelines were then further elaborated into 14 more specific and practical design recommendations pertaining to design for recycling. Another example is the study available at [50], wherein overarching design guidelines relevant to various CE strategies were compiled. Specifically, they underlined the frequent conflict between guidelines centered on disassembly and those targeted at recycling. Then, the study conducted at [51] examined and categorized the design guidelines originating from various DfX methodologies; they defined a synthesis of eco-design strategies, including design for environment, for remanufacturing, for upgradability, for assembly, for disassembly, for modularity, for manufacturing, and for reliability and relate them with the multiple lifecycle options of reuse, remanufacturing, and recycling. The authors linked the design guidelines with each of these approaches, asserting that the combined implementation of these strategies is crucial for achieving circular design in upcoming products. The same finding has been confirmed also in the work available

at [52], wherein the need of integrating different DfX methodologies to facilitate the transition towards CE was highlighted. They also presented a set of ten guidelines that should be considered within the field of circular product design. Instead, the work [53] linked product attributes with CE strategies through design guidelines that serve as supporting tool for circular product design. Moreover, the work [54] analyzed design guidelines that facilitate CE strategies, encompassing repairing, refurbishing, and remanufacturing; they introduced a structured classification of design guidelines for CE strategy within product design. These guidelines were organized into four principal categories ease of cleaning, ease of diagnosis, disassembly and reassembly, and ease of storage.

As it is possible to note, the literature about guidelines on circular product design is relatively extensive. These works undoubtedly offer valuable support for circular product design activities. However, as already asserted, the CE adoption is still low and with a declining trend. In fact, the design team needs reference targets to be achieved during the design process, but, to date, such quantitative targets (product requirements) are currently missing.

3.2.2 Optimization of disassembly and EoL activities

The second category of works is represented by quantitative works, which provide numerical outcomes aiming to support circular product design, often with a special focus on the disassembly process. For example, the work [55], presented a pair of EoL disassembly diagrams, illustrating both the environmental implications and the cumulative costs associated with the disassembly process of a product. These charts serve distinct purposes: the first supports product design decisions, while the second aids in identifying the optimal stage for disassembly of a product. [56], instead, developed a quantitative framework that assigns time-based numerical indices to various design factors influencing disassembly. These factors encompassed aspects such as the manual force required for disassembly, the precision needed for tool placement, weight, size, materials and shapes of disassembled components, and the use of hand tools, among others. The work [57], then, developed a method to concurrently establish the optimal spatial arrangement of components, locators, and fasteners considering the geometries of individual components and their associated revenues in the recovery process. The overarching objective is to facilitate an economically efficient disassembly process. The work [58], instead, approached the disassembly problem from the perspective of a multi-criteria decision-making problem considering that disassembly process can be influenced by a large number of parameters. They adopted a hybrid approach

integrating design of experiment and the Technique for Order of Preference by Similarity to Ideal Solution (TOPSIS). The primary objective was to establish a disassembly model to compute the disassemblability index for any given pair of components. The work [59] introduced a technique termed "eDiM," which stands for "ease of Disassembly Metric." Their objective was to quantify the time required for disassembly, thereby providing a means to assess the ease of disassembly, facilitate comparisons among different product designs, and gauge recoverability potential. The work [60], finally, introduced a novel approach to design for disassembly by developing a tool known as LeanDfD. The latter is aimed at assisting the design team in implementing redesign strategies to enhance both product de-manufacturability and EoL performances. By employing appropriate indicators, the LeanDfD tool enables a quantitative assessment of the disassemblability and recyclability of mechatronic products.

It is worth noting that the literature relating to quantitative approaches include also works with a broader scope than disassembly. For example, the work [61] developed a design tool known as the EoL Design Advisor (ELDA) aiming at facilitate EoL strategy decisions based on some influential product attributes. The EoL strategies considered in her tool were reuse, service, remanufacture, recycling with assembly, recycling without disassembly, and disposal, while the influential product attributes were wear-out life, technology cycle, level of integration, number of parts, design cycle, and reason for redesign. The decision-making process of the design tool relied on the recycling experiences of designers and product managers of different industries. Another example is represented by the work [62] where a method, known as the Early Design Phase EoL Scenario Evaluation Method (ELSEM), was developed to systematically assess different product EoL options during the initial design phase. ELSEM relied on a multi-criteria decision-making process suitable to deal with the uncertainty and subjectiveness in the early product development stages, i.e. the fuzzy technique for order preference by similarity to ideal solution. A similar approach was adopted also by the work [63] to quantitively assess the sustainability across economic (residual value), environmental (eco-indicator), and social impact (job creation, human toxic potential, and land use) dimensions for each EoL options based on fuzzy logic. The work [64], instead, conducted a study with the objective of enhancing product life extension, through prolonged lifetime, refurbishment, and remanufacturing, as well as product recycling. Guided by the Waste Framework Directive, they identified three primary strategies aligning with product life extension and recycling: prevention, reuse, and

recycling. A key consideration when addressing any of these strategies is the comprehensive definition of a product lifetime, considering both environmental and economic aspects. One of the central challenges lies in determining the optimal application of each product life extension strategy. To address this challenge, the researchers put forth a methodology aimed at quantitatively assessing the ideal product lifetime. Furthermore, the work [65] started with a systematic reorganization of 46 design guidelines through the lens of the CE approach and also introduced novel design guidelines. Such guidelines were then categorized into five key circular design clusters: elongating product lifespan, facilitating disassembly, promoting product and component reuse, and enabling material recycling. Finally, they introduced a methodology designed to quantitative evaluate the alignment of an existing product design with the CE principles, by computing the degree of circularity of a product design.

All these works offer valuable tools to enhance various aspects of the CE, often with a notable emphasis on disassembly characteristics related to disassembly cost. However, no work addresses the issue to analyze the reference values for the disassembly cost that render the CE model more convenient than the LE. Furthermore, no work establishes reference values for what concerns the product quality, although is recognized as one of the main parameters affecting the implementation of the CE. This work addresses such issue by studying the product requirements that render the CE paradigm more convenient than the LE one. Such product requirements serve as the targets for the design team during their innovation activities.

3.3 Methodology

The traditional methods of product design and development focused on creating products that meet customer needs with the required quality and at lowest production cost and time [28]. However, considering the environmental crise that human population is currently experiencing, it is imperative to broaden the scope of product development beyond customer needs by integrating also the environmental ones. Therefore, the principles of a CE must be integrated into the development of manufactured products since the early phases of a technological innovation. The classical model of a product life cycle, which includes *sourcing*, *transformation*, *assembly*, *product use*, and *product EoL* [48], [66], [67], is used to define the problem of the current analysis, as depicted in Figure 10**.**

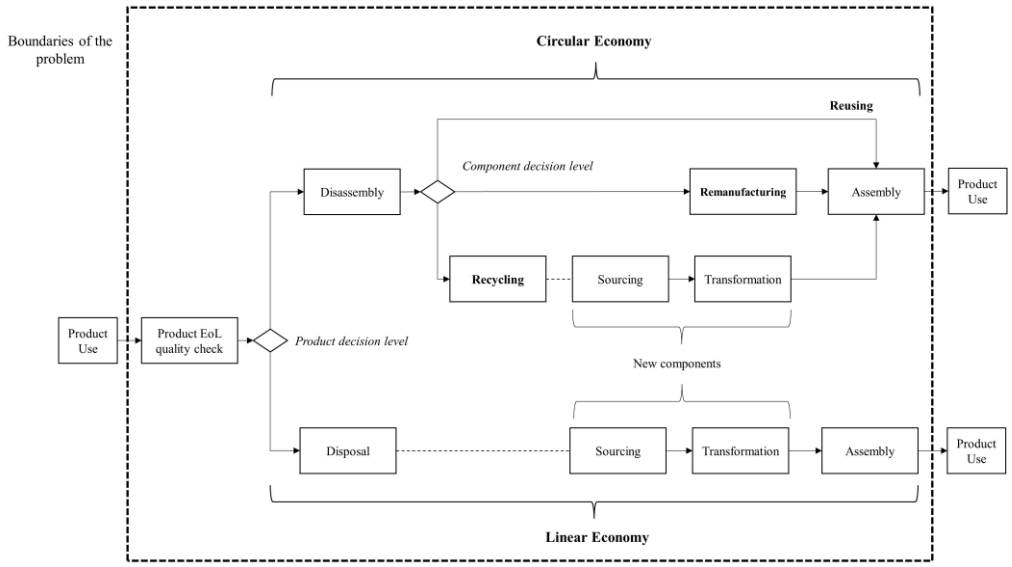


Figure 10. Life cycle model considered in this work.

The diagram outlines the process when a manufacturing company takes back its products (multi-component products) after use, i.e. when they have reached their EoL. Once products received, these go through a quality check to assess their condition (as well as the components they are made of). This can be done visually by human operators or through advanced technologies such as image recognition software or data from sensors embedded in the products. At this point, the decision on whether an LE or CE business model should be adopted needs to be taken.

In the LE model, the product is disposed in a landfill and to then be reproduced in new form: raw materials and/or components are purchased (*sourcing*), those materials are eventually transformed into components (*transformation*), which are then assembled (*assembly*), together with components purchased in the *sourcing* phase (if any), to create the final product.

In the CE model, the product needs to be disassembled into its different components. At this stage, each component should be either recycled, remanufactured, or reused. If a component is recycled, a new one needs to be produced through the *sourcing* and *transformation* phases described above. However, if a component is remanufactured, it needs to be restored to its nominal level of quality. If the component exhibits a quality equal to its nominal level, it can be reused directly. The new components, remanufactured and reused alike, are then assembled to form the final product. Notably, it is assumed that all the components

are recyclable and recoverable, with recovered components being restored to the same quality level as that of an entirely new product.

As it will be explained in the next section, these decisions are driven by economic and environmental criteria: the decision of whether to apply an LE or CE business model aims to minimize the sum of the economic and environmental criteria (with the latter considered in terms of $CO_{2,eq}$). Specifically, the environmental impact is monetized through the carbon tax implementation so that both economic cost and carbon footprint can be expressed in monetary terms and, hence, with a unique metric, total cost.

A systematic approach has been adopted to develop the analysis. Initially, a mathematical model is formulated to assess both the economic and environmental performance of each business model, i.e., the LE and the CE. This requires to express the total cost of each business model as a function of the performance (economic and environmental) of the product life cycle phases identified in Figure 9. The comparison of each business model's total cost represents the response of the mathematical model, i.e., the business model that leads at the lowest total cost. Once that the mathematical model is defined, the investigation of the most impactful model parameters must be performed. Thus, the mathematical model is implemented in MATLAB and a series of computer-based experiments are performed as follows. Specifically, a 2-levels factorial experiment is performed where all the model parameters vary on their two extreme values, and the response of the mathematical model is observed. Then, the impact of each model parameter is evaluated by means of the main effects and interaction plots. After such evaluation, model parameters that show no impact are held constant, assuming the mean value between their two extreme admissible values. Conversely, model parameters that influence the response are varied at multiple levels to carry out a new computer-based multi-level factorial experiment. The goal of this new experiment is to create a multi-scenario dataset corresponding to many different combinations of the values of the most impactful parameters. Finally, such dataset is processed with a Machine Learning (ML) algorithm, specifically a decision tree algorithm, to develop a decision-making tool that aid manufacturing organizations in establishing product requirements for a CE. It is worth noting that this systematic procedure is performed two distinct times: one at product level (to select LE or CE), and another one at component level (to select recycling, remanufacturing, or reusing). Furthermore, the effect of the carbon tax on the decision-making process and, thus, on the product requirements for a CE, is investigated. In this case, carbon tax level curves are built in order to evaluate the minimum carbon tax value that

make the environmental criterion impactful, and, hence, make at least one environmental parameter belonging to the set of product requirements for a CE. The adopted methodology is detailed in the following.

3.3.1 Mathematical model

To ensure the generality of the mathematical model, it is formulated to account for a generic product composed of n components (indexed as i for the i-th component). Additionally, for enhanced flexibility, each economic input parameter is represented as a fraction of the overall product manufacturing cost ($c_{product}$), denoted as rc_x, with the subscript x referring to the specific product life cycle phase considered (e.g., assembly, transformation, etc.). Similarly, each environmental input parameter is expressed as a fraction of the carbon footprint of product manufacturing ($cf_{product}$) and denoted as rc_x, with x signifying the respective product life cycle phase considered. To clarify further, $c_{product}$ and $cf_{product}$ pertain to the cost and carbon footprint associated with the product manufacturing, respectively, which encompasses the aggregation of sourcing, transformation, and assembly phases, as discussed earlier. It is essential to differentiate $c_{product}$ from the selling price, as they are distinct concepts in this context.

Before providing the mathematical formulation for the two business models, the notation adopted in this study is reported in the following Tables (Table 1 for the model variables and Table 2 for the model parameters).

Table 1: Model variables.

Model variable	Description	Units of measure
tc_{LE}	Total cost of linear economy paradigm	€
tc_{CE}	Total cost of circular economy paradigm	€
$tc_{product}$	Total cost of product manufacturing	€

$c_{disposal}$	Cost of product disposal	€
$cf_{disposal}$	Carbon footprint of product disposal	ton $CO_{2,eq}$
$tc_{disposal}$	Total cost of product disposal	€
$c_{disassembly}$	Cost of product disassembly	€
$cf_{disassembly}$	Carbon footprint of product disassembly	ton $CO_{2,eq}$
$tc_{disassembly}$	Total cost of product disassembly	€
$c_{assembly}$	Cost of product assembly	€
$cf_{assembly}$	Carbon footprint of product assembly	ton $CO_{2,eq}$
$tc_{assembly}$	Total cost of product assembly	€
$c_{sourcing,i}$	Cost of sourcing of i-th raw material/component	€
$cf_{sourcing,i}$	Carbon footprint of sourcing of i-th raw material/component	ton $CO_{2,eq}$
$tc_{sourcing,i}$	Total cost of sourcing of i-th raw material/component	€
$c_{trasnformation,i}$	Cost of transformation of i-th raw material/component	€
$cf_{trasnformation,i}$	Carbon footprint of transformation of i-th raw material/component	ton $CO_{2,eq}$
$tc_{trasnformation,i}$	Total cost of transformation of i-th raw material/component	€

$tc_{reusing,i}$	Total cost of reusing the i-th component	€
$tc_{remanufacturing,i}$	Total cost of remanufacturing the i-th component	€
$tc_{selling,i}$	Total cost of selling the i-th used component to recycler	€
$tc_{recycling,i}$	Total cost of recycling the i-th component	€

Table 2: Model parameters.

Input parameter	Description	Units of measure
$c_{product}$	Cost of product manufacturing	€
$cf_{product}$	Carbon footprint of product manufacturing	ton $CO_{2,eq}$
ct	Carbon tax	€/ ton $CO_{2,eq}$
n	Number of components	-
$rc_{disposal}$	Relative cost of product disposal	-
$rcf_{disposal}$	Relative carbon footprint of product disposal	-
$rc_{disassembly}$	Relative cost of product disassembly	-
$rcf_{disassembly}$	Relative carbon footprint of product disassembly	-

$rc_{assembly}$	Relative cost of product assembly	-
$rcf_{assembly}$	Relative carbon footprint of product assembly	-
cqi_i	Component quality index of the i-th component	-
$rc_{sourcing,i}$	Relative cost of sourcing of the i-th item	-
$rcf_{sourcing,i}$	Relative carbon footprint of sourcing of the i-th item	-
$rc_{transformation,i}$	Relative cost of transformation of the i-th item	-
$rcf_{transformation,i}$	Relative carbon footprint of sourcing of the i-th item	-
α_i	Multiplicative factor of remanufacturing cost of the i-th item	-
β_i	Multiplicative factor of remanufacturing carbon footprint of the i-th item	-
γ_i	Ratio between the selling price of scrap to recycler and its purchasing cost of the i-th item	-

Linear economy paradigm

As it can be seen from Figure 10, the LE business model is considered as followed: after the product quality check, the product is *disposed* in landfill and a new product needs to be fabricated from scratch going through the *sourcing*, *transformation*, and *assembly* phases as already described above. To each of these phases is associated both an economic cost and an environmental one, leading to the total cost tc_{LE} expressed as following:

$$tc_{LE} = tc_{disposal} + tc_{product} = tc_{disposal} + tc_{sourcing} + tc_{transformation} + tc_{assembly} \quad (1)$$

The different phases will be now described in detail.

Disposal

The phase *product disposal* refers to the product discard in landfill, encompassing any associated transportation contribution. The cost of disposal $c_{disposal}$ and its associated carbon footprint $cf_{disposal}$ are computed respectively by referring to the relative cost of product disposal $rc_{disposal}$ and to the relative carbon footprint of product disposal $rcf_{disposal}$ as follows:

$$c_{disposal} = rc_{disposal} \cdot c_{product} \quad (2)$$

$$cf_{disposal} = rcf_{disposal} \cdot cf_{product} \quad (3)$$

The total cost of disposal $tc_{disposal}$ is the sum of the economic cost and the environmental cost defined as follows:

$$tc_{disposal} = rc_{disposal} \cdot c_{product} + ct \cdot rcf_{disposal} \cdot cf_{product} \quad (4)$$

Sourcing

The phase *sourcing* refers either to the acquisition of raw materials that need further transformation to create components or to the direct acquisition of outsourced components, encompassing any associated transportation contribution. The cost of sourcing $c_{sourcing}$ and its carbon footprint $cf_{sourcing}$ is obtained by summing the cost and carbon footprint of each raw material/component i, respectively.

$$c_{sourcing} = \sum_{i=1}^{n} c_{sourcing,i}, \quad (5)$$

$$cf_{sourcing} = \sum_{i=1}^{n} cf_{sourcing,i}, \quad (6)$$

The economic cost and the carbon footprint of sourcing each raw material/component i are evaluated through the relative cost of sourcing $rc_{sourcing,i}$ and the relative carbon footprint of sourcing $rcf_{sourcing,i}$, respectively.

$$c_{sourcing,i} = rc_{sourcing,i} \cdot c_{product}, \qquad \forall i \in n \tag{7}$$

$$cf_{sourcing,i} = rcf_{sourcing,i} \cdot cf_{product}, \qquad \forall i \in n \tag{8}$$

The total cost of sourcing $tc_{sourcing}$ is hence the sum of the economic cost and the environmental cost for all the acquired raw materials/components n needed to create the product.

$$tc_{sourcing} = c_{product} \cdot \sum_{i=1}^{n} rc_{sourcing,i} + ct \cdot cf_{product} \cdot \sum_{i=1}^{n} rcf_{sourcing,i} \tag{9}$$

Transformation

The phase *transformation* refers to any transformation that the company applies to the acquired raw materials/components. The total cost of transformation $tc_{transformation}$ is the sum of the economic cost $c_{transformation}$ and the environmental cost of its carbon footprint $cf_{transformation}$ for all the transformed raw materials/components; each of them can be computed in relative terms as done for the sourcing phase through the parameters $rc_{transformation,i}$ and $rcf_{transformation,i}$.

$$c_{transformation} = \sum_{i=1}^{n} c_{transformation,i}, \tag{10}$$

$$cf_{transformation} = \sum_{i=1}^{n} cf_{transformation,i}, \tag{11}$$

$$c_{transformation,i} = rc_{transformation,i} \cdot c_{product}, \tag{12}$$

$$cf_{transformation,i} = rcf_{transformation,i} \cdot cf_{product}, \tag{13}$$

$$tc_{transformation} = c_{product} \cdot \sum_{i=1}^{n} rc_{transformation,i} + ct \cdot cf_{product} \cdot \sum_{i=1}^{n} rcf_{transformation,i} \tag{14}$$

Assembly

The phase *product assembly* refers to the process of components assembling to get the final product. The total cost of product assembly $tc_{assembly}$ is computed by considering the economic cost $c_{assembly}$ and its carbon footprint $cf_{assembly}$. Each of them is assessed in relative terms through $rc_{assembly}$ and $rcf_{assembly}$, respectively.

$$c_{assembly} = rc_{assembly} \cdot c_{product} \tag{15}$$

$$cf_{assembly} = rcf_{assembly} \cdot cf_{product} \tag{16}$$

$$tc_{assembly} = c_{product} \cdot rc_{assembly} + ct \cdot cf_{product} \cdot rcf_{assembly} \tag{17}$$

Circular economy model

According to Figure 10, the CE business model is composed of the following phases: after the product quality check, the product is *disassembled* into its components and new decisions need to be made at component-level. Specifically, each component *i* can be either *reused, remanufactured,* or *recycled.* The CE strategy selected per each component is the one characterized by the lowest total cost. After having collected all the needed components, these need to be *assembled* together to get the final product. The formulation of the total cost of circular economy tc_{CE} is expressed as follows:

$$tc_{CE} = tc_{disassembly} + \sum_{i=1}^{n} \min\{tc_{reusing,i}, tc_{remanufacturing,i}, tc_{recycling,i}\} + tc_{assembly} \tag{18}$$

Each phase is detailed below.

Disassembly

The phase *product disassembly* is the deconstruction of the product in its components. The total cost of product disassembly $tc_{disassembly}$ is computed by summing the economic cost $c_{disassembly}$ and the cost associated to its carbon footprint $cf_{disassembly}$. Each of them is assessed in relative terms respectively through $rc_{disassembly}$ and $rcf_{disassembly}$.

$$c_{disassembly} = rc_{disassembly} \cdot c_{product} \tag{19}$$

$$cf_{disassembly} = rcf_{disassembly} \cdot cf_{product} \tag{20}$$

$$tc_{disassembly} = c_{product} \cdot rc_{disassembly} + ct \cdot cf_{product} \cdot rcf_{disassembly} \tag{21}$$

Reusing

This work considers that the CE business model regenerates a product to the same quality level as a new one. Because of this, a component can be reused only if its quality level is equal to the nominal level. As done in the literature [68], [69], the quality of a component can be represented by a numeric index ranging from 0 (fully damaged) to 1 (fully performing). Hence, an input parameter named component quality index cqi_i is defined to represent the quality of a component. In this case, the reusing option is permissible only when the quality of a component is entirely preserved (i.e. $cqi_i = 1$). This leads to a total cost $tc_{reusing,i}$ that is null since no actions are needed.

$$\begin{cases} tc_{reusing,i} = 0, \ if \ cqi_i = 1. \\ tc_{reusing,i} = \emptyset, \ otherwise. \end{cases} \tag{22}$$

Remanufacturing

The phase *remanufacturing* refers to restoring the used component to its nominal quality level [70]. The total cost of remanufacturing the i-th component $tc_{remanufacturing,i}$ can be computed by referring to the total cost of creating the i-th new component as done in the literature [68]. The literature, in fact, assumes that

the economic cost of remanufacturing a component depends on the economic cost of manufacturing a new one. More in details, the literature assumes a linear relationship which is linked to the quality of the component. Hence, according to the literature, the cost of remanufacturing a component can vary between 0% and 100% of the cost of a new component [68], [71]. The present work assumes a linear relationship as well, but, to make the model more flexible, we consider that the economic cost of remanufacturing a component can be higher than 100% of the economic cost of creating a new one, and we express its maximum through the parameter α_i. The same relationship and assumptions are made for the environmental cost, where β_i takes the place of α_i.

$$tc_{remanufacturing,i} = \alpha_i \cdot c_{product} \cdot \left(rc_{sourcing,i} + rc_{transformation,i}\right) \cdot (1 - cqi_i) + \beta_i \cdot ct \cdot cf_{product} \cdot \left(rcf_{sourcing,i} + rcf_{transformation,i}\right) \cdot (1 - cqi_i), \quad \forall i \in n \tag{23}$$

Note that if $cqi_i = 1$, then $tc_{remanufacturing,i} = 0$, and the component can be reused.

Recycling

The phase recycling refers to sell to recyclers the component. This implies two main consequences. First, earning a profit from the sale of the scrap, which can be represented as percentage of the cost of sourcing through the parameter γ_i, encompassing any associated transportation contribution. Second, sending to recycler a component means the need of creating a new one from scratch (and hence going through the sourcing and transformation phases described above). Thus, the total cost of component recycling can be expressed as follows.

$$tc_{recycling,i} = tc_{selling,i} + tc_{sourcing,i} + tc_{transformation,i} = -\gamma_i \cdot c_{product} \cdot rc_{sourcing,i} + c_{product} \cdot \left(rc_{sourcing,i} + rc_{transformation,i}\right) + ct \cdot cf_{product} \cdot \left(rcf_{sourcing,i} \cdot + rcf_{transformation,i}\right), \ \forall i \in n \tag{24}$$

Definition of the class variables

As previously stated, two different types of analysis are conducted, one at product level and another one at component level. Therefore, it is necessary to create two different class variables.

The product-level decision that the company must accomplish is the one with the lowest total cost between LE and CE. Therefore, it is possible to define a class variable, called product decision class pdc, as follows.

$$pdc = \begin{cases} 0 & if\ tc_{CE} \leq tc_{LE} \\ 1, & otherwise. \end{cases} \tag{25}$$

Similarly, the component-level decision that the company must accomplish is the one with the lowest total cost between reusing, remanufacturing and recycling. Since reusing option only depends on the quality of component, the component-level decision needs to be performed between remanufacturing and recycling only. Thus, it is possible to define a class variable, called component decision class cdc, as follows.

$$cdc = \begin{cases} 0 & if\ tc_{remanufacturing,i} \leq tc_{recycling,i},\ \forall i \in n \\ 1, & otherwise. \end{cases} \tag{26}$$

Model constraints

The mathematical model is subjected to a set of constraints, mainly related to the limit values that the input parameters can assume.

The cost of product manufacturing is considered ranging from 1 € and 500 €. As described above, this coincides with the aggregated cost of sourcing, transformation and assembly operations and not with the selling price.

$$1 \leq c_{product} \leq 500 \tag{27}$$

The carbon footprint of product manufacturing relating to consumer products considered in this work can vary between 0.01 ton $CO_{2,eq}$ up to 0.500 ton $CO_{2,eq}$ [72]. Also in this case, the carbon footprint of product manufacturing refers to the aggregated carbon footprint of sourcing, transformation, and assembly operations.

$$0.01 \leq cf_{product} \leq 0.500 \quad (28)$$

According to [73], carbon tax values can vary between less than 1 € per each ton $CO_{2,eq}$, up to almost 140 €, and therefore we round up the values as described in the following constraint.

$$1 \leq ct \leq 140 \quad (29)$$

As discussed above, only multi-components products are considered. In this work, based on experience and discussion with practitioners, it is assumed that a product can be composed of maximum 50 components. Therefore, the following constraint applies to the number of components n.

$$2 \leq n \leq 50 \quad (30)$$

The relative cost of sourcing for each item $i \in n$ can potentially vary between 0 and 1, with extreme values excluded. The same constraint applies to the relative carbon footprint of sourcing.

$$0 < rc_{sourcing,i} < 1 \quad (31)$$

$$0 < rcf_{sourcing,i} < 1 \quad (32)$$

The relative cost of transformation for each item $i \in n$ can potentially vary between 0 (included) and 1 (excluded). The case equal to 0 represents the situation in which the company acquires outsourced components and assembly them to create a product without perform any transformation. The same constraint applies to the relative carbon footprint of transformation.

$$0 \leq rc_{transformation,i} < 1 \quad (33)$$

$$0 \leq rcf_{transformation,i} < 1 \quad (34)$$

The relative cost of product assembly can vary between 0 (excluded), when the cost of assembly is negligible, and 0.50 [74], [75]. The same constraint can be applied to the relative carbon footprint of assembly.

$$0 < rc_{assembly} \leq 0.50 \quad (35)$$

$$0 < rcf_{assembly} \leq 0.50 \quad (36)$$

The economic costs of sourcing, transformation and assembly ($c_{sourcing}$, $c_{transformation}$ and $c_{assembly}$, respectively) concur to the economic cost of product manufacturing $c_{product}$, and therefore the sum of the corresponding relative costs need to be equal to one.

$$\sum_{i=1}^{n}\left(rc_{sourcing,i} + rc_{transformation,i}\right) + rc_{assembly} = 1 \quad (37)$$

The same type of constraint applies also for what concerns the relative carbon footprint of sourcing, transformation, and assembly.

$$\sum_{i=1}^{n}\left(rcf_{sourcing,i} + rcf_{transformation,i}\right) + rcf_{assembly} = 1 \quad (38)$$

The component quality index cqi_i can vary between 0 (fully damaged) and 1 (fully performing), [68], [76]:

$$0 \leq cqi_i \leq 1 \quad (39)$$

The relative cost of product disassembly $rc_{disassembly}$ can vary between 0 excluded, when the cost is negligible, and an upper limit. The value of the upper limit is unknown in the literature. However, based on experience and on discussions with practitioners, it is reasonable to assume the same upper limit as for the relative cost of assembly. The same constraint is applied to the relative carbon footprint of disassembly $rcf_{disassembly}$.

$$0 < rc_{disassembly} \leq 0.50 \quad (40)$$

$$0 < rcf_{disassembly} \leq 0.50 \quad (41)$$

The literature also lacks data on the relative cost of product disposal $rc_{disposal}$. Again, through discussions with practitioners, it was decided to apply the same variation as the relative cost of product disassembly $rc_{disassembly}$. The same constraint is applied to the relative carbon footprint of product disposal $rcf_{disposal}$.

$$0 < rc_{disposal} \leq 0.50 \quad (42)$$

$$0 < rcf_{disposal} \leq 0.50 \quad (43)$$

The multiplicative factor of the relative cost of remanufacturing α_i can vary between 1 and 3 based on authors experience and from discussions with practitioners. The same constraint applies for the multiplicative factor of the relative carbon footprint of remanufacturing β_i.

$$1 \leq \alpha_i \leq 3 \quad (44)$$

$$1 \leq \beta_i \leq 3 \quad (45)$$

The ratio between the selling price of the scrap to recyclers and the cost of sourcing a new item can vary between 0 excluded (if the profit from recycling is negligible), and 0.6 (according to authors experience and from discussions with practitioners).

$$0 < \gamma_i \leq 0.6 \quad (46)$$

3.3.2 Bi-level computer-based factorial experiment

The second step of the methodology deals with the evaluation of whether or not all the model parameters (Table 2) affect the model response. Therefore, the mathematical model is implemented in MATLAB and a bi-levels computer-based factorial experiment is performed.

A factorial experiment involves to investigate all possible combinations of the independent variables' levels. When dealing with multiple independent variables, a factorial experiment is regarded to be more efficient than the traditional one wherein the independent variables' levels vary one at a time. In fact, the purpose of a factorial experiment is to systematically investigate the effects of multiple independent variables (model parameters) on a dependent variable (model response). This is usually performed through the analysis of the main effects plot and interactions plot. A main effect plot is a graphical representation used to visualize the impact of individual independent variables (model parameters) on a dependent variable (model response), while keeping the other model variables

constant at specific levels. Each independent variable is typically plotted on the x-axis, and its corresponding effect is shown on the y-axis. To show how changes in the levels of each independent variable affect the outcome of the dependent variable, the plot typically consists of a line. This makes it easy to understand the relative importance of the independent variables in the experiment. An interaction plot, instead, allows to visualize the interaction effects between two or more independent variables (model parameters) on a dependent variable (model response). Interaction effects occur when the impact of one independent variable on the dependent variable varies depending on the level of another independent variable [77].

The factorial experiment in this research was conducted on two levels, where the values assumed by each input parameter coincided with their admissible extreme values according to the constraints described above and reported for convenience in Table 3. It is worth mentioning that all the component-related input parameters are assumed to follow a triangular distribution of cardinality n with the lower and upper limits equal to the admissible values and with the peak of each distribution that can vary within the allowed domain. The choice of the triangular distribution is due to the fact that it is often employed in business simulation whose distribution is unknown [78], [79].

Table 3: Values adopted for the 2-levels computer-based factorial experiment.

Model parameter	Values	Units of measure	Reference
$c_{product}$	[1, 500]	€	Authors experience and discussions with practitioners.
$cf_{product}$	[0.01, 0.5]	ton $CO_{2,eq}$	[72]
ct	[1, 140]	€/ ton $CO_{2,eq}$	[73]

n	[2, 50]	-	Authors experience and discussions with practitioners.
$rc_{disposal}$	[10e-06[1], 0.5]	-	Authors experience and discussions with practitioners.
$rcf_{disposal}$	[10e-06[1], 0.5]	-	Authors experience and discussions with practitioners.
$rc_{disassembly}$	[10e-06[1], 0.5]	-	Authors experience and discussions with practitioners.
$rcf_{disassembly}$	[10e-06[1], 0.5]	-	Authors experience and discussions with practitioners.
$rc_{assembly}$	[10e-06[1], 0.5]	-	[74], [75]
$rcf_{assembly}$	[10e-06[1], 0.5]	-	Authors experience and discussions with practitioners.
cqi_{peak}	[0, 1]	-	[68], [76]
$rc_{sourcing,peak}$	[10e-06[1], 1)	-	Authors experience and discussions with practitioners.
$rcf_{sourcing,peak}$	[10e-06[1], 1)	-	Authors experience and discussions with practitioners.

[1] A value of 10e-06 has been assigned to represent the case of 0 excluded.

[1] A value of 10e-06 has been assigned to represent the case of 0 excluded.

$rc_{transformation,peak}$	[0, 1)	-	Authors experience and discussions with practitioners.

Note that for what concerns the second analysis (that dealing with the selection of the optimal CE strategy at component-level), the input parameters $rc_{disposal}$, $rcf_{disposal}$, $rc_{disassembly}$, $rcf_{disassembly}$ were not considered in the 2 levels analysis because they do not take part in the decision-making process (they only affect the choice of the suitable paradigm at the product-level).

After the execution of the bi-level computer-based experiments, both at product level and component level, the main effects plot and the interaction plot were analysed.

3.3.3 Multi-level computer-based factorial experiment

After performing the main effects and interaction plots, the model parameters with a negligible impact on the model response (the product decision class at product level, and the component decision class at component level) were excluded from the subsequent analyses. Conversely, the model parameters influencing the determination of the model response were selected for the further analyses.

Thus, a new multi-level factorial experiment was performed with the purpose of generating the datasets necessary for training the decision tree algorithms in the subsequent step. Parameters found to have no impact on the model response were kept constant in this new experiment, assuming the mean value between their two admissible values reported in Table 3. Instead, model parameters that influenced the determination of the model response were varied at multiple levels. The extreme values remained the same as listed in Table 3 and additional intermediate values were considered. Specifically, each selected model parameter was varied over four different levels evenly spaced. By following this approach, a dataset comprising 4,194,304 scenarios was generated at product level (for the choice between LE or CE), and another dataset of 65,536 scenarios was generated at component level (for the choice between remanufacturing and recycling, if CE is the selected business model).

3.3.4 Decision tree

This step involves the utilization of a decision tree algorithm both at product level and at component level to obtain two easy-to-use decision-making tools that assist practitioners in the determination of product requirements for a CE. The decision tree algorithm is a supervised classification technique that predicts the class to which an item belongs based on a given set of features [80], [81]: in this case, the set of features consists of the non-negligible model parameters derived from the second step of the discussed methodology, and used in the multi-level computer-based experiment for the generation of the multi-scenario dataset, while the class variables are pdc and cdc. The choice of adopting a decision tree algorithm is to be found on its user-friendly nature, as the predicted class can be easily and quickly identified by evaluating only few input parameters. This is regarded to effectively support the design team in the product development process. To ensure the necessary user-friendliness, as well as to avoid overfitting issues during tree generation, the decision tree was pruned to maintain a maximum tree depth of four levels [82]. Detailed information about the decision tree algorithm can be found in the literature [83], [80].

To evaluate the accuracy of the decision-making tools, the decisions suggested were evaluated considering four key performance indicators (KPIs) related to the leaves of the trees, i.e. the accuracy of the leaf (a), the percentage of predictions in the leaf (p), the average percentage total cost loss encountered when the decision-making tool suggests the wrong option (tcl), and the average percentage total cost savings achievable when the decision-making tool suggests the correct decision (tcs). The definitions of these KPIs are provided in the following.

The accuracy of each leaf (a) can be calculated as follows:

$$a = \frac{CP_{leaf}}{CP_{leaf} + WP_{leaf}} \cdot 100 \tag{47}$$

where e CP_{leaf} represents the number of correct predictions made by each leaf and WP_{leaf} the number of wrong predictions.

The percentage of predictions in each leaf (p) is considered as follows:

$$p = \frac{TP_{leaf}}{TP_{tree}} \cdot 100 \tag{48}$$

where TP_{leaf} is the total number of predictions in the leaf and (TP_{tree}) is the total number of predictions in the tree.

The average percentage total cost loss encountered when the decision-making tool suggests the wrong option (tcl) is computed as follows:

$$tcl = \frac{\sum_{k=1}^{WP_{leaf}} \frac{tc_{WP,k} - tc_{CP,k}}{tc_{CP,k}}}{WP_{leaf}} \cdot 100 \quad (49)$$

where tc_{WP} represents the total cost of the wrong prediction, and tc_{CP} stands for the total cost of the correct decision.

Finally, the average percentage total cost saving for each leaf (tcs) is calculated as follows:

$$tcs = \frac{\sum_{k=1}^{CP_{leaf}} \frac{tc_{WP,k} - tc_{CP,k}}{tc_{WP,k}}}{CP_{leaf}} \cdot 100 \quad (50)$$

3.3.5 Carbon tax level curves

The mathematical model developed in the previous section deals with two different criteria, i.e. the economic and environmental criteria. Each criterion has an importance that depends on the corresponding weight, i.e. the cost of product $c_{product}$ for the economic criterion, and the algebraic product between the carbon footprint and the carbon tax $cf_{product} \cdot ct$ for the environmental one. The cost of product manufacturing $c_{product}$ and the carbon footprint of product manufacturing $cf_{product}$ rely just on the manufacturing company capabilities of creating products that are economically and environmentally affordable. The carbon tax ct, instead, is an external factor for manufacturers, and its value can alter the importance of the environmental criterion.

In this analysis, it is investigated how the carbon tax can alter the importance of the environmental criterion of the mathematical model. Specifically, this analysis aims to understand which is the minimum value that the carbon tax should assume to make at least one environmental parameter influencing the model response.

The Pareto rule is leveraged to discriminate whether or not the environmental criterion affects the model response. The Pareto Rule, also known as the 80/20 rule, is a principle that suggests that a significant portion of the effects (typically 80%) comes from a relatively small number of causes (typically 20%) [84]. In this analysis, the Pareto rule is applied to the relative importance of the model parameters computed by the Minimum Redundance Maximum Relevance (MRMR) algorithm [85], [86]. The latter allows to identify a set of features that are both maximally dissimilar from one another and highly effective in representing the response variable [86]. The algorithm identifies the best set S of parameters that maximizes V_S, the relevance of S concerning the response variable y, and minimizes W_S, the redundancy of S.

V_S and W_S are defined using the mutual information I:

$$V_S = \frac{1}{|S|}\sum_{x\epsilon S} I(x,y) \tag{51}$$

$$W_S = \frac{1}{|S|^2}\sum_{x,z\ \epsilon S} I(x,z) \tag{52}$$

$|S|$ is the cardinality of S, x and z are two generic parameters belonging to the parameters set, i.e., model parameters listed in Table 2. For each parameter, the algorithm computes the mutual information quotient MIQ_x, which is used to determine the most important parameters.

$$MIQ_x = \frac{V_x}{W_x} \tag{53}$$

V_x and W_x are the relevance and redundancy of a parameter:

$$V_x = I(x,y) \tag{54}$$

$$W_x = \frac{1}{|S|}\sum_{z\ \epsilon S} I(x,z) \tag{55}$$

MIQ_x can be used to rank parameters through an importance score. In this way, the Pareto rule can be applied on the importance scores and understand which are the most important parameters on the determination of the model response. The MRMR algorithm was implemented in MATLAB.

The key idea is to alter the carbon tax value until when the relative importance of one environmental parameter is included in the cumulative importance of 80%. Thus, the minimum value that the carbon tax should assume to make the environmental criterion influencing the model response is the value such that at least one environmental input parameter is included in the cumulative importance of 80%. However, as it will be better explained during the presentation of the results, this value depends on values assumed by the cost of product $c_{product}$ and by the carbon footprint $cf_{product}$, and therefore a unique value of carbon tax cannot be defined. In the light of this, it is possible to develop carbon tax level curves which allow to depict the different minimum carbon tax values depending on the cost of product $c_{product}$ and on the carbon footprint $cf_{product}$.

To develop such carbon tax level curves, a series of bi-levels computer-based factorial experiments were carried out, where the values of product manufacturing cost $c_{product}$ and of product manufacturing carbon footprint $cf_{product}$ were kept fixed, while the carbon tax value ct varied until the above-mentioned condition was met. Such procedure was repeated for different combinations of $c_{product}$ and $cf_{product}$; in this way, it was possible to develop the carbon tax level curves representing, for different combinations of product manufacturing cost $c_{product}$ and of product manufacturing carbon footprint $cf_{product}$, the minimum carbon tax values ensuring that at least one environmental input parameter influences the model response.

3.4 Results and discussion

In this Section the results from the application of the methodology are presented and discussed. Specifically, three different sub-sections are reported, one for the application of the methodology at product level, one for the application of the methodology at component level, and another one for the development of the carbon tax level curves to investigate the role of carbon tax.

3.4.1 Decision-making tool at product level

The first step involved the implementation of the mathematical model in MATLAB to perform a bi-levels computer-based factorial experiment. The resulting main effects plot are displayed in Figure 11.

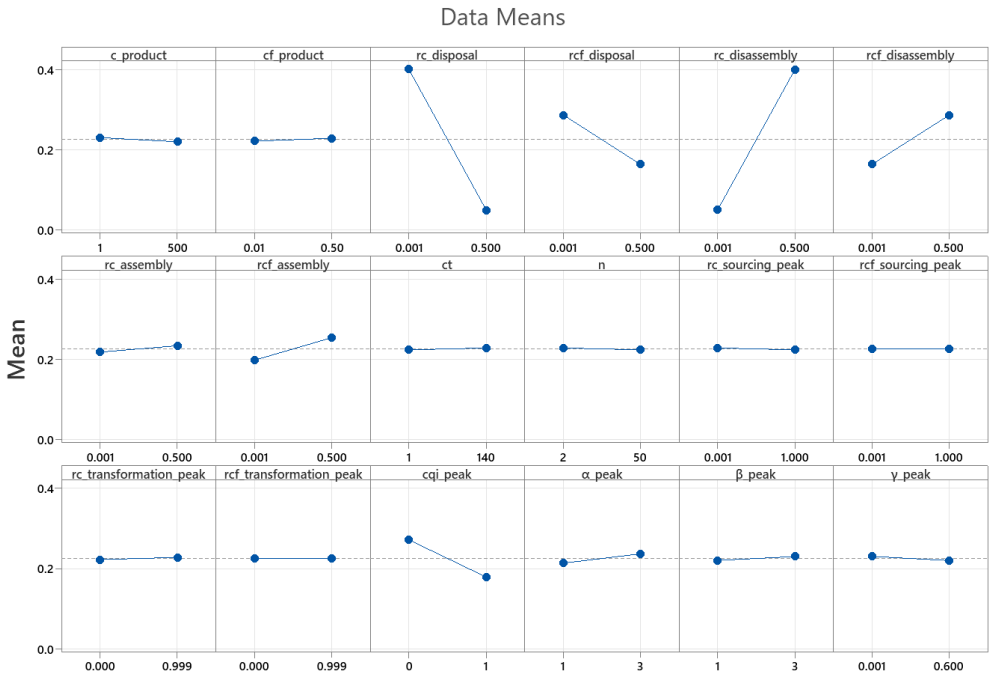


Figure 11: Main effects plot at product level; in the y-axis the class value for the product decision class is reported ('0' stands for CE and '1' for LE).

As it can be seen from the Figure, five model parameters clearly impact the model response at product level and, hence, the decision on the preferable business model between LE and CE. Specifically, the relative cost of product disposal $rc_{disposal}$ and the relative cost of product disassembly $rc_{disassembly}$ have the largest impact on the determination of the business model. They are followed by the relative carbon footprint of product disposal $rcf_{disposal}$, the relative carbon footprint of product disassembly $rcf_{disassembly}$, and the peak of the triangular distribution adopted for the component quality index cqi_{peak}.

After the main effects plot, the interactions plot was investigated to understand whether or not the model parameters with a negligible main effect became impactful when considered in combination with other input parameters. The strongest interactions found are displayed in Figure 12.

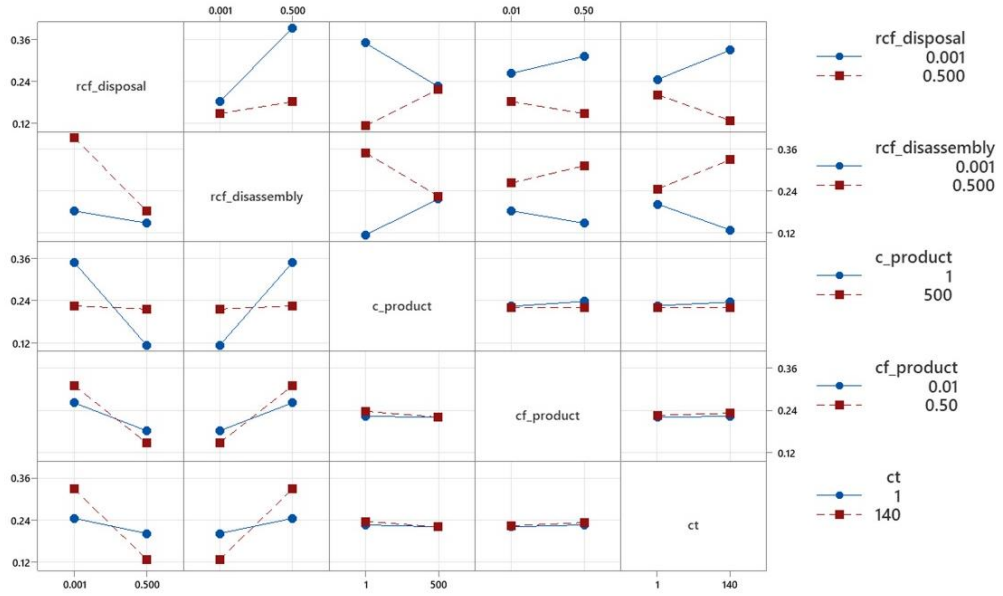


Figure 12: Strongest interaction plot between the model parameters for the business model selection at product level.

It stands out that the impact of the environmental parameters of product disposal $rcf_{disposal}$ and product disassembly $rcf_{disassembly}$ heavily depend on carbon tax value ct, carbon footprint of product manufacturing $cf_{product}$, and cost of product manufacturing $c_{product}$. This is because the cost of product manufacturing represents the weight of the economic criterion, while the carbon footprint of product manufacturing multiplied by the carbon tax represent the weight of the environmental criterion. Based on such evidence, the model parameters $c_{product}$, $cf_{product}$, and ct were also included in the selected parameters. Moreover, although with lesser intensity, also $rc_{assembly}$, $rcf_{assembly}$, and α_{peak} show several interactions with many parameters and, hence, they are included in the selected input parameters.

Overall, 11 model parameters were selected to perform a multi-level factorial experiment at product level for the selection of the preferable business model between LE and CE.. These 11 parameters were varied on four equally spaced levels to create the dataset necessary to feed and train the machine learning algorithm for the development of the data-driven decision-making tool at product level. This resulted in a dataset consisting of 4^11 = 4 194 304 different scenarios. Table 4 reports the values considered per each parameter.

Table 4: Values adopted for the multi-level computer-based factorial experiment at product level.

Model parameter	Values	Units of measure
$c_{product}$	[1, 150, 300, 500]	€
$cf_{product}$	[0.010, 0.150, 0.300, 0.500]	ton $CO_{2,eq}$
ct	[1, 50, 100, 140]	€/ ton $CO_{2,eq}$
n	25	-
$rc_{disposal}$	[10e-06, 0.150, 0.300, 0.500]	-
$rcf_{disposal}$	[10e-06, 0.150, 0.300, 0.500]	-
$rc_{disassembly}$	[10e-06, 0.150, 0.300, 0.500]	-
$rcf_{disassembly}$	[10e-06, 0.150, 0.300, 0.500]	-
$rc_{assembly}$	[10e-06, 0.150, 0.300, 0.500]	-
$rcf_{assembly}$	[10e-06, 0.150, 0.300, 0.500]	-
cqi_{peak}	[0, 0.350, 0.700, 1]	-
$rc_{sourcing,peak}$	0.500	-
$rcf_{sourcing,peak}$	0.500	-
$rc_{transformation,peak}$	0.500	-

$rcf_{transformation,peak}$	0.500	-
α_{peak}	[1, 1.7, 2.4, 3]	-
β_{peak}	2	-
γ_{peak}	0.3	-

The obtained dataset was then used to feed and train a decision tree algorithm in order to create a data-driven and user-friendly decision-making tool at product level that can support practitioners in the determination of product requirements for a CE. The decision tree, with the corresponding KPIs, is displayed in Figure 13.

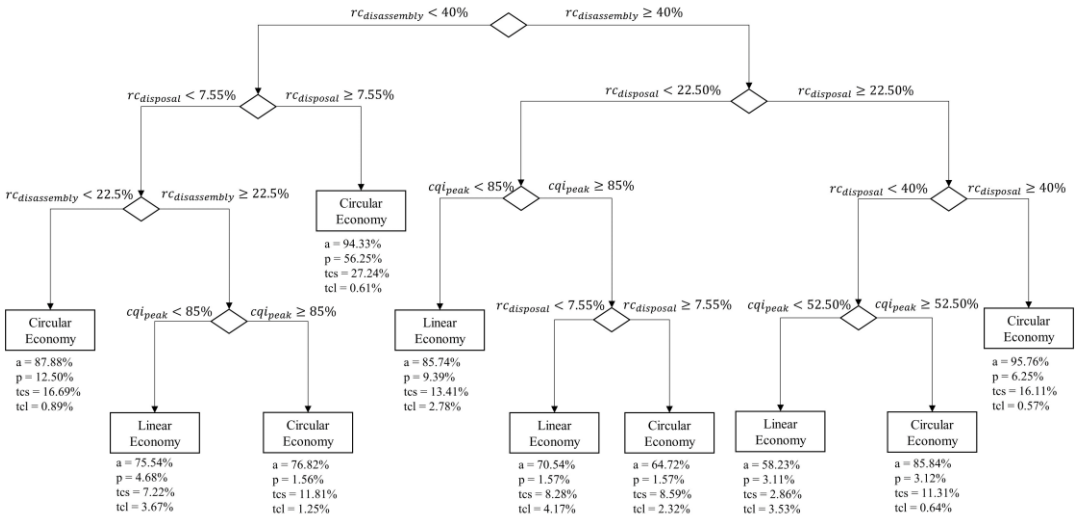


Figure 13: Decision tree for the selection of the most performing business model. The decision rules to apply represent the product requirements for a CE.

As can be seen, the decision tree is a user-friendly graphical representation of the product requirements needed to achieve a CE. In fact, by applying few decision rules on the most important parameters, it allows to determine the most performing decision between LE and CE, with an high global accuracy, i.e. 89.43%. Moreover, it shows the average percentage of total cost savings and the average percentage of total cost loss for each leaf of the tree. In this case, practitioners can be informed

also about the expected outcomes associated with particular product requirements. Finally, it is possible to draw the following general insights.

First, the economic cost of product disassembly $rc_{disassembly}$ drives the main product requirements. If this cost remains under 40% of the cost of product manufacturing, the CE is almost always the preferable business model. This holds true, in fact, for all the scenarios where the economic costs of product disposal $rc_{disposal}$ are not very low (i.e. higher than 7.55% of the product manufacturing cost). In other scenarios where the product disposal costs are very low, however, the LE becomes the preferable business model, notably if the quality of the components is low. Things change when the economic cost of the product disassembly increases (i.e. $rc_{disassembly} \geq 40\%$). From the right-hand side of the decision tree, it is clear that the CE is no longer the predominant business model suggested and that the suitability of the CE and LE business models depends greatly on the combination of the values assumed by the economic costs of product disposal $rc_{disposal}$ and the peak of the component quality index distribution cqi_{peak}. In particular, much depends on the economic costs of product disposal $rc_{disposal}$: when this is high (i.e. greater than 22.5% of product manufacturing cost), the CE is the preferable business model, unless the peak of the component quality index distribution cqi_{peak} is very low; instead, when the relative cost of product disposal is low, the LE can be the preferable business model, even when the peak of the component quality index distribution cqi_{peak} assumes high values.

As mentioned above, the product requirements are based only on economic parameters ($rc_{disassembly}$ and $rc_{disposal}$) and not on environmental parameters, although these have been included in the multi-level factorial experiments. This means that the choice of the preferable business model is not influenced by the $CO_{2,eq}$ emissions of the different life cycle phases. This will be further investigated later, but it turns out that, with the current values of the carbon tax ct, the economic criterion dominates the decision-making process and the environmental criterion is negligible and, thus, no environmental parameters are needed in the product requirements for a CE. This negligible impact of the environmental terms is confirmed by the relative importance of the different model parameters, represented in Figure 14 below.

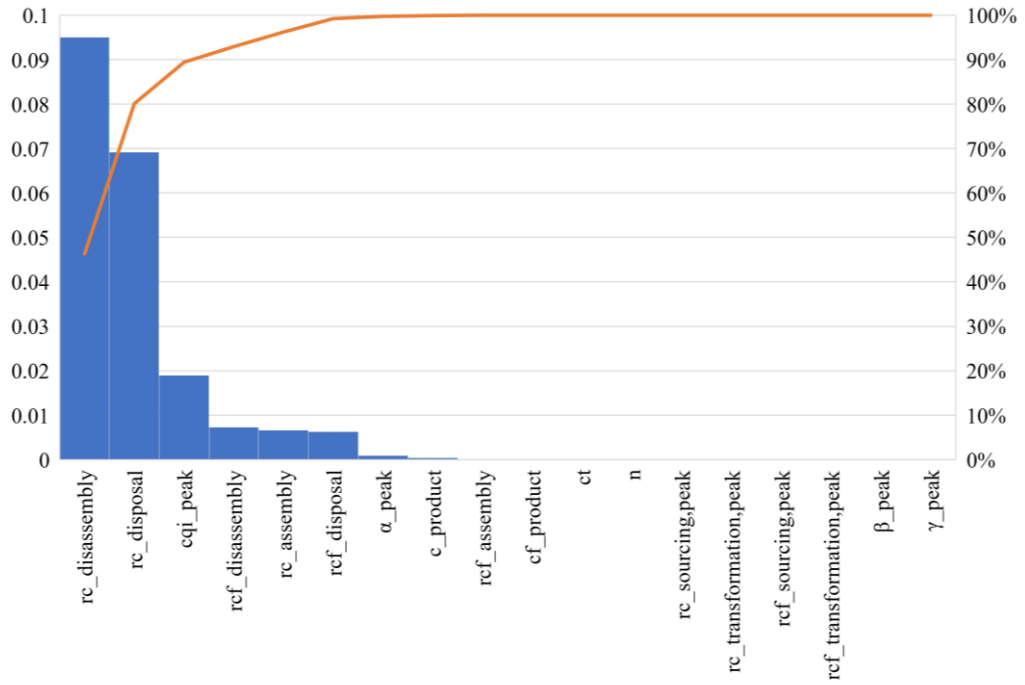


Figure 14: Relative importance of the model parameters at product level.

Finally, it is worth analyzing the performance provided by each business model when it represents the preferable choice in order to demonstrate the convenience in pursuing CE business models. Specifically, the cost savings, the carbon footprint savings, and the total cost savings are represented in the box and whisker plot in Figure 15.

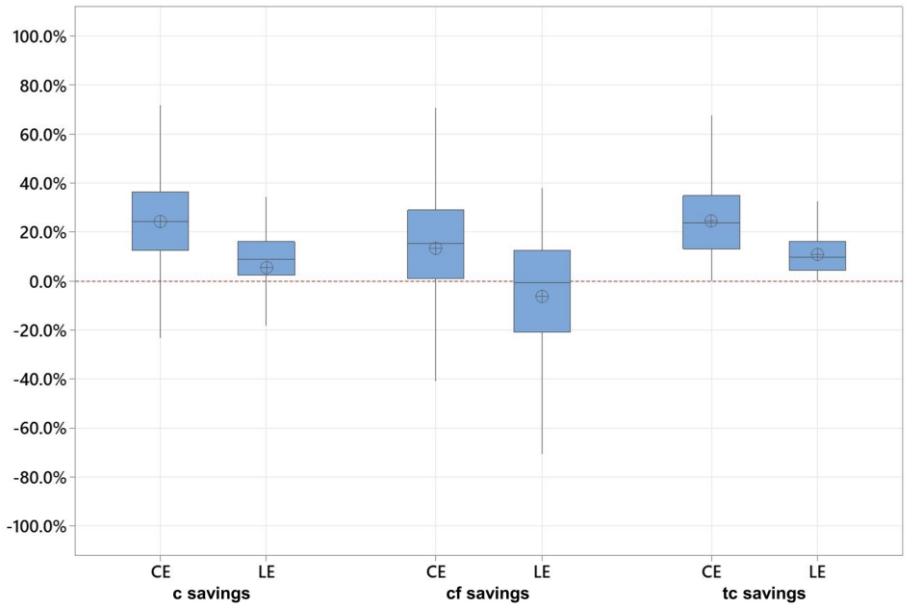


Figure 15: Box and whisker plot of the performance provided by each business model when it represents the preferable choice. The horizontal line represents the median value, while the target symbol represents the mean value.

Clearly, the CE business model exhibits superior performance to that of the LE in both criteria, i.e. economic (represented by the cost savings) and environmental (represented by the carbon footprint savings), as well as in the integration of the two (total cost savings). This shows companies the preferability of pursuing a CE rather than an LE business model because the former provides greater advantages, both in economic and environmental terms. Moreover, the average carbon footprint savings of the LE business model are negative, corresponding to an average increase of $CO_{2,eq}$ emissions. This further demonstrates that the choice of the preferable business model is exclusively driven by the economic criterion, while the environmental criterion is negligible in the decision-making process of the business model selection. Indeed, it is possible to observe that for both business models, the average value of the total cost savings coincides approximately with the average economic cost savings, further proving that the $CO_{2,eq}$ emissions have no impact on the decision-making process.

3.4.2 Decision-making tool at component level

As described earlier, a decision-making tool at component level is also created. This tool enables the determination of the CE strategy between recycling and remanufacturing based on the minimum total cost. Since the reusing strategy exclusively depends on the component quality, this CE strategy is not included in the development of the decision-making tool.

Also in this case, the first step was to analyze the main effects plot to understand the impact of the different model parameters on the model response at component level. The results are represented in Figure 16, where in the ordinate axis the component decision class (cdc) is reported ('0' for the remanufacturing strategy and '1' for the recycling one). It is worth noting that the reusing strategy is not included as component decision class since its adoption depends only on one model parameter, i.e. the component quality index cqi_i.

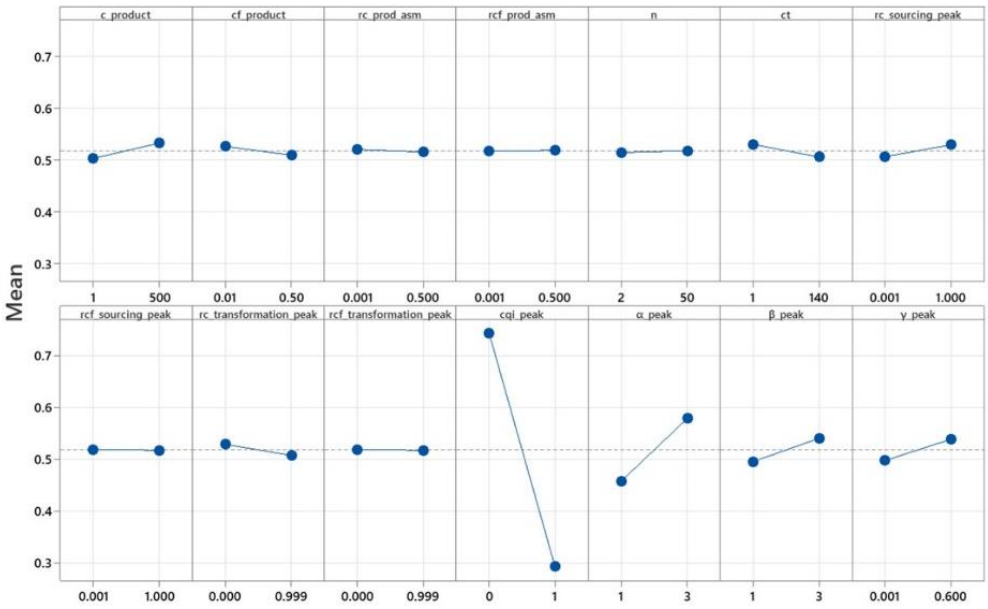


Figure 16: Main effects plot at component level; in the y-axis the class value for the CE strategy is reported ('0' stands for Remanufacturing and '1' for Recycling).

In this case, it is possible to note that the peak of the component quality index distribution cqi_{peak} has the largest impact on the determination of the CE strategy. The peak of the multiplicative factor of remanufacturing cost distribution (α_{peak}), the peak of the multiplicative factor of remanufacturing carbon footprint

distribution (β_{peak}), and the peak of the ratio between the selling price of scrap to recycler and its purchasing cost distribution (γ_{peak}) have also a non-negligible effect. Then, as done for the first decision-making tool at product level, an examination of the interaction plots was conducted to understand whether or not the model parameters with a negligible main effect became relevant when considered in combination with other parameters. The strongest interactions discovered are depicted in Figure 17.

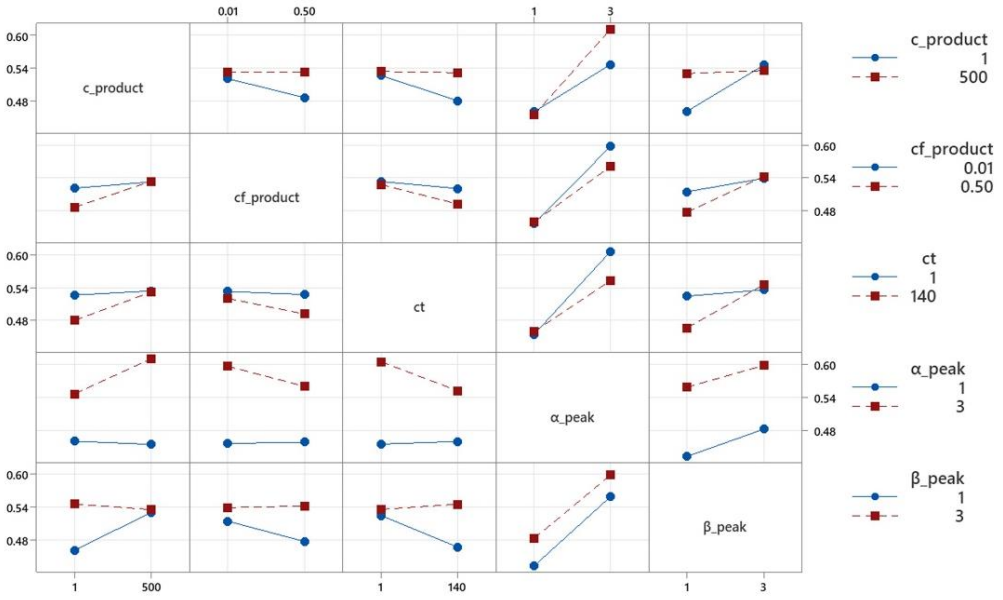


Figure 17: Strongest interaction plot between model parameters for the CE strategy selection.

From the analysis of the interaction plots, the cost of product manufacturing $c_{product}$, the carbon footprint of product manufacturing $cf_{product}$ and the carbon tax ct were added. These, in fact, exhibit a strong interaction between each other and with the peaks of the multiplicative factors of remanufacturing cost α_{peak} and carbon footprint β_{peak} distributions. Moreover, the peak of the relative cost of sourcing distribution $rc_{sourcing_peak}$ shows a slight interaction with the percentage of selling scrap to recycler γ_{peak}, and it was also included as relevant parameter.

Overall, 8 model parameters were selected to perform the multi-level factorial experiments at component level. Also in this case, the 8 parameters were varied on four equally spaced levels resulting in the creation of a dataset of 65,536 scenarios

(4^8). In particular, the extreme values for each model parameter remained as those indicated in Table 3, and the two intermediate values were selected to obtain an equal spacing among the four values. In contrast, the non-selected model parameters were assigned a fixed value corresponding to the average of the extreme values defined by the constraints. The considered values for each parameter are reported in Table 5.

Table 5: Values adopted for the multi-level computer-based factorial experiment at component level.

Model parameter	Values	Units of measure
$c_{product}$	[1, 150, 300, 500]	€
$cf_{product}$	[0.010, 0.150, 0.300, 0.500]	ton $CO_{2,eq}$
ct	[1, 50, 100, 140]	€/ ton $CO_{2,eq}$
n	25	-
$rc_{assembly}$	0.250	-
$rcf_{assembly}$	0.250	-
cqi_{peak}	[0, 0.350, 0.700, 1]	-
$rc_{sourcing,peak}$	[10e-06, 0.350, 0.700, 1]	-
$rcf_{sourcing,peak}$	0.500	-
$rc_{transformation,peak}$	0.500	-
$rcf_{transformation,peak}$	0.500	-
α_{peak}	[1, 1.7, 2.4, 3]	-

β_{peak}	[1, 1.7, 2.4, 3]	-
γ_{peak}	[10e-06, 0.2 0.4, 0.6]	-

The dataset obtained from the multi-level factorial experiment was then processed with a decision tree algorithm with the aim of creating a user-friendly decision-making tool that can support practitioners in the determination of product requirements for a CE at component level. The decision tree, with the corresponding KPIs, is displayed in Figure 18.

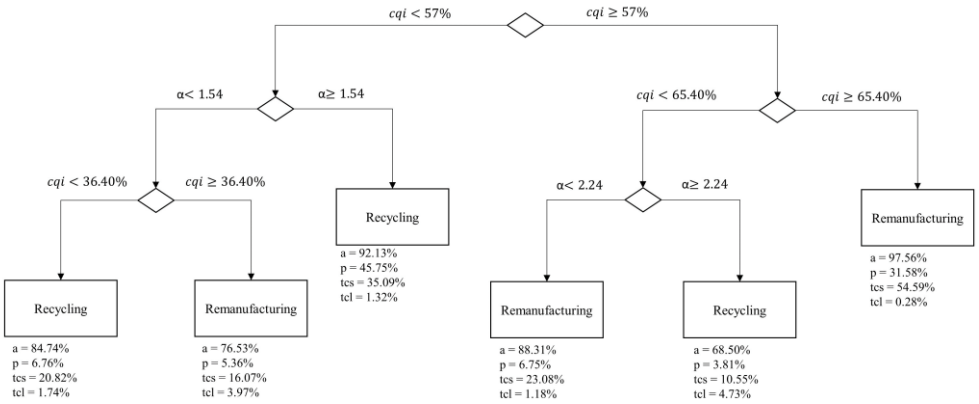


Figure 18: Decision tree for the selection of the CE strategy between recycling and remanufacturing. The decision rules to apply represent the product requirements for a CE at component level.

The developed decision tree represents a user-friendly decision-making tool, enabling practitioners to quickly determine the preferable CE strategy by applying just few decision rules (up to three). The decision rules to apply for the determination of the choice represent the product requirements for a CE at component level. The global accuracy provided is high, i.e. 91.35%. The data-decision tree enables to draw some general insights.

The primary driving factor in the decision-making process is the component quality index (cqi). If the quality of component is preserved with a component quality index equal or greater than 65.40%, remanufacturing strategy is always preferred. Conversely, when the component quality index is very low (i.e. below 36.40%), recycling strategy is selected. In all the other intermediate cases, the

choice depends on how much it costs to remanufacture a component (i.e. it depends on the multiplicative factor of remanufacturing cost α). Moreover, it can be observed also here that the environmental parameters do not affect the final choice since they do not appear in the decision tree and, thus, in the product requirements for a CE. This is further highlighted by the computation of the relative importance of the input parameters through the MRMR algorithm (Figure 19).

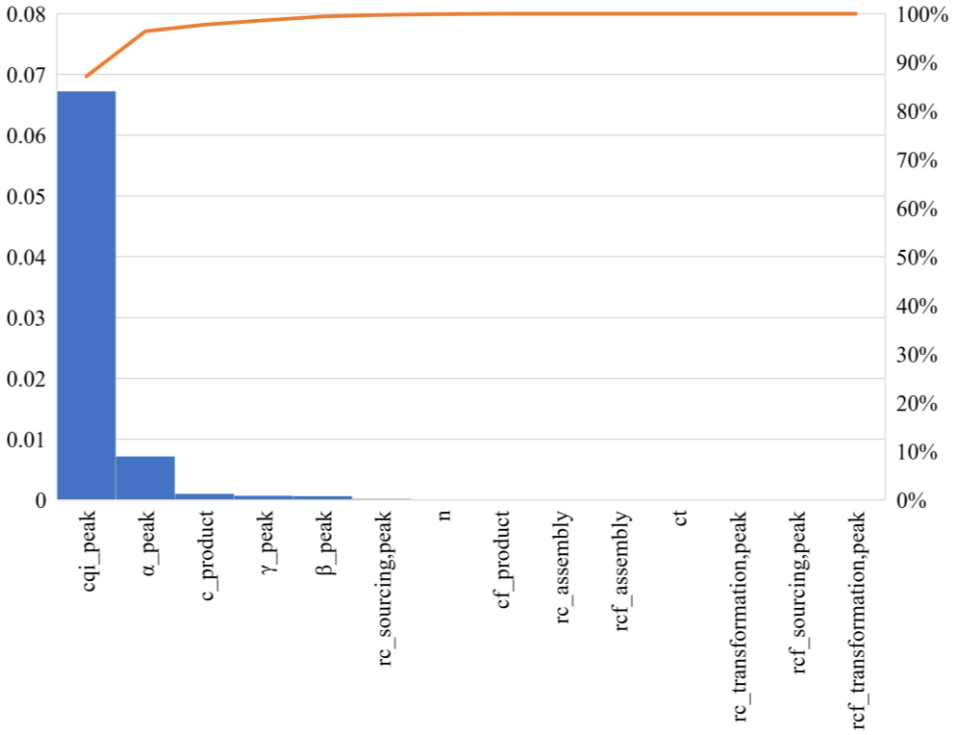


Figure 19: Relative importance of the model parameters for CE strategy selection.

From the Figure, in fact, it can be observed that the relative importance of the environmental parameters is null, with the decision-making process being largely dominated by the component quality index cqi. Of minor importance is then the peak of the triangular distribution relating to the multiplicative factor of remanufacturing cost α_{peak}, which is however non negligible, further confirming the insights derived from the analysis of the decision tree.

Finally, it is worth investigating the performance provided by each CE strategy when it represents the preferable choice. Hence, Figure 20 reports the box and whisker plot of the cost savings, carbon footprint savings, and total cost savings of

the two CE strategies (in the Figure 'REC' stands for recycling and 'REM' for remanufacturing).

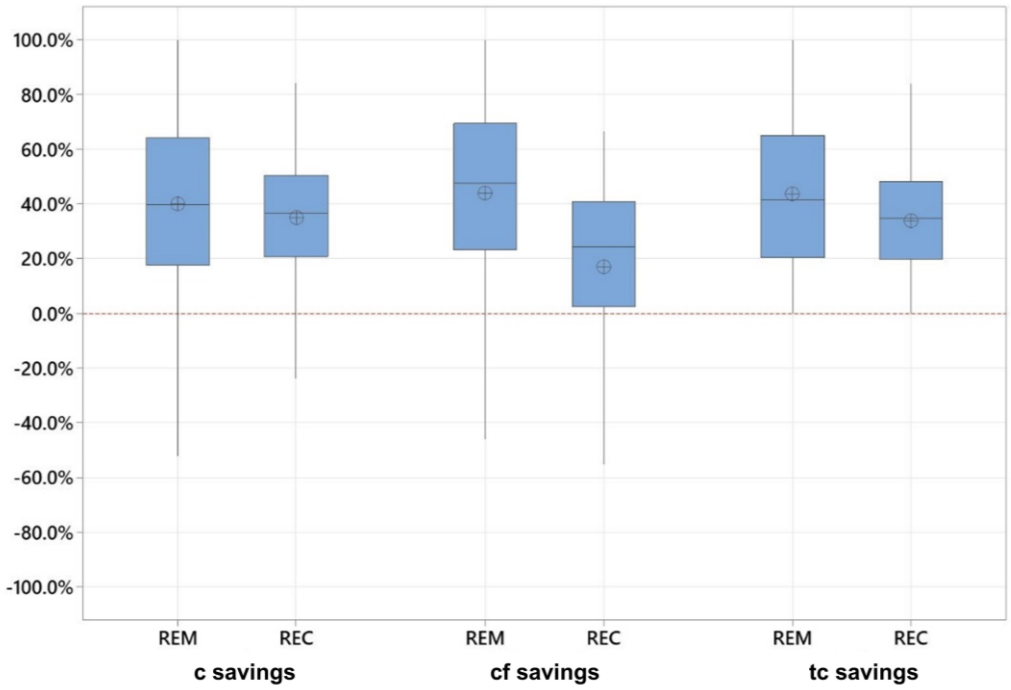


Figure 20: Performance provided by each CE strategy ('REC' stands for recycling and 'REM' for remanufacturing) when it represents the preferable choice. The horizontal line represents the median value, while the target symbol represents the mean value.

It turns out that remanufacturing strategies are on average more convenient than recycling ones both economically (cost savings) and environmentally (carbon footprint savings), as well as when considering their integration (total cost savings). Also in this case, for both CE strategies, the average value of the total cost savings reflects the average value of the cost savings. This is a further proof that the environmental criterion has a negligible impact on the choice of the preferable CE strategy, which is instead exclusively driven by the economic criterion.

3.4.3 Carbon tax level curves

As shown in the interaction plot of the model parameters in Section 3.4.1 (Figure 12), the environmental parameters strongly interact with the cost of product

manufacturing $c_{product}$, the carbon footprint of product manufacturing $cf_{product}$, and the carbon tax ct. This means that the importance of the environmental parameters on the decision-making process for the business model selection depends on the values assumed by these three parameters. As discussed before, of these three, only the carbon tax ct is an external factor that can be modified, and it represents the main discriminating factor about the relevance of the environmental parameters (and hence the environmental criterion) on the decision-making process. As has been shown by the analysis of the decision tree, the current values of carbon tax ct are such that the impact of the environmental criterion on the decision-making process is negligible. Understanding the minimum carbon tax value that renders the environmental criterion impactful is crucial to the decision-making process; it is achieved by finding the minimum carbon tax value that identifies at least one environmental input parameter belonging to the cumulative importance of 80%. Based on the above discussion, it is not possible to identify a unique value of carbon tax ct. Rather, the value of the carbon tax ct—such that the environmental criterion becomes relevant to the decision-making process—depends on the values of both the cost of product manufacturing $c_{product}$ and the carbon footprint of product manufacturing $cf_{product}$. Therefore, it is necessary to develop carbon tax level curves showing the minimum carbon tax ct value rendering the environmental criterion relevant to the decision-making process. This relevance is based on the combination of the values assumed by the cost of product manufacturing $c_{product}$ and by the carbon footprint of product manufacturing $cf_{product}$. The development of the carbon tax level curves has followed the methodology explained in Section 3.3.5, and their graphical representation is displayed in Figure 21.

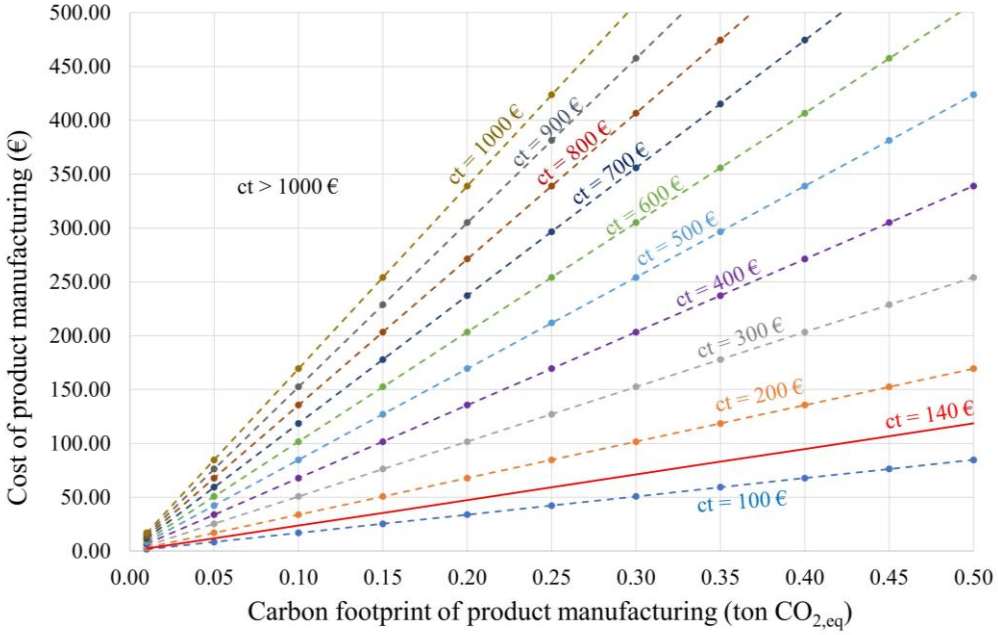


Figure 21: Carbon tax level curves. The solid red line represents the maximum value currently present.

Each level curve discerns the importance of the environmental parameters: given a certain level curve (i.e. a certain value of the carbon tax ct), the environmental parameters are relevant to the decision-making process if a product's cost of manufacturing $c_{product}$ and carbon footprint $cf_{product}$ lies on or below the level curve, otherwise the decision-making process is driven exclusively by the economic input parameters (i.e. by the economic criterion). These carbon tax level curves represent an important tool for policymakers to understand how to define their carbon tax policies to truly reduce CO_2 emissions. Even considering the highest carbon tax value currently adopted (around 140 €/ ton $CO_{2,eq}$), carbon tax level curves barely impact the decision-making process: only a small portion of products—with high $CO_{2,eq}$ emissions and low manufacturing costs—lie below the corresponding level curve (in red) and are hence affected by the environmental criterion; the majority of the products lie above and are thus not affected by any environmental considerations.

Based on these observations, it was decided to investigate how a new carbon tax regime, able to render the environmental criterion relevant in the decision-making process, would change the decision tree both at product and component levels. To make comparable the decision-making processes (that with the current

carbon tax regime and that with the new carbon tax regime), the same scenarios described above were investigated, i.e. the same model parameters were varied over the same 4 levels, but adopting different values of carbon tax that would ensure the relevance of the environmental criterion. To do this, per each combination of the cost of product manufacturing $c_{product}$ and of the carbon footprint of product manufacturing $cf_{product}$, the carbon tax value was varied over four equally spaced levels, ranging from the value indicated in the carbon tax level curves in Figure 20 to twice that value. Therefore, for each decision tree, a new multi-level factorial experiment was performed with new values of carbon tax, and the corresponding new decision trees are described in the following.

Decision tree at product level under new carbon tax regime

The decision tree developed for the selection of the preferable business model considering the new carbon tax regime is displayed in Figure 22 with the corresponding KPIs.

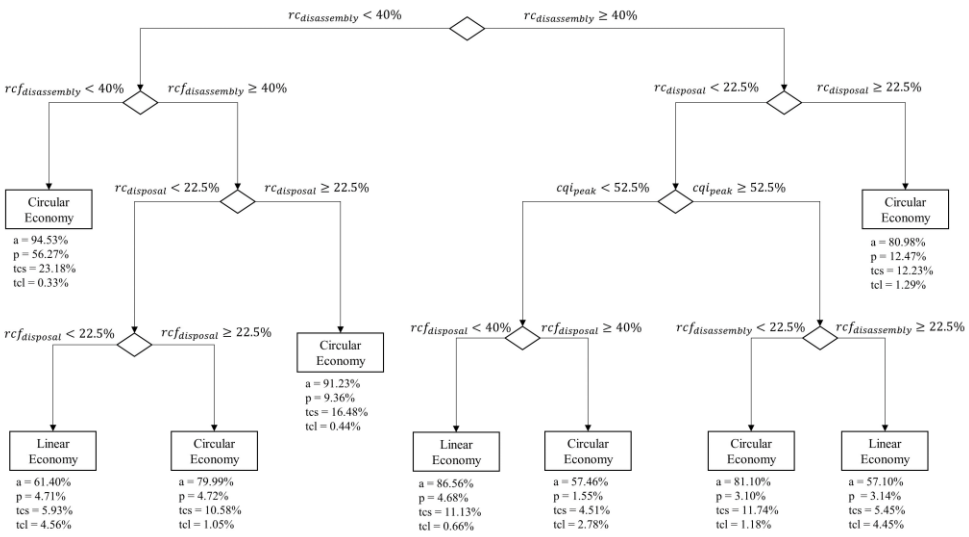


Figure 22: Decision tree for business model selection with the new carbon tax regime.

Also in this case, practitioners can detect the product requirements for a CE by looking at the decision rules of the decision tree, which has a global accuracy of 87.74 %.

Focusing on the comparison of the decision trees for the business model selection developed for the two carbon tax regimes (Figure 13 and Figure 22), it is

possible to note that the main driver of the decision-making process remains the relative costs of product disassembly $rc_{disassembly}$. However, with the new carbon tax regime, environmental parameters appear now in the decision tree, proving their non-negligible impact on the decision-making process and, thus, belonging to the set of product requirements for a CE. This is the case of the relative carbon footprint of product disassembly $rcf_{disassembly}$ and of product disposal $rcf_{disposal}$. Specifically, when the relative cost of product disassembly $rc_{disassembly}$ is low (i.e. below 40%), the decision-making process is now mainly driven by the relative carbon footprint of product disassembly $rcf_{disassembly}$ and not by the relative cost of product disposal $rc_{disposal}$. Moreover, in these scenarios of low $rc_{disassembly}$ (i.e. left-hand side of the decision tree), the quality of components, i.e. the peak of the component quality index distribution cqi_{peak}, do not affect the decision-making process, which is only governed by the economic and environmental parameters of product disassembly and disposal. Conversely, when the relative cost of product disassembly $rc_{disassembly}$ is high (i.e. above 40%), the environmental parameters of product disassembly and disposal still affect the decision-making process, but they have a lower impact than the relative cost of product disposal $rc_{disposal}$ and the quality of components.

This increased importance of the environmental parameters on the decision-making process is confirmed analyzing the relative importance of the model parameter (Figure 23). It can be seen, in fact, that the new carbon tax regime conveys a redistribution of the relative importance of the model parameters: while the relative cost of product disassembly and disposal are still the most important parameters of the decision-making process, the corresponding environmental parameters have now gained significant importance, surpassing even the peak of the component quality index distribution in their influence.

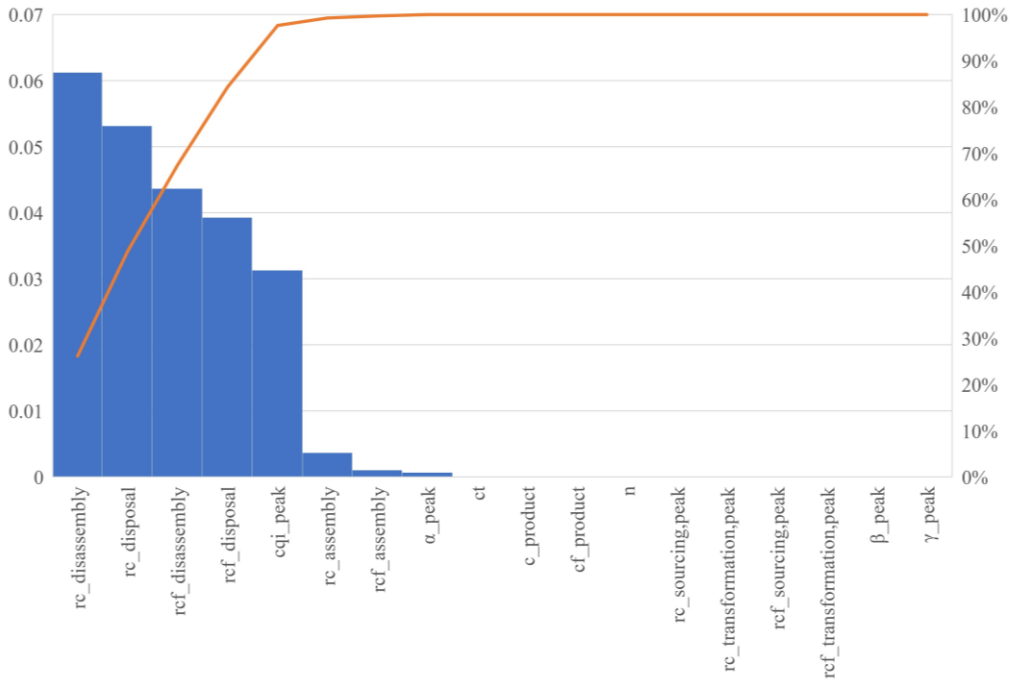


Figure 23: Relative importance of the input parameters for the business model selection with new carbon tax regime.

Finally, it is interesting to analyse how the new carbon tax regime affects the performance of each selected business model. Figure 24 displays, for each selected business model, the performance comparison in terms of cost savings, carbon footprint savings and total cost savings for the current and new carbon tax regime.



Figure 24: Comparison of each business model performance when it represents the preferable choice under different carbon tax regimes: a) CE comparison; b) LE comparison.

The adoption of a new carbon tax regime affects the performance for both the business models (CE and LE). On the one hand, both the CE and LE business models experience higher carbon footprint savings under the new carbon tax regime compared to the current regime. This suggests that the new carbon tax regime encourages businesses to reduce their carbon emissions, leading to environmental benefits. On the other hand, the new carbon tax regime results in a small reduction in cost savings for both the business models. Indeed, under the new carbon tax regime, the economic criterion, despite remaining the primary driver in the decision-making process, is characterized by a significance that slightly diminishes in favor of a greater emphasis on the environmental criterion. Finally, under the new carbon tax regime, the average $CO_{2,eq}$ savings for the LE business model becomes positive (under the current carbon tax regime they are negative).

Decision tree at component level under new carbon tax regime

The decision tree at component level developed for the selection of the suitable CE strategy considering the new carbon tax regime is displayed in Figure 25 with the corresponding KPIs.

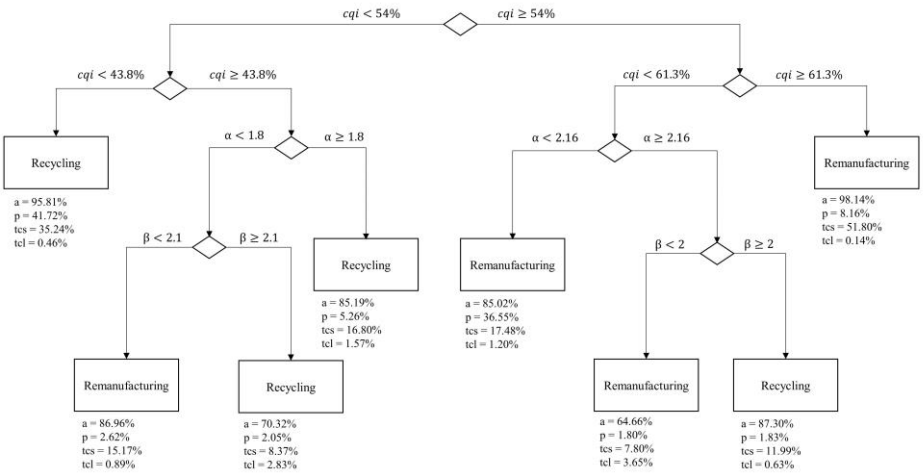


Figure 25: Decision tree for CE strategy selection with the new carbon tax regime.

Also in this case, practitioners can detect the product requirements for a CE at component level by looking at the decision rules of the tree, which has a global accuracy of 93.76 %.

In this case, the change in the carbon tax regime has a lower effect in the decision-making process at component level than in the one at product level. When dealing with the CE strategy selection, in fact, the decision-making process keeps

being highly dominated by the quality of component, i.e. the component quality index (cqi), followed by the multiplicative factor of remanufacturing cost α (as it was for the current carbon tax regime, cf. Figure 18). Nevertheless, the new carbon tax regime renders the decision-making process influenced by the environmental criterion through the multiplicative factor of the remanufacturing carbon footprint (β). All these considerations are confirmed by the analysis of the relative importance of the input parameters (Figure 26).

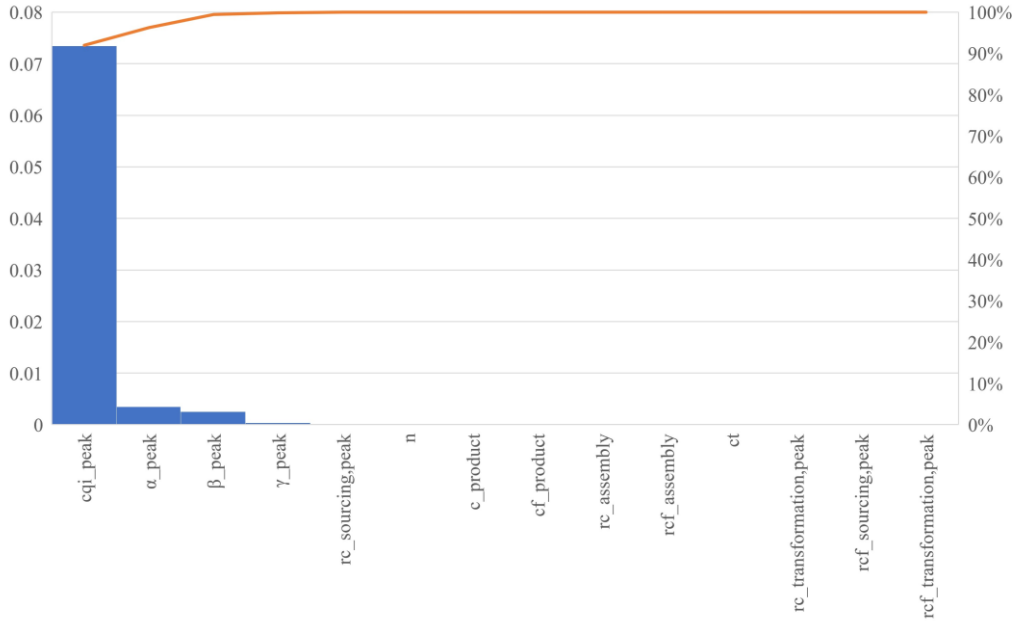


Figure 26: Relative importance of model parameters for CE strategy with new carbon tax regime.

This, in fact, confirms that the peak of the component quality index distribution cqi_{peak} continues to dominate the decision-making at component level, with an importance score much higher than all the other model parameters. However, now, in addition to the economic parameters related to the multiplicative factor of remanufacturing operations (α_{peak}), also the environmental counterpart (β_{peak}) has a non-negligible importance score.

Finally, it is interesting to evaluate if the change in the carbon tax regime affects the performance of the selected CE strategy. The performance comparison considering the two carbon tax regimes (current and new), for each selected CE

strategy, are displayed in Figure 27 in terms of cost savings, carbon footprint savings, and total cost savings.

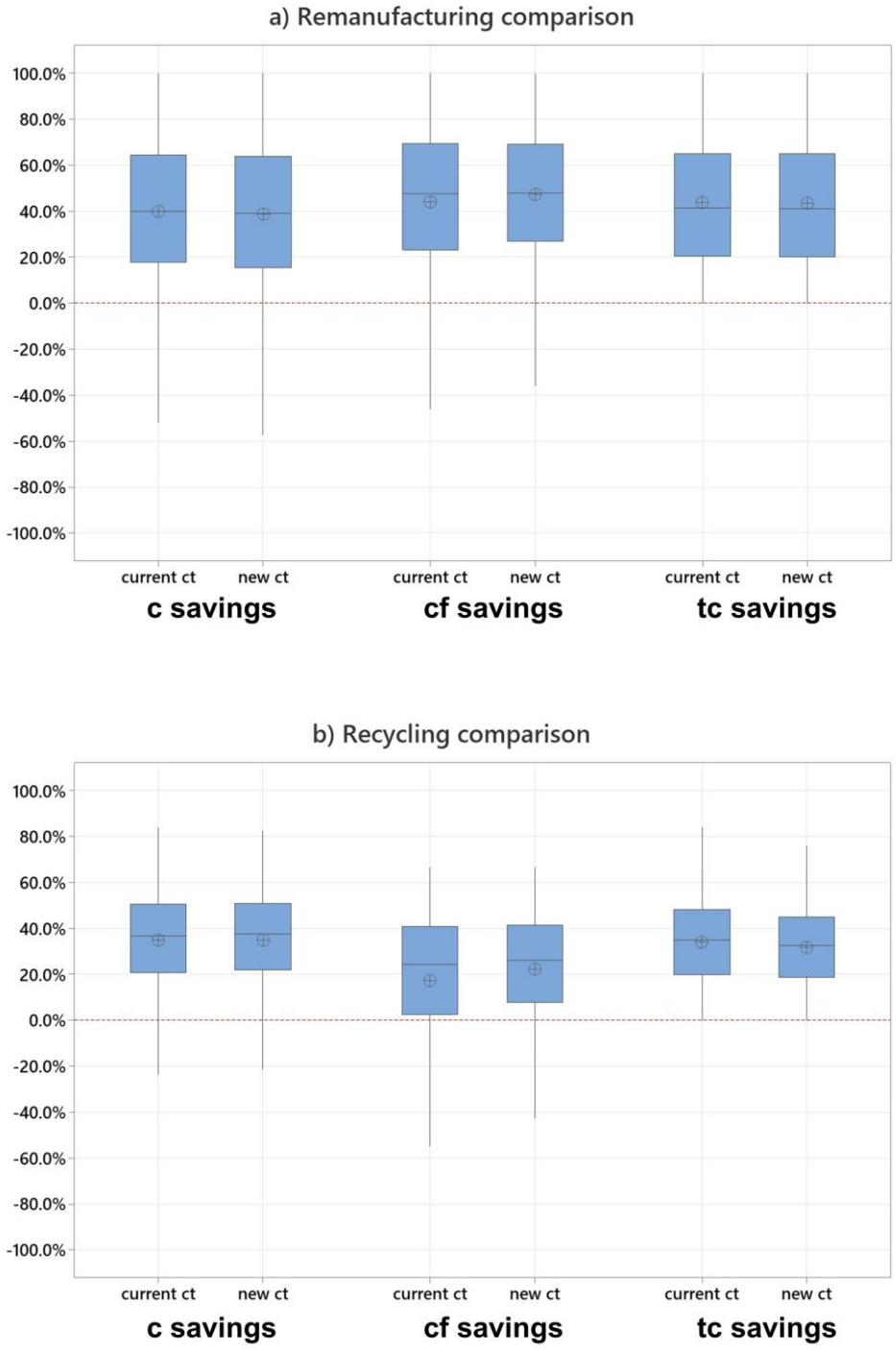


Figure 27: Comparison of each CE strategy performance when it represents the preferable choice under different carbon tax regimes: a) Remanufacturing comparison; b) Recycling comparison.

The effect of the new carbon tax regime on the performance of the CE strategy closely mirrors the findings observed in the comparison of the business model performances. Specifically, both the analyzed CE strategies, i.e. remanufacturing and recycling, show an average increase in carbon footprint savings. At the same time, there is a negligible decrease in cost savings for both CE strategies. In essence, the new carbon tax regime positively influences the environmental gains of the CE strategies while only slightly affecting their cost savings.

However, it is worth mentioning that higher carbon taxes may affect the entire supply chain, as companies could face increased costs for raw materials, transportation, and other inputs. This, in turn, might lead to a cascading effect on the overall cost structure of the product. Moreover, to meet emission reduction targets and comply with carbon regulations, companies may need to invest in new technologies and equipment. The initial costs of adopting cleaner and more sustainable technologies can impact budgets and profitability of manufacturing organizations. More research is needed to analyse the economic implications of more severe carbon tax measures.

3.5 Main contributions and limitations

The CE is an attractive business model that aims to tackle the impending alarming environmental challenges. However, despite its potential, the adoption of such a business model remains low, with a declining trend in recent years. A reason for this low adoption is the lack of suitable tools that support designers in the development of products suitable for a CE. Indeed, the current literature aimed to support the circular product design by developing both qualitative and quantitative tools, but without knowing which requirements they need to meet in order to make the product suitable for a CE. This work aims to overcome these limitations developing two user-friendly decision trees, one at product level and another one at component level, that allow designers and engineers to quickly identify the requirements needed to make a product suitable for a CE.

The developed decision trees are based on economic and environmental criteria, respectively represented by the economic cost and the $CO_{2,eq}$ emissions associated with product life cycle phase. The environmental criterion is monetized through the carbon tax, allowing both criteria to be expressed in monetary terms. To develop such decision tree, a systematic methodology has been adopted, involving the formulation of a mathematical model regarding the total cost of CE and LE business models at product level, and the total cost of the CE strategy at

component level. Then, for each level of the analysis, a bi-level computer-based factorial experiment was performed to identify the most impactful model parameters, followed by a multi-level computer-based factorial experiment to generate a multi-scenario dataset. These datasets are fed by a decision tree algorithms. This resulted in the development of two user-friendly decision trees, which are characterized by high accuracy and an assessment of the expected outcomes in terms of average percentage of total cost savings coming from the application of the requirements suggested by the decision tree. The developed decision tree offers also valuable insights to practitioners. Specifically, under the current carbon tax regime, the decision-making process is not affected by any environmental parameters. In fact, decision rules are applied relying on just three model parameters: the relative cost of product disassembly, the relative cost of product disposal, and the peak of the triangular distribution of the component quality index. Thus, one major thing has emerged, i.e. that the environmental parameters have no impact on the decision-making process. This is due to the current carbon tax regime, since carbon tax values control the weight of the environmental parameters.

Therefore, this work has also studied the role of the carbon tax on the decision-making process by analyzing which is the minimum carbon tax value that render the environmental parameters relevant. More in detail, since it is not possible to identify a unique value of carbon tax ct that makes the environmental criterion relevant, carbon tax level curves have been developed. In fact, the effect of the carbon tax depends by the values assumed by the cost of product manufacturing $c_{product}$ and the carbon footprint of product manufacturing $cf_{product}$ and, thus, a unique value cannot be established. Carbon tax level curves show the minimum value of carbon tax ct that renders the environmental criterion relevant in the decision-making process depending on the values assumed by the cost of product manufacturing $c_{product}$ and by the carbon footprint of product manufacturing $cf_{product}$. In such a way, this work aiming to tackle policy makers interested in environmental sustainability.

Moreover, the decision trees mentioned above have been updated according to a new carbon tax regime based on the carbon tax level curves. This change significantly affects the decision rules that determine the CE business model and the CE strategies, as the decision-making process is now influenced by some environmental parameters. In particular, the relative carbon footprint of

disassembly and disposal phases now appear in the decision tree at product level and, hence, in the product requirements. Similarly, although with less importance, the multiplicative factor of carbon footprint of remanufacturing process now appear in the decision tree at component level. Furthermore, the environmental performance both at product level and component level, measured as $CO_{2,eq}$ savings, surpassed the performance achievable under the current carbon tax regime.

The establishment of product requirements for a CE can be useful to enhance the sustainability-oriented innovation at product level of manufacturing organizations. As product requirements are primarily addressed in the initial phases of the product development process, this contribution may find greater relevance during the early stages of a technology lifecycle. However, its validity holds true across the entire technology lifecycle, as shown in Figure 8.

However, this study also has some limitations that should be acknowledged. Firstly, for the development of a holistic decision-making tool, it is essential to include the social criterion in the decision-making process. Unfortunately, the lack of objective methodologies in the field of social sustainability poses a challenge in incorporating such criterion into the analysis. Moreover, the scope of the environmental criterion should not be limited solely to $CO_{2,eq}$ emissions. Other essential environmental indicators, such as water consumption, resource usage, pollution emissions, and more, should also be considered in the decision-making process to obtain a more comprehensive understanding of the environmental impact [87]. Additionally, the number of CE strategies could be expanded beyond the ones explored in this study. Options like repair, refurbishment, repurposing, and others should be considered to offer a broader range of sustainable choices for businesses and decision-makers.

Chapter 4

Technological innovation at system level for sustainable manufacturing

The present research is also published in an article titled “Integrating Absolute Sustainability and Social Sustainability in the Digital Product Passport to promote Industry 5.0” in the Sustainability journal [87].

4.1 Theoretical background

The introductive section of the present doctoral thesis has described the importance of addressing sustainability issues in manufacturing at product, process, and system levels. As emphasized by the work [88], product and process innovation approaches are just a part of the solution to pursue, and there is a growing need to adopt a system-level perspective that encompass the entire value chain to tackle the sustainability challenge [33]. After having proposed a method to set product requirements for a CE and support sustainability-oriented innovation activities suitable in the early phases of a technology lifecycle, the second research of the doctorate has focused on system level technological innovations. In fact, as discussed in the sustainability-oriented technological innovation framework proposed in Section 2 (Figure 7), the innovation activities are different based on the technology lifecycle phase. In the initial phases of the technology lifecycle, the primary focus is on product innovation. Then, as the dominant design emerges and the core product architecture is established, innovation efforts can shift towards enhancing the value chain system. This transition is logical because the value chain system is intricately linked to the product architecture. Thus, following the technology lifecycle model, the product innovation activities can be followed by system innovation activities, which is the scope of this chapter.

The application of CE principles in manufacturing at system-level entails to create circular value chain systems. One of the main obstacles in the realization of a circular value chain is the lack of an efficient and effective information flow

among the stakeholders involved in the value chain. In fact, as stated by Berg and colleagues [26], a circular value chain needs information relating to location, conditions, and availability of materials, as well as it requires a coordination between material and information flows. Therefore, to effectively implement CE principles in a value chain, an efficient flow of information is required. This represents one of the main difficulties, mainly due to the following reasons as reported in the work [89]: (i), limited awareness of the necessity for circular information; (ii), absence of systems for sharing information throughout the value chain (iii), uncertainty regarding information on resources; (iv), constrained information sharing caused by concerns about competition. (v), insufficient understanding of resource recovery at the end of their use.

Many scholars have written about the importance of these points. For example, in the work available at [90], the lack of information exchange systems is regarded the key barrier to achieve a circular value chain in the textile sector. They dissert that the establishment of platforms that enable stakeholders to exchange information and collaborate, would represent a prominent solution for addressing this issue. Then, in the work available at [91], it is claimed that establishment of digital platforms for resource sharing among stakeholders would facilitate the extension of product lifecycles by improving resource efficiency within the value chain system. A similar finding was reported in the literature review available at [92], wherein the authors claimed that the expanded utilization of sharing platforms can support the implementation of an efficient circular value chain. Similarly, the literature review available at [93] recognizes the absence of stakeholder involvement throughout the product lifecycle as a key point hindering the application of CE principles in the value chain. Again, in the work available at [94] it is asserted that the current barriers to implementing circular strategies in the manufacturing sector are related to the lack of information along the value chain.

The achievement of an effective circular and sustainable value chain system could be greatly improved by digitally identifying products and their associated resources using a digital passport known as the digital product passport (DPP), a concept envisioned by the European Commission (EC) [95], [96]. The primary goal of the DPP is to promote sustainability, facilitate the transition to a Circular Economy (CE), and assist consumers in making responsible purchasing decisions by providing product-related information that is tracked throughout its lifecycle. Indeed, the conceptualization of DPP encompasses data and information relevant to all stages of the product lifecycle, involving sourcing, manufacturing, assembly, usage, and recovery.

As reported in [95]–[98] the creation of the DPP is regarded to offer a multitude of advantages. Designers and engineers, by utilizing the lifecycle data contained in the DPP, have the opportunity to improve the eco-design features of products, such as their durability, reliability, reusability, repairability, re-manufacturability, recyclability, energy efficiency, and waste reduction. Manufacturers can optimize their operations by improving traceability, which is valuable, for example, to manage warranty claims and recalls. Service providers specializing in repairs and maintenance can deliver more efficient and effective services by exploiting the technical and historical data available in the DPP. Remanufacturers can gain advantages from having access to data concerning component disassembly and their condition. Recyclers can make well-informed decisions by exploiting information about the presence of hazardous or valuable materials within products. In the end, consumers can make more environmentally conscious choices when making purchases by gaining insights into a product's environmental performance. It turns out that all the stakeholders involved in a product value chain can gain advantage by the establishment of a DPP.

Furthermore, the DPP can serve as a valuable tool for ensuring compliance. Recent regulations in the European Union (EU) and the United States (US) require businesses to produce Sustainability Reports (SRs) regarding their operations. The data contained in the DPP can serve as an evidence of compliance with these requirements. The information contained in the DPP can be seamlessly integrated into SRs, enhancing brand image and corporate reputation. Additionally, third-party organizations can get DPP data to assess sustainability indices. Having strong performance in this field can convey a competitive advantage [99], [67].

Therefore, the second research of the present doctoral thesis is focused on the establishment of a DPP to support sustainability-oriented technological innovations at system level. This research proposes the data requirements for the DPP, aimed at conducting a comprehensive evaluation of absolute environmental sustainability that aligns with the Earth's ecological limits. This assessment is grounded in the Life Cycle Assessment (LCA) methodology and the Planetary Boundaries (PBs) framework. Environmental attributes, environmental impact indicators with corresponding thresholds, are proposed to be integrated in the DPP. Moreover, a conceptual framework for the establishment of a DPP is discussed. Specifically, a framework based on Cyber-Physical Systems (CPSs) is proposed to facilitate the automated collection of both technical and environmental data for the DPP. This framework is constructed based on the well-established 5C architecture, a widely recognized architecture in the existing literature [100]. Therefore, in this chapter,

the second set of RQs will be addressed aiming to support sustainability-oriented technological innovation at system level:

2.1 What are the sustainability-oriented data requirements for the digital product passport ?

7.2 How can these data automatically collect and store in the DPP?

This work contributes to the establishment of a DPP and, thus, it provides a sustainability-oriented system innovation to enhance the implementation of CE principles in manufacturing.

4.2 Literature analysis and current state of DPP

This section introduces the primary academic articles that address the emerging subject of the DPP. It also offers an overview of the current status of the DPP, covering essential requirements and technical implementation issues.

4.2.1 Literature analysis

The analysis of the literature involved searching articles within the Google Scholar database using the keyword 'Digital Product Passport.' Only journal articles and conference papers in the English language were considered. All the identified papers were reviewed, and the most pertinent ones have been incorporated into this section and are summarized below.

The research on DPP is an emerging research area and the works available in the literature mainly focus on the types of data and information to include in the DPP, and different frameworks for their management.

Regarding the works connected with the study of data and information requirements, the main contributions can be found at [99], [101]–[103]. For instance, Jensen et al. investigated the data requirements for digital product passports in a mechatronics context. They identified seven clusters of data: (1) usage and maintenance, (2) product identification, (3) products and materials, (4) guidelines and manuals, (5) supply chain and reverse logistics, (6) environmental data, and (7) compliance. A survey was conducted to evaluate the significance, accessibility, and sensitivity of specific data points, involving three original equipment manufacturers, their customers, service partners, suppliers, and third-party recycling companies. The findings highlighted distinct data needs across these

stakeholders, but indicated that the exchange of data and the supporting infrastructure for closing resource loops are still at a relatively early stage of development [99]. A classification system for product data in the DPP was introduced by Stratmann et al. The development of this system involved a systematic literature review and a case study research conducted on typical operational information systems. The classification system comprises three levels and encompasses 62 data points, which are organized into four main categories: (1) Product information, (2) Utilization information, (3) Value chain information, and (4) Sustainability information [101]. Jansen et al. studied the requirements for a DPP system based on stakeholder involvement and literature from science and industry. They identified 8 different groups of requirements that are: (1) legal obligations, (2) functional suitability, (3) security, confidentiality, and IP protection, (4) interoperability, (5) modularity and modifiability, (6) accessibility, (7) availability and time behavior, (8) portability. For each of this group, a list of requirements is provided [102]. Finally, King et al. conceptualized the digital product passport as a collaborative and socio-technical system of systems. This innovative approach involves shared ownership among various stakeholders throughout the product lifecycle. They analyzed the requirements relating to this new kind of system-based concept [103].

Regarding the development of frameworks for the establishment of a DPP, the main contributions can be found at [97], [104]–[106]. Koppelaar et al. presented a conceptual design of the DPP to circular supply chain management. Their work was oriented to facilitate the recovery and reuse of critical raw materials at both component level and material levels. They conducted an assessment of existing information management practices for critical raw materials and surveyed the information needs of 10 manufacturers, producer responsibility organizations, collectors, and recyclers. Based on these needs, 14 key processes and exchanges for product information management were identified, forming the basis of the DPP circular supply management system [104]. Berger and colleagues presented a conceptual framework aimed at creating a digital battery passport for electric vehicles. Their work focused on providing the necessary information to effectively implement the digital battery passport, considering four distinct perspectives, which include: (i), battery: (ii), sustainability and circularity; (iii), diagnostics, performance, and maintenance; (iv) value chain actors. The objective was to facilitate the decision-making process for the sustainable management of electric batteries [120]. The same authors presented a conceptual framework that showcases how data science and machine learning techniques can facilitate the secure

exchange of data among stakeholders in the electric vehicle battery value chain in the context of DPP. By enabling confidentiality-preserving data exchange, their framework aimed to address concerns related to data sharing and enhance sustainability data management for electric vehicle batteries [105]. Plociennik et al., instead, proposed a framework for a digital lifecycle passport which relies on the asset administration shell and a cloud-based application. They also implemented a case study to demonstrate the improvement of the sorting process of an electronic waste [97]. Finally, Adirson et al., through a desk research and stakeholder workshops, discussed some design issues of the DPP with the expected benefits for the stakeholders of a product value chain [106].

All these works are valuable contributes for the development of the DPP. Different information requirements have been conceptualized and some use cases have been presented in the literature. However, an absolute perspective of environmental sustainability that respect the Earth's carrying capacity is not considered, and the literature does not propose how technical and environmental data can be automatically collected throughout the value chain system to be stored in the DPP. This research aims to bridge these existing gaps. First, it discusses the inclusion of environmental impact indicators, along with associated threshold values derived from the PBs framework, to enable an absolute assessment of product environmental sustainability. Then, a framework based on CPSs is proposed for the automatic collection of technical and environmental data throughout the value chain system to store in the DPP.

4.2.2 Current state of the DPP

In order to provide a general background on the current state of the DPP, the essential requirements and its technical implementation issues are described in the following.

Essential requirements

The EC established the essential requirements for the creation of the DPP. A data carrier that is physically attached to the product is required to connect the DPP to a unique product identifier. Both the data carrier and the unique product identifier must adhere to ISO/IEC 15459:2015 standard [107].

Data in the DPP must adhere to several rules. It should be machine-readable, structured, searchable, and constructed using open standards in an interoperable

format. Readers can refer to [96] for a detailed summary of the general requirements..

The EC also establishes the necessary technical requirements. It is anticipated that the DPP will be compatible with other DPPs, guaranteeing smooth data transfer and end-to-end communication across technological, semantic, and organizational domains. Users of the DPP will be able to freely access the information within the DPP in accordance with their individual access rights. Security, privacy, authenticity, and integrity of data must all be guaranteed, and fraud must be prevented [96]. Guth-Orlowski, then, emphasizes the importance of an inclusive and adaptable architecture for the DPP. The involvement in the DPP should not result in prohibitively high expenses or pose technical barriers that could marginalize small-scale economic participants. To deal with the dynamic of the present global value chains, DPP needs a flexible structure. This implies that it must be simple to add new product features or characteristics and to remove actors or information that is no longer needed [98].

The aforementioned requirements have been also proposed and extended in the recent study of Boukhatmi et al. [108], wherein they identified several requirements based on practical insights from interviews and surveys. The requirements were grouped in 11 categories as follows: (i), accessibility, i.e., grant complete platform access exclusively to specific parties via login process; (ii) completeness, i.e., provide additional information to the already present technical datasheets; (iii) consistency, i.e., promote uniform data sharing among stakeholders involved in the value chain; (iv) efficiency, i.e., streamline operational processes for the collection of product information; (v) inter-operability, i.e., allow the smooth integration of new information from different stakeholders; (vi) security, i.e., guarantee the hosting of the platform by an external and impartial entity; (vii) sensitivity, i.e., restrict the access to sensitive information; (viii) traceability, i.e., provide the history of the product life cycle via comprehensive data tracking; (ix) transparency, i.e., establish openness by means of sharing data; (x) time performance, i.e., reduce the time and effort spent by stakeholders in collecting information about the product; (xi) visibility, i.e., set up distinct levels of information visibility according to specific stakeholder groups.

To fulfil the aforementioned requirements, the following principles can be followed [98]:

- Data responsibility of the originators: stakeholders within the value chain provide declarations regarding their actions on the product, which are organized in a structured data sheet.

- Collection of data sheets: the DPP primarily encompasses a collection of data sheets generated by value chain's stakeholders, spanning from material production to the product's end of usage.

- Decentralized storage: the storage location is determined by the stakeholders, leading to the distributed storage of the DPP across multiple data stores. There is no centralized system for managing DPP information.

- Verifiability of the data: the digital signature of stakeholders ensures the verifiability of the data sheets, enabling the identification of the source of the provided product information, and preventing denial of its origin. This significantly boosts the trustworthiness of the DPP and the overall data quality. A signed data sheet serves as a certification.

Finally, it is essential to emphasize that a successful deployment of the DPP necessitates an appropriate governance framework [109]. This entails the establishment of comprehensive regulations, an active role played by the EC as a platform or registry manager, and vigilant supervision by the relevant authorities [110].

Regarding the type of information to be stored in the DPP, the EC provides two categories of information, that are: (i) track and trace information; (ii) attributes.

The first category comprises information related to the stakeholder and associated events. This may encompass details such as the manufacturer's name, registered trade name, global trade item number, TARIC code, global location number, and information that supports legal compliance, among others.

The second category comprises technical and sustainability-related information concerning the product. The EC offers general examples of attributes that should be incorporated into the DPP. These attributes may include product details like size, color, and images, information about the origin of raw materials, environmental impact indicators, product environmental footprint, circularity indicators, social indicators, chemical content, recycled content, usage instructions, manuals, disassembly instructions, and more [95], [96].

Technical implementation of the DPP

Guth-Orlowski suggests the utilization of decentralized technologies for the digital implementation of the product passport. Digital Decentralized Identifiers (DID) can be applied to individuals, products, machinery, processes, or organizations and are typically anchored on a blockchain (BC). In this scenario, a software tool for generating and overseeing decentralized identifiers is required, allowing all value chain stakeholders to establish their unique identifiers. DID have been nowadays standardized by the World Wide Web Consortium (W3C), which is one of the most important standardization bodies for Internet protocols.

Verifiable Credentials (VC) are digitally readable certificates signed with the private key of a DID. VC can be verified through their signatures, ensuring data integrity and access control. In fact, each stakeholder has the possibility to regulate access to these certificates, safeguarding company secrets from competitors and permitting access only to authorized entities like auditors, customers, or government agencies. This capacity makes VC well-suited for implementing certificates within the DPP. As mentioned earlier, a wallet can create and manage DIDs, but it can also be utilized for the generation, signing, and management of VC. The connection between one VC and another, known as "credential chaining," serves as the link between various pieces of information in the DPP..

The extensive adoption of the DPP, as envisioned by the EC, necessitates that every company within the value chain possesses a digital wallet. Interactions between multiple wallets are established on standardized protocols, thus preventing vendor lock-in. Through these wallets, each company can generate its own DID, accumulate VC pertaining to its operations, and issue VC related to other businesses and products. These credentials may encompass details such as disassembly instructions and repair guidelines.

Leveraging decentralized technology offers numerous benefits, including end-to-end verifiability, data accuracy, access control, real-time updates, inclusivity, flexibility, and establishing a trust anchor [98].

In such a context, in the last years BC technologies have gained importance and their role in the transition towards CE has been investigated by several researchers. According to [111], BC is an information technology that can be defined as a “digital, decentralized and distributed ledger in which transactions are logged and added in chronological order with the goal of creating permanent and tamperproof records”.

By adopting a distributed ledger architecture, BC eliminates the need for complex data center infrastructure while establishing a secure and dependable network. This decentralized approach eases the participation of multiple stakeholders, with cryptographic algorithms ensuring data validation and consistency in the sharing process [35]. Protocols designed for information security and seamless updates expand the capacity to store a wide range of data, including events, records, and transactions [36]. Rusch et al. [112] have underlined how BC enables effortless information sharing, efficient exchange of life cycle inventory data, and real-time monitoring of product conditions. These findings highlight BC's potential to enhance transparency, traceability, and sustainability within value chain operations, promoting environmentally responsible and socially conscious practices.

As a result, BC has the capacity to streamline the operations of a circular value chain [113]. For instance, BC can optimize recycling procedures by enabling the precise monitoring of waste streams and promoting integration within recycling networks. It provides a secure and transparent framework for monitoring and verifying the flow of recycled materials, ensuring their appropriate disposal or reutilization. This, in turn, plays a significant role in enhancing the efficiency and sustainability of recycling practices and, consequently, the CE as a whole [114], [115]. For instance, the research conducted by Erol et al. highlights the pivotal role of BC in promoting the adoption of CE. BC enhances supply chain traceability, encourages cooperation and coordination within business ecosystems, and fosters higher levels of trust [116]. These findings are further confirmed by Kayikci et al., underscoring the importance of network collaboration for the successful development of BC-based CE [117]. Additionally, Chaudhuri et al. conducted interviews with four small and medium enterprises (SMEs) actively engaged in CE. Their focus was on initiatives that leveraged digital technologies, including BC, to support the transition towards CE. The analysis revealed that SMEs involved in these initiatives were able to optimize their recycling facilities, establish well-defined circular economy processes, make informed decisions about raw materials, and optimize their manufacturing processes [118].

Furthermore, BC can be integrated with the Internet of Things (IoT) to further boost the implementation of circular value chain. These technologies hold the potential to improve the efficiency of reverse supply chain systems, streamline data collection and analysis regarding end-of-life products, and enhance traceability [119]. Consequently, through the application of these technologies, stakeholders within the circular value chain can boost eco-efficiency and enhance the resilience

of the entire supply chain [120]. Magrini et al. [121] investigated the use of IoT and BC technologies in the e-waste sector. Their research unveiled significant benefits from combining IoT and BC, including the ability to track products throughout their entire lifecycle, promote CE practices, and facilitate well-informed decision-making. This combination enables organizations to effectively monitor product usage, maintenance, and e-waste management, thereby advancing sustainability efforts and optimizing resource utilization. An example of an e-waste management system based on the Ethereum BC can be found in [122].

In conclusion, the incorporation of BC into value chain systems provides a means to uphold human rights and equitable labor practices. Transparent product history records offer consumers the assurance that their purchases originate from environmentally responsible sources. Additionally, smart contracts hold the potential to autonomously enforce the monitoring and validation of sustainable regulations and policies [123].

As a consequence, BC can play a central role in advancing the technical aspects of the DPP.

4.3 Methodology

As done for the establishment of product requirements for a CE, the classical model of a product life cycle, which includes sourcing, transformation & assembly, product use, and product EoL [48], [66], [67], is used as a reference value chain system in this work.

As mentioned earlier, the EC has already specified various environmental attributes to be included in the DPP [94]. The identification of these environmental attributes largely relies on a well-established methodology known as Life Cycle Assessment (LCA), which is standardized by ISO 14044:2006 [124]. LCA analysis is designed to collect data on resource consumption and emissions throughout a product's lifecycle, allowing for the assessment of multiple environmental impact categories. One commonly used method for quantifying these product environmental impact categories within the LCA framework is the Environmental Footprint (EF) method, which serves as a reference in the EU [125]. The definition of the environmental impact categories according to the EF method is reported in Table 6.

Table 6. Definition of environmental impact according to the EF method [125].

EF impact category	Indicator	Units of measure
Human toxicity, cancer	Comparative Toxic Unit for humans	CTUh
Human toxicity, non cancer	Comparative Toxic Unit for humans	CTUh
Particulate matter	Impact on human health	Disease incidence
Photochemical ozone formation	Tropospheric ozone concentration increase	kg NMVOC eq
Ionising radiation	Human exposure efficiency relative to U^{235}	kBq U235 eq
Water use	User deprivation potential	m^3 world eq
Ecotoxicity, freshwater	Comparative Toxic Unit for ecosystems	CTUe
Climate change	Radiative forcing as Global Warming Potential (GWP100)	kg CO_2 eq
Resource use, fossil	Abiotic resource depletion – fossil fuels	MJ
Ozone depletion	Ozone Depletion Potential (ODP)	kg CFC-11 eq
Eutrophication, marine	Fraction of nutrients reaching marine end compartment (N)	kg N eq
Eutrophication, freshwater	Fraction of nutrients reaching freshwater end compartment (P)	kg P eq
Land use	Soil erosion	kg soil loss
Eutrophication, terrestrial	Accumulated Exceedance (AE)	molc N eq
Acidification	Accumulated Exceedance (AE)	molc Hþ eq
Resource use, minerals and metals	Abiotic resource depletion (ADP ultimate reserves)	kg Sb eq

However, it is important to note that determining environmental impact categories based on LCA provides a relative assessment of the ecological performance of technologies but does not offer information about whether these technologies are sustainable in absolute terms [126]. Therefore, there is a critical

need to transition from a relative sustainability assessment to an absolute one in order to achieve sustainable manufacturing. Notably, there is a growing emphasis on integrating the Planetary Boundaries (PBs) framework into LCA analysis for an absolute sustainability assessment [127]. By establishing threshold values for environmental impact categories based on PBs, a clear understanding of whether a product lifecycle is sustainable in absolute terms can be achieved. The existing literature offers a comprehensive framework for PBs [4], [1]. The definition of such framework is presented in Table 7.

Table 7. Definition of Planetary Boundaries [6].

Earth-system process	Control variable	Boundary value in 2023	Current value
Climate change	Atmospheric carbon dioxide concentration (ppm by volume)	350	417
	Total anthropogenic radiative forcing at top-of-atmosphere (W/m2) since the start of the industrial revolution (~1750)	1	2,91
Change in biosphere integrity	Genetic diversity: Extinction rate measured as E/MSY (extinctions per million species-years)	<10	>100
	Functional diversity: energy available to ecosystems (NPP) (% HANPP)	<10%	30%
Biogeochemical	Phosphate global: P flow from freshwater systems into the ocean; regional: P flow	Phosphate global: 11 Tg of P $year^{-1}$; regional: 6.2 Tg of P $year^{-1}$ mined and	Global: 22 Tg of P $year^{-1}$; regional:

	from fertilizers to erodible soils (Tg of P $year^{-1}$)	applied to erodible (agricultural) soils.	17.5 Tg of P $year^{-1}$
	Nitrogen global: industrial and intentional fixation of N (Tg of N $year_{-1}$)	62	190
Ocean acidification	Global mean saturation state of calcium carbonate in surface seawater (omega units)	2,75	2,80
Land use	Part of forests rested intact (percent)	75 from all forests including 85 from Boreal forest, 50 from Temperate forests and 85 from Tropical forests.	Global: 60
Freshwater change	Blue water: human induced disturbance of blue water flow.	Upper limit (95th percentile) of global land area with deviations greater than during preindustrial, Blue water: 10.2%	18,2%
	Green water: human induced disturbance of water available to plants (% land	11,1%	15,8%

	area with deviations from preindustrial variability)		
Ozone depletion	Stratospheric ozone concentration (Dobson units)	276	284,6
Atmospheric aerosol	Interhemispheric difference in AOD	0,1	0,076
Novel entities	Percentage of synthetic chemicals released to the environment without adequate safety testing	0	Transgressed

Sala et al. [125] applied the PBs framework within the EF methodology to set limits for environmental impact indicators. The relations between the EF impact categories and PBs are represented in Figure 28.

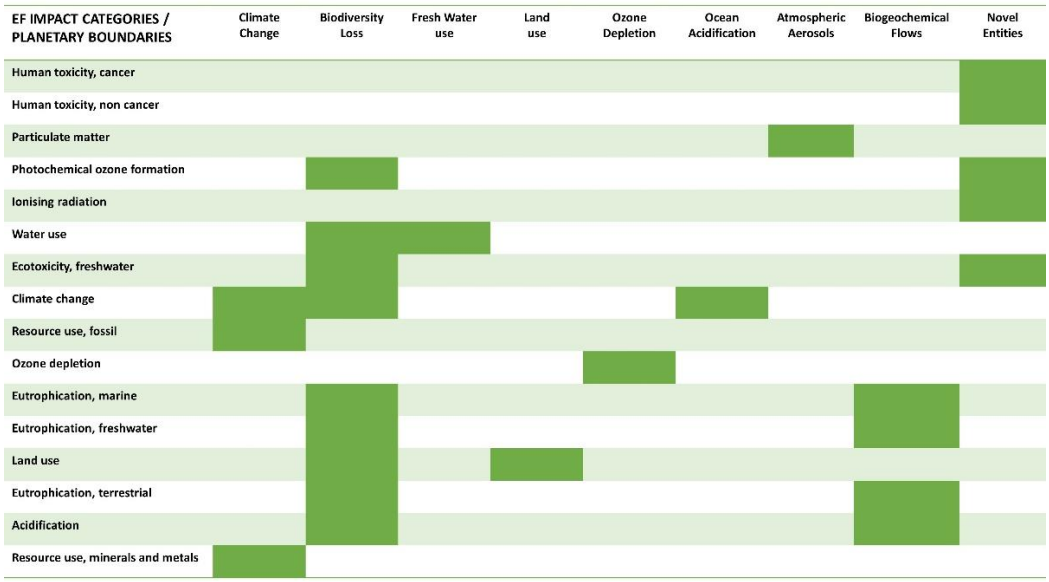


Figure 28. Relations between EF impact categories and PBs based on [125].

This application allows for an assessment of absolute sustainability. They specifically established a connection between the environmental impact categories of the EF method and the PBs framework determining numerical threshold values for environmental impact indicators based on PBs. The environmental impact category of EF methodology, its indicators, and the corresponding threshold values are reported in Table 8.

Table 8: Planetary Boundaries applied to Environmental Footprint impact categories based on [125].

EF impact category	**Indicator**	**Units of measure**	**Threshold values based on PBs**
Human toxicity, cancer	Comparative Toxic Unit for humans	CTUh	9.62E+05
Human toxicity, non cancer	Comparative Toxic Unit for humans	CTUh	4.10E+06
Particulate matter	Impact on human health	Disease incidence	5.16E+05
Photochemical ozone formation	Tropospheric ozone concentration increase	kg NMVOC eq	4.07E+11
Ionising radiation	Human exposure efficiency relative to U^{235}	kBq U235 eq	5.27E+14
Water use	User deprivation potential	m^3 world eq	1.82E+14
Ecotoxicity, freshwater	Comparative Toxic Unit for ecosystems	CTUe	1.31E+14
Climate change	Radiative forcing as Global Warming Potential (GWP100)	kg CO_2 eq	6.81E+12
Resource use, fossil	Abiotic resource depletion – fossil fuels	MJ	2.24E+14
Ozone depletion	Ozone Depletion Potential (ODP)	kg CFC-11 eq	5.39E+08

Eutrophication, marine	Fraction of nutrients reaching marine end compartment (N)	kg N eq	2.01E+11
Eutrophication, freshwater	Fraction of nutrients reaching freshwater end compartment (P)	kg P eq	5.81E+09
Land use	Soil erosion	kg soil loss	1.27E+13
Eutrophication, terrestrial	Accumulated Exceedance (AE)	molc N eq	6.13E+12
Acidification	Accumulated Exceedance (AE)	molc Hþ eq	1.00E+12
Resource use, minerals and metals	Abiotic resource depletion (ADP ultimate reserves)	kg Sb eq	2.19E+08

Therefore, environmental attributes, environmental impact indicators with corresponding thresholds, are proposed to be integrated in the DPP based on the above mentioned methodologies.

These environmental data, together with the technical ones, can be efficiently gathered through the utilization of Industry 4.0 technologies, particularly Cyber-Physical Systems (CPSs). CPSs integrate physical assets, like products, machinery, and plants, with their corresponding digital representations. Within a CPS, sensors capture data from the physical assets and transmit it to the digital environment, where this data is converted into information that improves the decision-making process of manufacturing organizations [128].

CPSs can be configured using various architectures, with the 5C architecture, as outlined in the literature [100], being one of the most widely adopted and serving as a reference for the present work. Numerous works have already adopted the 5C architecture, with several examples available in [129], [130], [131]. The DPP can be established by focusing on three primary layers of the 5C architecture. The initial layer, known as the Connection Level, is composed by the assets under monitoring and the sensors utilized for data collection. The data collected is then transmitted to the second layer, referred to as the Conversion Level, where data is transformed into information through various analytical methods, including statistical analysis

and machine learning algorithms. Finally, the third layer, known as the Cyber Level, harnesses the data and information to generate knowledge, primarily employing data analytics and artificial intelligence tools.

The following section presents the relevant data to be stored in the DPP for enabling an absolute assessment of sustainability (which represents the answer to RQ2.1) and introduces the conceptual framework created to automatize data collection throughout the value chain within the DPP (which represents the answer to RQ2.2).

4.4 Results and discussion

As discussed in the methodology section, the DPP should contain not only the environmental data necessary to compute the environmental impact indicators, but also the corresponding threshold values that represent the natural limits that our planet can withstand. To this purpose, the work available at [125] can be used as a reference. They quantitatively assessed the threshold values based on the PBs framework to apply for each environmental impact category of the EF methodology.

Besides the inclusion of environmental impact indicators for each relevant phase of the value chain, along with the associated threshold values based on Table 8, the DPP should also include technical information to track product quality throughout its lifecycle. This promotes the flow of product information necessary to drive the implementation of the CE principles in the value chain as previously discussed.

The subsequent sections present different environmental attributes to be gathered across a product value chain. Additionally, technical attributes to be stored in the DPP for each phase of the product value chain are proposed. Depending on the particular product and its application, some fields may remain empty or unspecified.

4.4.1 Sourcing data

The sourcing process rigorously complies with international standards related to operational safety, environmental impact mitigation, and material property certification. In these phases, the data is routinely standardized, often measured in kilograms (kg) or tons, and categorized in the DPP as follows [67], [11], [125]:

• Environmental attributes: embodied energy, water consumption, $CO_{2,eq}$ emissions, NOx emissions, Sox emissions, particulates, solid wastes, liquid wastes, etc.

• Environmental impact indicators and related PB-based thresholds: particulate matter, climate change, resource use (fossil), water use, land use, etc., (refer to Table 6).

• Technical attributes: Chemical (chemical composition, toxicity, corrosion resistance, etc.), Mechanical (density, elastic modulus, tensile strength, fatigue strength, etc.), Thermal (thermal conductivity, thermal expansion, melting point, etc.), Electrical (electrical resistivity, capacitance, dielectric constant, etc.), etc.

4.4.2 Transformation and Assembly data

Manufacturing operations rigorously comply with established standards, with a focus on human safety, environmental impact reduction, and product performance certification. The DPP can function as a repository for a wide range of information that should be recorded and stored, encompassing the following examples:

• Environmental attributes: processing energy, water consumption, $CO_{2,eq}$ emissions, NOx emissions, Sox emissions, particulates, solid wastes, liquid wastes, etc.

• Environmental impact indicators and related PB-based thresholds: particulate matter, climate change, resource use (fossil), water use, land use, etc., (refer to Table 6).

• Technical attributes: Technological (process type, etc.), Geometrical (2D drawing of the part, CAD model, etc.), Assembly (assembly instructions, assembly time, etc.), eventual update of previous properties.

4.4.3 Use data

During operations, products experience alterations over time caused by various wear mechanisms. It is essential to recognize and track the most notable changes to maintain the accuracy of the DPP:

• Environmental attributes: use energy, water consumption, $CO_{2.eq}$ emissions, NOx emissions, Sox emissions, particulates, solid wastes, liquid wastes, etc.

• Environmental impact indicators and related PB-based thresholds: particulate matter, climate change, resource use (fossil), water use, land use, etc., (refer to Table 6).

• Technical attributes: Operations (usage time, usage mode, product health indicators, etc.), Maintenance (maintenance mode, maintenance time, etc.), update of previous properties.

4.4.4 End of Life data

Upon reaching the end of its usage, the product's recovery or disposal activities must be monitored and incorporated into the DPP. As previously mentioned, the recovery process varies depending on the chosen strategy.

• Environmental attributes: processing energy, water consumption, $CO_{2,eq}$ emissions, NOx emissions, Sox emissions, particulates, solid wastes, liquid wastes, etc.

• Environmental impact indicators and related PB-based thresholds: particulate matter, climate change, resource use (fossil), water use, land use, etc., (see Table 6).

• Technical attributes: Disassembly (disassembly instructions, disassembly time, etc.), update of previous properties.

4.4.5 Reusing, Remanufacturing, Recycling data

Upon reintegration of the material/component/product into the economy, there are three potential pathways: re-use, remanufacturing, or recycling. Depending on the chosen scenario, relevant updates need to be made in the DPP reflecting new information regarding Usage, Manufacturing, or Materials sourcing.

4.4.6 DPP platform based on CPSs

Environmental and technical data can be systematically collected through the utilization of Industry 4.0 technologies, particularly CPSs. These CPSs establish a

connection between physical assets (products, machinery, plants, etc.) and their digital counterparts. Within CPSs, data is captured by sensors in the physical realm and transmitted to the digital domain, where this data is transformed into information utilized to inform the decision-making process [128].

As Ahmed et al. asserted [132], CPSs are increasingly integrated into all phases of a product value chain. During the material sourcing phase, where primary materials are often obtained through extraction processes associated with significant environmental impacts and potential human health risks, CPSs offer the opportunity to automate operations efficiently. This results in reduced environmental impacts and decreased human health risks while concurrently capturing environmental and technical data related to the process. In the transformation and assembly phase, CPSs play a crucial role in machine monitoring, production scheduling, and maintenance activities. These activities provide opportunities to record both environmental and technical data. Additionally, CPSs are progressively employed to monitor products throughout their usage phase, facilitating the prediction of maintenance requirements. In this context as well, sensors embedded within products enable the detection and collection of technical and environmental data [67]. Given these considerations, CPSs present a valuable means to obtain environmental and technical attributes throughout a product's value chain and store them in DPP.

CPSs can be designed with various architectures, although the 5C architecture, as widely mentioned in the literature [100], serves as a key reference for this study. Numerous valuable works have already adopted the 5C architecture, and specific examples can be found in [129], [130], [131].

The development of the DPP can rely on just three layers of the 5C architecture. The initial layer, known as the Connection Level, encompasses the asset under monitoring along with the sensors employed for data collection. The collected data is then transmitted to the second layer, referred to as the Conversion Level, where data is processed into information using techniques like statistical analysis and machine learning algorithms. Finally, the third layer, termed the Cyber Level, utilizes the data and information to generate knowledge primarily through data analytics and artificial intelligence tools.

In this context, every stakeholder can utilize the Connection Level of their CPS to collect the necessary technical and environmental attributes for the DPP. The Conversion Level is tasked with processing this data and transmitting it to the Cyber

Level, where technical parameters, environmental impact indicators based on the EF methodology, and the corresponding thresholds are made accessible. Consequently, each stakeholder's digital space will contain pertinent product technical parameters and environmental impact indicators along with associated PBs thresholds, which can then be forwarded to the DPP. This process can be facilitated, for instance, through decentralized technologies as previously detailed in the Section 4.2.2 of the present doctoral thesis. Figure 29 illustrates the envisioned framework for the digitization of the product value chain and the completion of the DPP, using a generic product value chain phase as an example. The extent to which each level is populated can vary depending on the particular product and stakeholder in question. For example, a stakeholder supplying raw materials to a product manufacturer would transmit information solely pertaining to the initial 2 levels (connection and conversion). Conversely, a stakeholder contributing a component to the product manufacturer would provide information encompassing all 3 levels of the CPS.

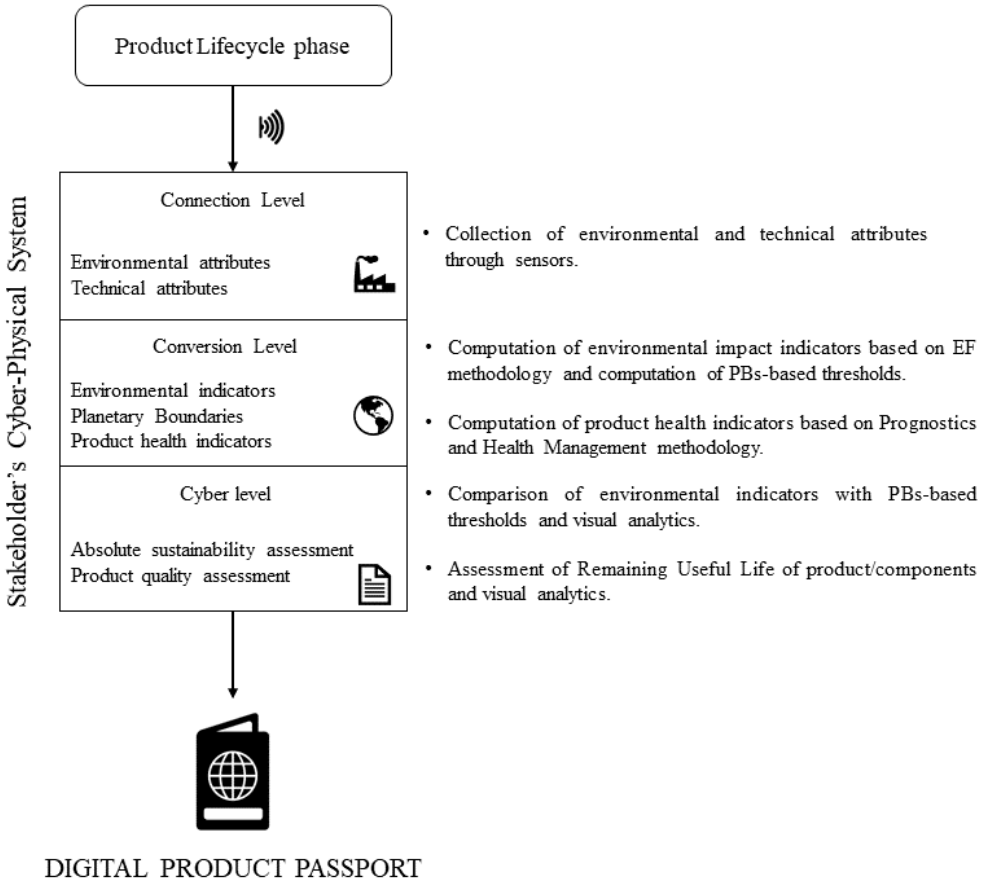


Figure 29: Use of stakeholder's CPS to fill the DPP.

In accordance with the value chain model adopted as a reference in this research, the stakeholders engaged in materials sourcing establish a linkage between their digital space and the DPP to transmit the identified environmental and technical attributes. As the materials progress to the subsequent stakeholders involved in the transformation and assembly phase, they will update the DPP by incorporating additional environmental and technical attributes from their own digital space.

When the product is delivered to the end-users, information can be collected through various methods. If the product is equipped with sensors, the DPP can be automatically updated by extracting environmental and technical attributes from sensor data. Alternatively, technical attributes can be directly ascertained at the end of the usage phase using Non-Destructive Testing techniques, including computed tomography, ultrasonic testing, thermographic inspection, and other relevant

methods. Furthermore, reverse engineering techniques like 3D scanning systems can be employed to detect alterations in the product's geometry resulting from wear mechanisms. These approaches contribute to maintaining the DPP with accurate and pertinent information.

Upon the conclusion of the usage phase, in alignment with the chosen recovery scenario, which can be broadly categorized as reusing, remanufacturing, or recycling, new environmental and technical attributes need to be documented. The stakeholders responsible for these actions will then update the DPP accordingly.

Figure 30 depicts the conceived framework applied to the entire circular value chain system.

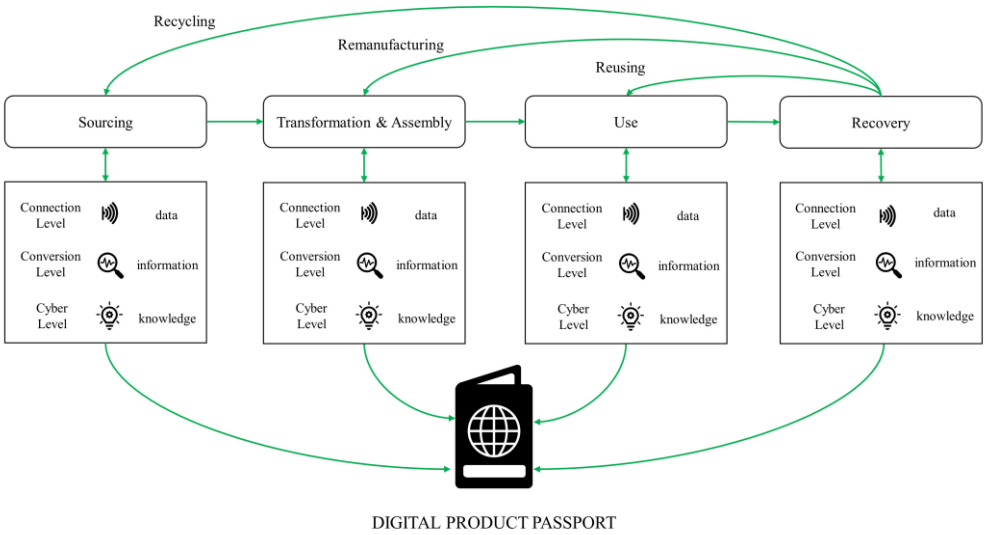


Figure 30: Use of CPSs for filling the DPP throughout the product lifecycle.

4.5 Main contributions and limitations

This research has presented the existing status of DPP and emphasized the necessity of incorporating an absolute environmental sustainability perspective into it. More precisely, a collection of environmental attributes and environmental impact indicators has been suggested, utilizing the LCA methodology, in conjunction with associated threshold values based on the PBs framework. The introduction of these proposed elements to the DPP will enable the evaluation of

products' absolute environmental sustainability. Introducing these novel concepts to the DPP literature serves the purpose of enhancing the decision-making process for the stakeholders within a product value chain. The intention of this research is not to replace existing frameworks and methodologies found in the literature related to the DPP, but to complement them, providing a more comprehensive perspective and enhance sustainability-oriented innovation at the value chain system level.

Furthermore, a framework based on CPSs to digitalize the product passport has been proposed, enabling the collection of environmental and technical information throughout the value chain. This digitalization process allows stakeholders in the product value chain to store and share all the necessary product-related information required for assessing its absolute environmental sustainability, as well as to implement CE principles. In fact, by saving all the relevant information into a single information system, i.e. the DPP, the information flow needed to implement a circular value chain discussed in section 4.1 can be finally realized.

Moving forward, some limitations can be acknowledged and addressed in the future. Firstly, the design and implementation of a software platform to support digital product passports will be crucial, considering aspects such as data security and standardization. To address data security concerns and protect stakeholders engaged in data sharing, the adoption of crypto-anchors and BC technologies can be considered, as they provide robust mechanisms for safeguarding data. Additionally, seamless data integration across various value chains should be ensured to maintain coherence and consistency.

Another critical research area concerns the incorporation of social data within the DPP. Social data, given their subjective nature and susceptibility to diverse cultural values and perceptions, demand standardization to ascertain which entity is responsible for gathering and documenting such data in the passport. According to United Nations Environmnet Program (UNEP) [133], social data collection often relies on licensed databases such as PSILCA. Alternatively, when primary data is necessary, it can be acquired by visiting specific production facilities or through collaboration with relevant organizations. Primary data can be obtained through direct engagement with organizations and companies, working alongside Non-Governmental Organizations (NGOs) or similar entities, observing on-site business and production procedures, or conducting interviews and surveys with affected stakeholders, such as workers.

Lastly, it is imperative to evaluate the sustainability of the digitization process itself. While digitalization holds significant promise for the CE, it is crucial to acknowledge that Information and Communication Technology (ICT) consumes a substantial amount of energy, leading to environmental emissions. In fact, ICT technology demands a noteworthy share of electricity, accounting for 5% to 9% of total electricity consumption, with an anticipated increase to 20% by 2030. Digitization presents invaluable prospects for advancing the CE, but this transition should be coupled with an increase in the adoption of clean energy sources and enhanced energy efficiency [26]. Therefore, efforts directed at digitalization must be accompanied by a simultaneous escalation in the utilization of clean energy sources and improved energy efficiency to counteract the environmental impact associated with ICT technologies.

The establishment of a DPP can be crucial to enhance sustainability at system level when the product architecture, strongly linked with the value chain configuration, is emerged. Thus, this work contributes to sustainability-oriented technological innovations at system level with a major applicability in the second phase of a technology lifecycle, i.e., when the dominant design emerges and, hence, the product architecture of a technology is affirmed in the market (Figure 8).

Chapter 5

Technological innovation at process level for sustainable manufacturing

This research is also published in an article titled “Use of electrode displacement signal for electrode degradation assessment in Resistance Spot Welding” in the Journal of Manufacturing Processes [134].

5.1 Theoretical background

After having presented an example of sustainability-oriented technological innovation at product level, more suitable during the onset of a technology lifecycle, and at system level, more suitable during the transition phase of a technology lifecycle when the dominant design is emerged, the last research carried out during the doctorate deals with the last type of innovation activities, focused on the process level. As explained in the chapter 2, this type of innovation is more suitable when both the product and value chain system are already optimized, and innovations can be achieved by optimizing process operations. To this end, the work developed in this chapter is presented directly on a case study relating to a manufacturing process that exhibits great opportunity in terms of incremental sustainability-oriented innovations, i.e., the Resistance Spot Welding (RSW) process.

In the context of ongoing global market expansion and escalating environmental challenges, the manufacturing sector needs to continuously enhance its operations. The maximization of asset value and resource efficiency becomes imperative to align with the goal of a sustainable manufacturing. Maintenance functions constitute a vital component of modern manufacturing organizations, contributing significantly to resource efficiency, downtime minimization, quality assurance, and the preservation of competitive advantages in the market. Maintenance activities in the manufacturing sector can account for a significant portion of the total production costs, ranging from 15% to 60% [135]. This

highlights the imperative for companies to enhance their maintenance tools. This, in turn, would result in a decrease in the overall production cost, as well as the price of the final product. Historically, manufacturers have consistently sought methods to achieve an equilibrium in maintenance operations, ensuring both system reliability and productivity are upheld [128].

However, a recent trend analysis, which involved interviews with over 230 senior European business leaders, revealed that approximately 93% of respondents suffer of inefficient maintenance policies [136].

As an example of the criticality linked with maintenance issue, it is reported that, for each minute of downtime, a typical automotive assembly line experiences a financial loss of $20,000 [128]. Resistance Spot Welding (RSW) is a widely used joining process in the automotive assembly line because of its ability to join sheet metal components, such as body panels and frames, with strong and reliable welds. This process is favoured for its speed, precision, and suitability for high-volume production, making it a key technology in automotive manufacturing [137].

In the RSW process, two electrodes initially apply pressure to the sheets being joined for a specified duration known as the *squeeze time*. Subsequently, a high electric current passes through the electrodes and the stack of sheets for a predetermined period referred to as the *weld time*. The heat generated by the Joule effect supplies the thermal energy necessary to locally melt the sheets and create the nugget, i.e. the junction. Figure 31 provides an illustrative representation of the RSW process.

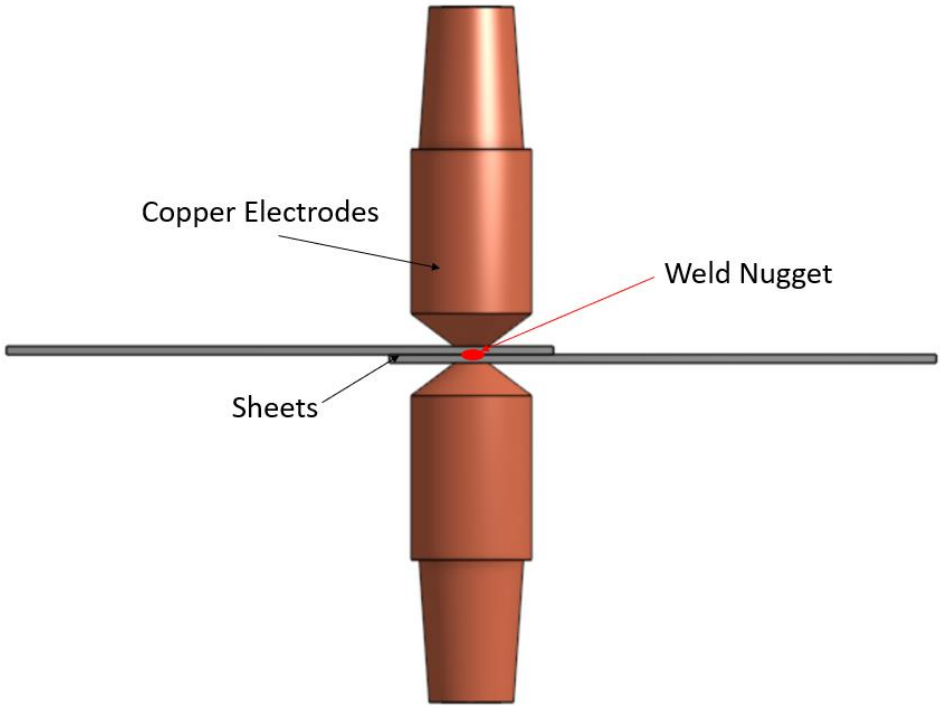


Figure 31: Schematization of the RSW process.

The quality of an RSW joint is significantly influenced by the nugget size, which is considered a primary key indicator of joint quality [138]. Achieving the desired nugget size begins with the accurate configuration of the spot weld cycle, schematically represented in Figure 32. This requires the definition of the following process parameters:

- Squeeze time: It represents the time duration (in milliseconds) during which pressure is applied to the electrode before activating the electric current.
- Weld time: It represents the time duration (in milliseconds) when the electric current flows through the electrodes.
- Hold time: It represents the time duration (in milliseconds) during which pressure is applied to the electrode after the electric current is turned off.
- Weld current: it is the intensity of electric current (kA).
- Electrode pressure: It represents the pressure (in bars) applied to the electrodes for clamping the material sheets.

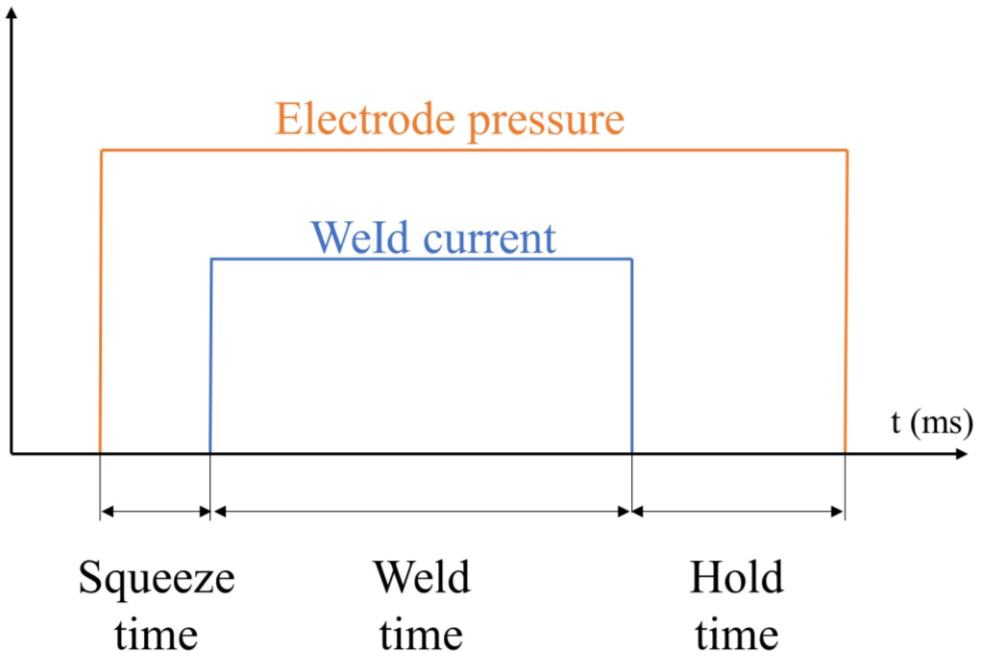


Figure 32: Schematization of a spot weld cycle

However, the correct definition of the process parameters does not guarantee a flawless joint. Other factors, including shunting, edge proximity, initial sheet gaps, and electrode degradation, can serve as potential sources of welding defects and, consequently, result in non-compliant joint quality [139]. The first three factors can be mitigated through appropriate joint design; instead, the electrode degradation plays a pivotal role. In fact, this process is currently struggling with significant inefficiencies associated with electrode degradation. It is estimated that approximately 60% of defective spot welds can be attributed to electrode wear [140]. For each car body, the literature reports that automotive manufacturers typically execute 20% more welds than necessary, which amounts to an excess of 1000-1200 welds, as a precaution to account for uncertainty related to the electrode conditions [140]. Moreover, it is estimated that a high-volume automotive production line produces approximately 7 million welds every day [141].

Electrodes are subjected to numerous complex and diverse forms of damage, including plastic deformation, pitting, creep, and thermal fatigue because of the simultaneous impact of extreme temperatures, significant mechanical pressure, and atomic diffusion between electrodes and sheets during the process. These factors render the prediction of electrode condition highly challenging [142].

Several resource-efficiency improvements may be achieved if the electrode state could be real-time monitored in the assembly production lines: fewer spots may be performed reducing both energy and resource consumption, the productivity would be increased, and the electrodes could be replaced or dressed only when needed [143], [144].

With the advent of Industry 4.0 paradigm, the cost in sensor equipment and computing resources has drastically decreased by enabling the adoption of intelligent monitoring systems. These systems facilitate the application of Prognostics and Health Management (PHM) techniques to a wide array of assets spanning various industries [136]. PHM is conceived as a proactive maintenance approach for modern manufacturing systems in recent years. In accordance with IEEE Standards (2008), PHM is defined as "*systematic approaches for maintenance and asset management, which utilizes signals, measurements, models, and algorithms to detect, assess, and track degradation, and to predict failure progression*" [145]. PHM typically encompasses functionalities such as condition monitoring, health assessment, fault detection and diagnostics, fault prognostication, and offering decision support for operation and maintenance towards sustainable manufacturing [145]. Thus, PHM activities can be strongly support the development of sustainability-oriented process innovations.

In this context, the present research aims to propose a data-driven tool for the health assessment of industrial assets in order to support sustainability-oriented process innovation activities. In contrast to the previous studies, the aim and novelty of this work are to develop a machine learning tool capable of predicting the quality in real-time the electrode degradation. This tool allows for an automatic assessment of the electrode contact area based on data collected from sensors, providing crucial insights for maintenance operations. By proactively replacing or dressing the electrode before it starts producing low-quality welds, redundant welds can be avoided or drastically reduced. Eliminating these unnecessary additional welds results in time, energy, and resource savings for manufacturers, thereby contributing to a substantial enhancement in the sustainability of the manufacturing process.

5.2 Literature analysis

Over the recent years, significant focus has been directed towards monitoring the welding process with the aim of extracting valuable information from welding

signals (e.g., welding voltage and power, electrode displacement, dynamic resistance of the sheet stack). This is done to manage the process effectively, ensure high-quality welds, and provide real-time predictions of nugget size and mechanical strength of the spot welds.

For instance, Zhao et al. [138] utilized features extracted from the electric power signal to train a Neural Network (NN) for predicting the nugget size of spot welds. In a similar way, X. Wan et al. [146] developed an NN using features extracted from the voltage signal to forecast various quality parameters, including weld strength and nugget size. Furthermore, the same authors [147] applied an NN to predict both the nugget dimensions and the mechanical strength of spot welds, based on features extracted from the electrical resistance signal. Additional research efforts have focused on weld quality prediction with an emphasis on analyzing electrode displacement during the welding process [148], [149]. Xia et al. [150], then, established a clear link between abrupt changes in electrode displacement during welding expulsion and the corresponding amount of expelled material. L. Zhou et al. [139] explored two distinct adaptive control strategies: one based on electrode displacement signals and the other on dynamic resistance signals, to monitor the welding process under non-optimal conditions. When welding spots were positioned close to the edges of sheets or when there were gaps between the sheets to be welded, the control strategy employing electrode displacement signals outperformed the one utilizing dynamic resistance signals from the sheet stack. Finally, Zhao et al. [151] harnessed process signals to determine optimal values for several welding quality indicators, including nugget size, mechanical strength, peak electrode displacement, and stored energy within the joint before reaching the point of failure.

In all these works, statistical methodologies and/or NNs were employed to forecast variables such as nugget size, failure load, and welding anomalies (e.g., metal expulsion). However, these studies did not take into account the impact of electrode wear. This phenomenon can be neglected in experimental tests where a limited number of spots are created with new, unused electrodes. However, it assumes significant importance in spot weld quality when electrodes are subjected to hundreds of cycles of use, as is common in industrial production. In such cases, electrodes undergo various complex forms of damage, including plastic deformation, pitting, creep, and thermal fatigue [142]. These issues result from the combined effects of high temperatures, substantial mechanical pressure, and atomic diffusion between the electrodes and the sheets [152]. This degradation manifests in various macroscopic evidences.

On the one hand, the irreversible deformation of the electrode tips leads to an increase in their contact area, which subsequently reduces the current density. Consequently, welding with the same current value as when the electrodes were new results in poor quality spots due to inadequate current density. On the other hand, electrode wear leads to an irregular distribution of electric current within the sheet stack, contributing to the deterioration of joint quality and a reduction in the repeatability of welding performance. For these reasons, parameters such as electrode tip diameter and contact area are commonly recognized as indicative of electrode degradation [149].

Numerous studies have examined the impact of electrode wear on weld quality, but they often lack precise methodologies for quantitatively predicting electrode degradation [153]. Traditional works [152]–[155] have explored the characteristics of electrode wear and their impact on spot weld properties providing valuable insights. Statistical process control techniques have been developed based on the electrode displacement signals for monitoring the welding process during electrode wear [156]. The electrode displacement signal was also used to monitor the electrode wear through a moving range chart [157]. Fan et al. investigated the relationship between the dynamic resistance signal and the electrode tip radius. They found that the average value of the signal during the nugget growth stage has a strong relation with the electrode contact radius [158]. Zhou et al. [140] used the dynamic resistance signal to evaluate electrode wear through similarity techniques among the signals of the welding parameters. The work available at [159] assessed inline electrode wear occurring during the welding process without the need for extra sensors. The tests conducted demonstrate a correlation between the deformed contact area and the change in electrode length. The study reveals that this alteration in electrode length is discernible in real-time process data, making it a suitable criterion for characterizing electrode wear. In the work [160], an adaptive control scheme employing fuzzy Proportional-Integral (PI) control is examined and developed to compensate the effect of electrode wear on the electric current. Within each control cycle, features from the dynamic resistance and welding power serve as inputs for the fuzzy controller. By using current closed-loop feedback control, the fuzzy PI controller output manages the full bridge inverter on and off switching to maintain a steady welding current. Simulation and experimental outcomes demonstrate that this approach offers several advantages compared to traditional PID control methods. The study [161], instead, investigated the effect of electrode wear by means of electrical-thermal-mechanical simulations. The model validity

was confirmed by comparing simulated temperature and voltage results with experimental measurements. Findings show that electrode wear leads to an increase in resistance and temperature at the electrode tip rather than a decrease. To address this, it is recommended to lower welding parameter values instead of increasing them. Consistently, maintaining a controlled temperature rise at the electrode tip is crucial for ensuring welding quality in the presence of electrode wear. Heilmann et al. [162] studied the electrode wear in RSW of aluminum sheets. Specifically, they proposed mitigating electrode wear by mechanically disrupting the oxide layer before welding. This study explored the impact of both translational and rotational movements of the electrode on wear, and the findings indicate that oxide layer disruption occurs even at low movements. However, achieving a uniform and extensive destruction is crucial for effectively reducing wear. More recently, Zhao et al. [163] investigated the degradation process of electrodes in baked hardening (BH) 220 steel. They identified several analytical relationships between the weld number and different nugget features, mechanical properties, and electrode characteristics. Noteworthy examples include the relationships between the weld number and the maximum displacement of the weld sample in mechanical tests, peak load, failure energy, and electrode diameter, with an adjusted coefficient of determination exceeding 0.90.

Although many studies have addressed the electrode wear problem in RSW, car manufacturers are still coping with the uncertainty associated with the electrode degradation process, forcing them to perform up to 20% of redundant welds. In an industrial setting, the evaluation of electrode degradation typically depends on the experience of human operators or qualitative assessment, rather than on quantitative methodologies. The absence of a real-time and objective system capable of relating the electrode degradation with joint quality results in an excess of approximately 1000-1200 spot welds in a car body. As already discussed, these extra welds are introduced as a precaution to account for the potential presence of substandard joints [140]. This leads to increased resource consumption. This includes higher energy usage for additional welds, which could otherwise be avoided if there were a real-time and objective system to accurately monitor electrode degradation and its impact on joint quality. Reducing the number of unnecessary welds would result in more efficient resource utilization in the automotive manufacturing process, which is especially crucial in an era of increased focus on sustainability and resource conservation. For these reasons, the capability of quantitively predict electrode degradation in real-time would result in a sustainability-oriented process

innovation that would contribute to advance sustainability in the automotive industry.

5.3 Methodology

Figure 33 displays the systematic approach adopted for the development of a data-driven health-assessment tool of industrial assets. Such methodology is based on the PHM approach and it is articulated in 5 main steps.

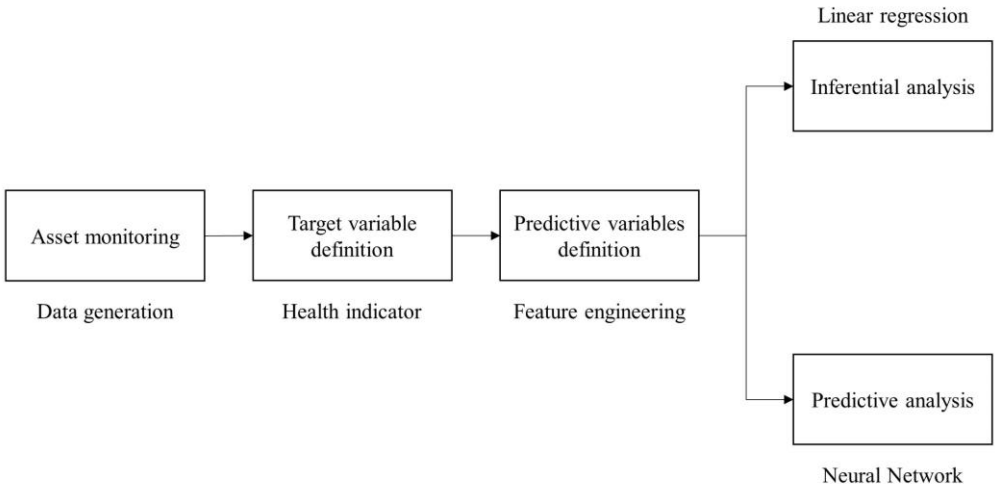


Figure 33. Data-driven methodology for the health assessment of industrial assets.

The initial step is the identification of the critical asset to be monitored; the essential components that exert a remarkable influence on the manufacturing process' performance, availability, reliability, and productivity, need to be detected. Subsequently, the condition of these components need to be continuously observed to detect and diagnose faults.

5.3.1 Asset monitoring

The first step involves designing an appropriate method for data generation. Data can be generated in different ways, such as simulation models, real experiments, etc. The goal of this step is to collect informative data to be furtherly processed. It is crucial to consider, since this step, how to induce the degradation process in the monitored asset, how to quantify it accurately by choosing one or more suitable health indicators, and to develop a preliminary concept for predicting

it/them. In this work, data are generated from real experiments that will be presented in the results section.

5.3.2 Target variable definition

The second step deals with the definition of an health indicator that is representative of the monitored asset. Different health indicators can be considered, and the one that most accurately reflects the asset's performance is selected as the target variable for the predictive tool. The health indicators considered in this work are different geometrical features of the electrode, while the asset's performance is represented by the mechanical strength of the spot weld. Thus, the health indicator that better represents the mechanical strength of the spot weld is chosen as target variable.

5.3.3 Predictive variables definition

Data collected in the step 1 are processed to obtain the predictive variables of the tool. Inspired by the approach outlined in the work [164], the procedure for defining predictive variables from the raw data obtained from real experiments is detailed in the subsequent section.

Pre-processing

A preliminary data processing is essential to check the data accuracy and obtain manipulable time series data. This sub-step encompasses data cleaning and validation and is typically entrusted to the edge computing components of the IoT system [165]. The primary functions of this sub-step include:

- Conducting a preliminary validation of each individual operation (ensuring correct manufacturing operations).
- Selecting the relevant time window (selection of the range of data relating exclusively to the period of machine operation).
- Smoothing of the time series to remove the noise from the signal and get manipulable data.

In experiments supervised by expert operators, the preliminary validation of manufacturing operation can rely on the operator's experience. As explained in earlier sections, the weld spot cycle initiates with the squeeze time and concludes with the hold time. Therefore, the electrode force signal can be utilized to determine the machine's activity period in RSW. Regarding the smoothing activity, a common

technique employed is the moving average smoothing. The latter is a statistical technique used to reduce noise or random variations in a time series data or signal. It involves calculating the average of a fixed number of data points within a moving window and using this average to represent the smoothed value at the center of the window. The purpose of moving average smoothing is to emphasize underlying trends or patterns in the data by removing short-term fluctuations.

Feature extraction

In this step, valuable information can be extracted from the time series data using feature extraction techniques. This approach helps conserve computational resources for subsequent algorithmic learning tasks. Time-domain statistics can be computed from various types of process signals. Depending on the nature of the sensor measurements, a range of features can be extracted, including but not limited to the mean, maximum, minimum, rise time, fall time, increase rate, decrease rate, amplitude increase, amplitude decrease, variance, skewness, Euclidean distance between consecutive curves, and more. A similar approach can also be applied in the frequency domain to augment the dataset with significant insights.

Feature selection

Lastly, a feature selection process is valuable to further reduce data dimensionality by retaining the most informative features. To create an effective feature selection strategy, various techniques can be applied, including correlation-based analysis among predictor variables, correlation-based analysis between predictor variables and target variables, hypothesis testing, monotonicity analysis, and predictability analysis [164].

Feature scaling

After selecting features from time series data, it is necessary to scale them to address differences in magnitude. Feature scaling aims to bring the data into a comparable range, enhancing the convergence of future algorithms. Two appropriate techniques for normalization are min-max normalization and standardization. Min-max normalization scales the data within a specific range, typically between 0 and 1. It works by mapping the minimum and maximum values of the data to 0 and 1, respectively, and then linearly scaling all other values in between. Min-max normalization is useful when it is needed to ensure that all features have the same scale and fall within a specific range Standardization, also known as Z-score normalization, transforms the data into a standard normal

distribution with a mean of 0 and a standard deviation of 1. It subtracts the arithmetic mean value from each data point and divides it by the standard deviation. This can be particularly useful when working with algorithms that assume the data is normally distributed [166].

5.3.4 Inferential analysis

The purpose of an inferential analysis is to identify an accurate mathematical model that define a relationship between the most informative and independent predictive variables and the target variable. From an inferential perspective, the issue of multicollinearity among predictive variables is of paramount significance. In cases where predictive variables exhibit interdependence, the attribution on the target variable's influence may be inaccurately assigned. Thus, the first step is to study the interdependence among the predictive variables in order to set a correct inferential analysis. An effective method for addressing this issue is to compute a correlation matrix, which shows the Pearson correlation coefficients for each pair of predictive variables. The correlation coefficient of two variables is a measure of their linear dependence. If each variable has N scalar observations, then the Pearson correlation coefficient is defined as follows [167]:

$$r(A,B) = \frac{1}{N-1}\sum_{i=1}^{N}\left(\frac{A_i-\mu_A}{\sigma_A}\right)\cdot\left(\frac{B_i-\mu_B}{\sigma_B}\right) \quad (56)$$

where μ_A and μ_B are the arithmetic mean of A and B, σ_A and σ_B are the standard deviation of A and B, respectively.

Once that the most explanatory predictive variables are selected, a linear regression model can be applied. In its general form, a linear regression model is defined as follows:

$$Y = b_o + b_1x_1 + b_2x_2 + \cdots + \varepsilon \quad (57)$$

where Y is the dependent variable (target variable), x_i is the i-th independent variable (independent predictive variable), b_i is the i-th estimated model parameter, and ε is the residual between the observed value and the predicted one.

The determination of the model parameter is typically performed through a method called ordinary least squares (OLS), which minimizes the sum of the squared differences between the observed and predicted values [167]. Some metrics can be used to assess the significance of the estimated model parameters. For instance, the p-value in a two-sided hypothesis test can be used. The latter is a statistical analysis used to assess whether there is a significant difference between

a sample mean and a hypothesized population mean. If the p-value related to a model parameter is greater than 0.05, so this term is not significant at the 5% significance level given the other terms in the model [77]. Moreover, the confidence interval, i.e. the range of possible values of the model parameter at fixed confidence level (usually 95%), can be used. The narrower the confidence interval, the more accurate the parameter estimate [77].

The evaluation of the model's goodness of fit, instead, can be performed with the coefficient of determination (R^2), which measures how well the model explains the variance in the data [167]:

$$R^2 = 1 - \frac{\sum_{i=1}^{N} {e_i}^2}{\sum_{i=1}^{N} (y_i - \mu_y)^2} \quad (58)$$

where y_i is the observed value, N is the number of observations, μ_y is the arithmetic mean of the observed data, and e_i is the residual, i.e., the difference between the observed data and the predicted one.

Finally, the underlying assumptions regarding the use of a linear regression model need to be checked. The first assumption is that the residuals are normally distributed. This assumption is crucial because it ensures that the statistical inferences made about the regression coefficients and predictions are valid. If the residuals are not normally distributed, it can affect hypothesis tests, confidence intervals, and p-values. This assumption can be graphically checked by means of histogram of residuals and normal probability plot of residuals. The second assumption is that the variance of the residuals is constant (homoscedastic) across all values of the independent variables (predictive variables). Homoscedasticity is important because it ensures that the error terms are spread uniformly across the range of the independent variable values. If homoscedasticity is not met, it can lead to biased parameter estimates and incorrect confidence intervals. Plotting the residuals against the predicted values can be a helpful way to visually assess whether the spread of residuals is uniform across the predicted values [77].

5.3.5 Predictive analysis

The final step deals with the application of a predictive algorithm. The role of the predictive algorithm involves taking input data, i.e., the predictive variables, and generating predictions for the target variables. Although these tasks can be

accomplished by any supervised statistical model, ML algorithms are generally preferred because of their superior predictive performance [165]. It is essential to partition the entire dataset obtained during the data processing phase into three subsets: the training set, the validation set, and the test set. The training set is employed to train the ML algorithms, the validation set is utilized to fine-tune the models' hyperparameters, while the test set assesses the overall performance of the chosen algorithm.

In this work, a Neural Network (NN) has been employed. A NN is a supervised regression algorithm capable of predicting a target variable based on the values of the explanatory features taken as inputs [81]. A NN is organized in layers, and each layer is composed by different computation units, called activation units, that represent the neurons of the network.

The vector of input features X feeding the network represent the first layer, called input layer. The second layer of the network represents the first hidden layer, and it is generated by multiplying a weight matrix W^1 to the vector of input features X, by adding a vector of bias unit b^1, and then by applying an activation function g. The same approach can be repeated multiple to create L hidden layers, where for each layer $l \epsilon L$, a vector of activation units A^l can be defined as follows.

$$A^l = g(W^l \cdot A^{l-1} + b^l) \tag{59}$$

The process is repeated until to reach the final layer, where the prediction of the target variable $y_{predicted}$ is contained.

$$y_{predicted} = g(W^L \cdot A^{L-1} + b^L) \tag{60}$$

The variable of the NN are the weight matrix $W^l, \forall l \in L$ used to go from one layer to another. The values of weight matrices are iteratively learned by getting the predictions as close as possible to the observed values. This is done by defining an average loss function J that must be minimized on the training set by means of optimization techniques. More details on the mathematical definition of NNs can be found at [81].

The number of hidden layers, the number of neurons per each layer, the choice of the activation function, and the choice of the optimization technique depend on the available computational resources, the desirable performance, as well as by the quantity and quality of training set data.

The performance of the NN can be assessed by computing several metrics, such as the mean error, the median error, and the standard deviation of the error, as well as their corresponding relative values.

At this point, a predictive tool is available to be used in real manufacturing setting. By gathering the predictive variables in real-time, the ML algorithm can provide predictions of the target variable, which represent the health assessment of the monitored asset. In such a way, the health state of the electrode can be known in real-time and the uncertainty connected with the electrode wear can be reduced, as well as the number of redundant welds. The application of such methodological framework is shown in the following section.

5.4 Results and discussion

The results coming from the application of the methodology described above are reported and discussed in the following.

5.4.1 Asset monitoring

As anticipated earlier, in this research the asset was monitored through real experiments. The experimental study encompassed over 1200 spot welds conducted on 1 mm thick DP590 galvanized steel sheets, a material commonly used in the automotive industry [149], [153], [134]. These sheets are frequently employed in the automotive industry for manufacturing car body components such as wheel webs, lightweight sections, strut mounts, fasteners, and more [168].

The spot welds were created using an industrial 650 kVA medium-frequency direct current (MFDC) RSW machine, equipped with a TE700 control unit manufactured by Tecna Industry. The measurement of electrode displacement was performed using a magnetostrictive linear position sensor, model Temposonics R-series, boasting a position resolution of 2 μm and an acquisition frequency of 40 kHz. This sensor utilizes a CANBasic communication protocol output with a baud rate of 500 kbit/s. The linear position sensor, shown in Figure 34, is a certified industrial solution commonly employed in advanced welding machines. Electrode displacement signals were acquired through a National Instruments NI-9862 CAN interface module and managed using LabVIEW software.

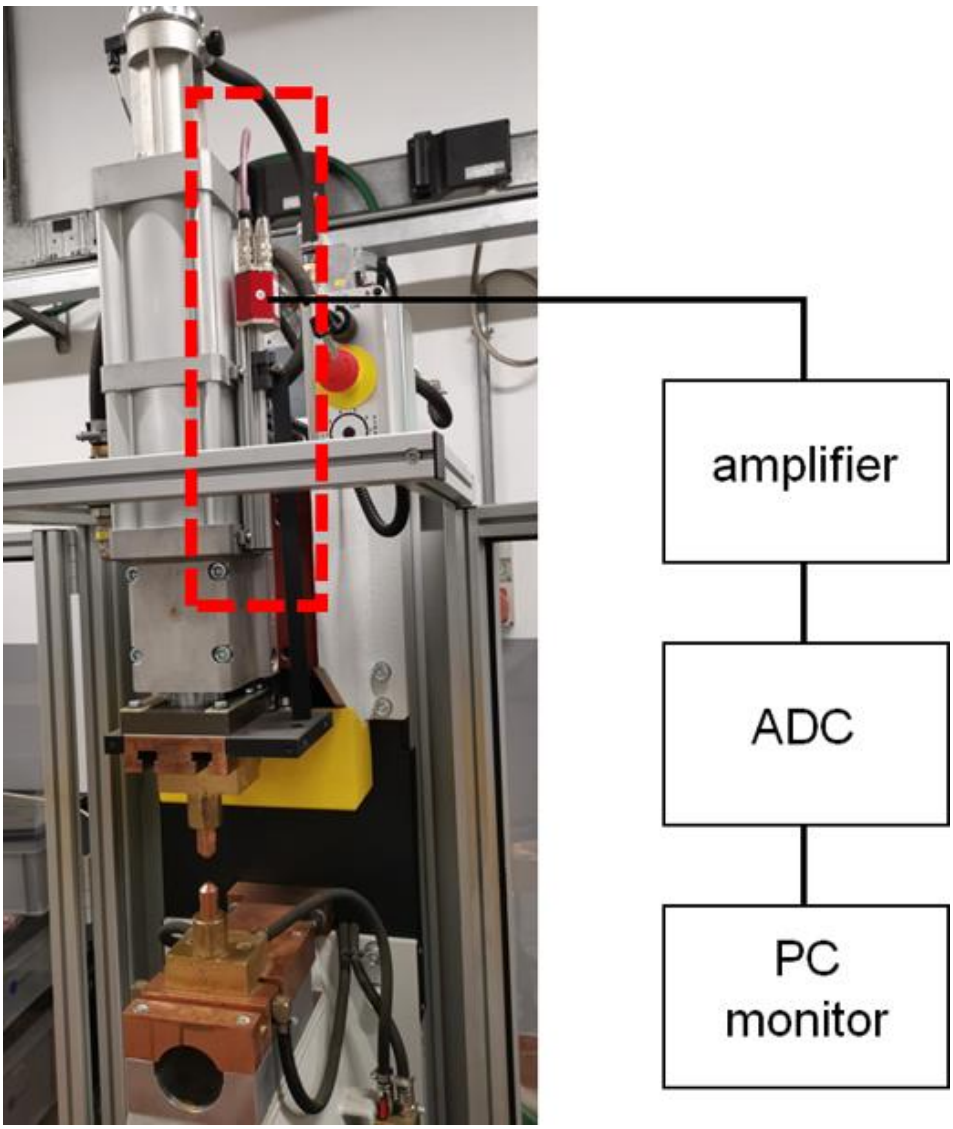


Figure 34: Linear position sensor embedded on the machine and structural block diagram.

The RSW machine was equipped with two truncated cone-shaped electrodes composed of Cu-Cr-Zr alloy, featuring a nominal contact diameter of 6 in accordance with the guidelines outlined in the AWS D8.9 M standard [169]. The detailed geometry of these electrodes is illustrated in Figure 35. Throughout the welding process, a water flow of 4 liters per minute was used to cool the electrodes. The lower electrode remained stationary, while the upper electrode moved to clamp the sheet stack.

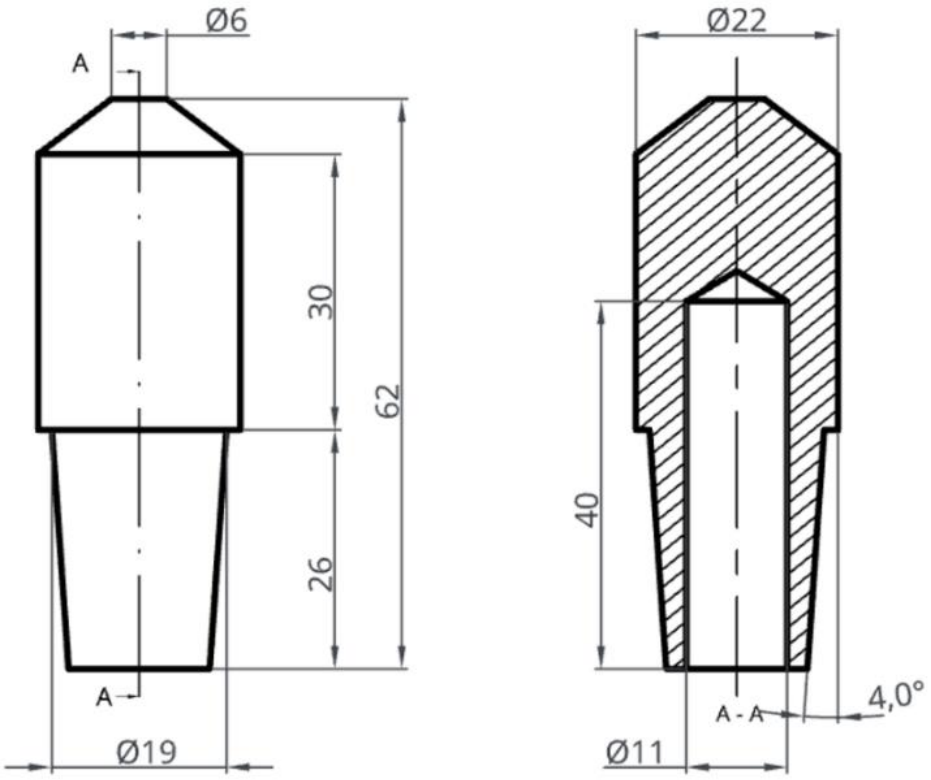


Figure 35: Geometry of the truncated cone electrodes.

An endurance test, conducted in compliance with the AWS D9.8 M standard, was undertaken to examine electrode degradation. Successive spot welds were produced employing the same welding cycle until the electrodes were fully worn out, determined based on the outcomes of shear tension tests. The spot weld cycle employed in the RSW tests is depicted in Figure 36. More in details, based on the material and thickness of the sheets, the AWS D9.8 M provides values for the electrode diameter, electrode force, and weld time. The electric current value was set as the maximum value before metal expulsion occurred. The RSW machine was set in 'current constant' mode, with the controller TE700 maintaining the set values of the electric current throughout the experiments.

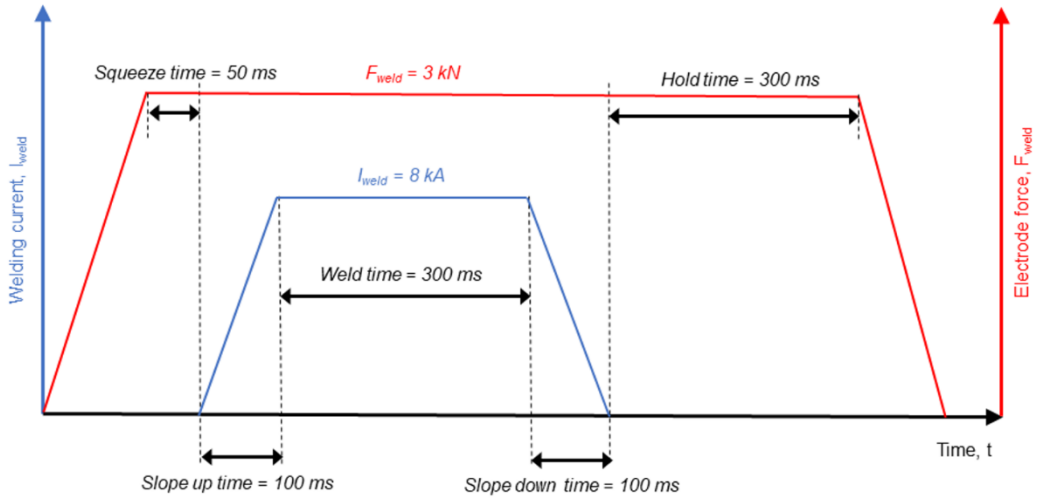


Figure 36: Schematization of the spot weld cycle used in the experimental campaign.

The endurance test involved the use of 9 pairs of overlapping sheets, referred to as panel welds, each measuring 300 mm x 200 mm (as illustrated in Figure 37). Each pair of sheets was subjected to spot welding along 9 rows, each consisting of 15 points. In total, 1215 spot welds were created. The prescribed edge and weld spacing distances, as well as the execution sequence, were consistent across all panel welds.

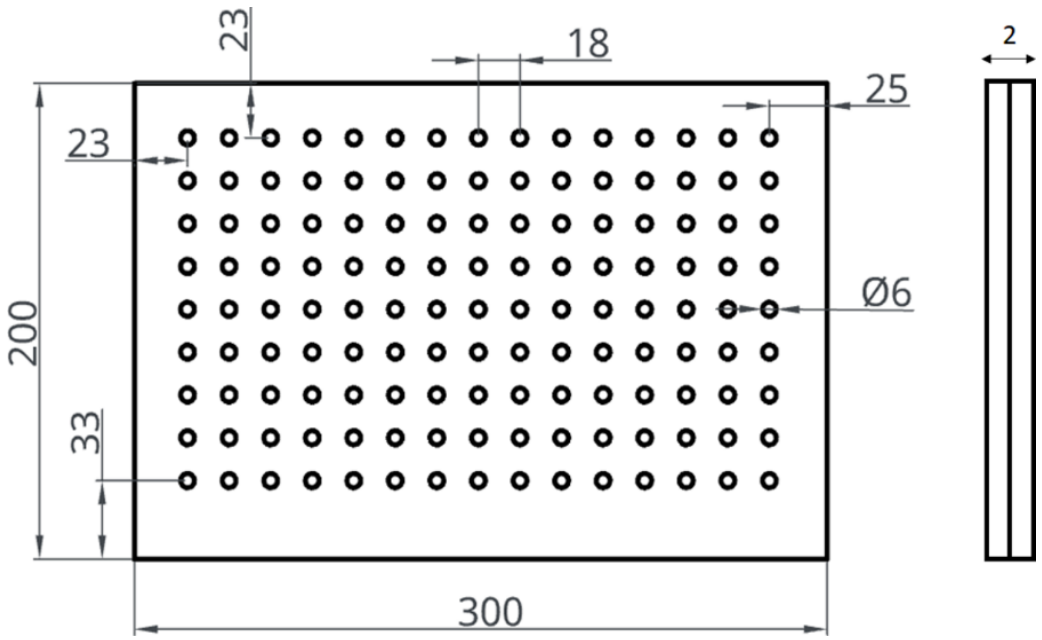


Figure 37: Edge and weld spacing distances used on the panel welds for the endurance test according to the AWS D9.8 M standard.

The welding campaign followed this procedure:

a) The initial contact area of unused electrode was assessed through a carbon imprint test. This involved using a metal sheet wrapped in two layers of paper. The outer layer was black carbon paper, while the inner layer was plain paper. A complete welding cycle was executed without electric current flow. The electrode imprints left by the carbon paper on the white paper served as a measure of electrode face damage. From the carbon imprint tests it is possible to extract geometrical characteristics to use as health indicator of the electrode.

b) The electrode displacement signal was zeroed by slightly closing the electrodes against the sheet stack without applying welding current. The zero signal was established when the electrode faces made contact with the sheet surfaces.

c) The first spot weld was made on the weld panel. Subsequently, three consecutive spot welds were performed on overlapped sheets to create three welded samples for shear tension testing. This allowed the determination of the mechanical strength of the weld spots produced using unused electrodes.

d) Additional spot welds were made on the overlapped sheets for the endurance test. After completing each row of 15 spot welds (as shown in Figure 37), electrode degradation was assessed through the carbon imprint test using imprints on plain paper. The endurance test continued, and after every 135 welds (equivalent to a couple of overlapped sheets), three welded samples were prepared for shear tension testing. This checkpoint of mechanical strength every 135 welds is a more stringent condition compared to the standard [169] (i.e., 200) and it allowed for a more detailed understanding of the impact of electrode degradation on the mechanical strength of spot welds.

e) These procedures were repeated for each of the 9 pairs of welded panels.

The shear tension samples, as per the JIS Z 3136 [170], measured 30 mm x 100 mm, with a 30 mm overlapping area, as illustrated in Figure 38. Shims were placed at the ends of the sheets to prevent bending of the weld panels during experimentation. Shear tension tests were conducted using a standard testing machine with a crosshead speed of 10 mm/min. The shear tension strength was determined as the maximum force attained during the test, and the peak load was used as the parameter to assess the impact of electrode degradation on joint quality. The critical wear damage of the electrode was identified as soon as the strength of

the spot welds fell below a predefined threshold value, set at 80% of the initial peak load [153], [155].

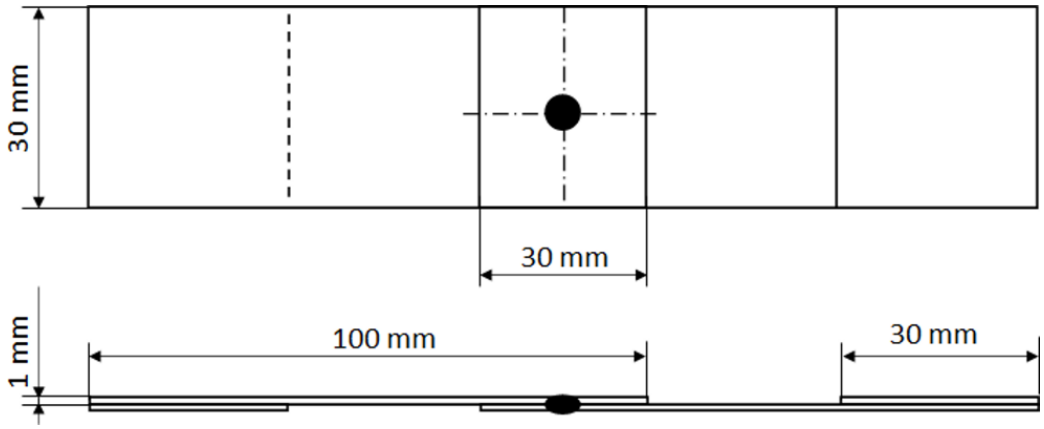


Figure 38: Geometry of the shear tension samples according to JIS Z 3136 standard.

The displacement of the moving electrode was recorded using a non-contact sensor for all spot welds conducted in the endurance test. These time-series data are used to subsequently define the predictive variables of this work.

The shear tension test results are presented in Figure 39. To distinguish weld spots with varying mechanical properties based on the number of welds, three colors (black, blue, and red) were employed. These colored points are also used in the subsequent figures in the main text.

- Black dots signify a region where the mechanical strength of the spot welds consistently exceeds the minimum shear strength value of 8 kN, displaying a narrow range of repetitive values (0-800 range).
- Blue dots represent a transitional zone in which the weld spots begin to exhibit decreased repeatability, accompanied by a significant reduction in weld strength (800-1000 range), with the occurrence of the first weld spot falling below the minimum value.
- Red dots denote an unstable welding process characterized by high variability in strength values, often dropping below the minimum shear strength. In this region (1000-1245 range), electrode wear is significant, resulting in undersized welded nuggets, frequently with localized unwelded areas.

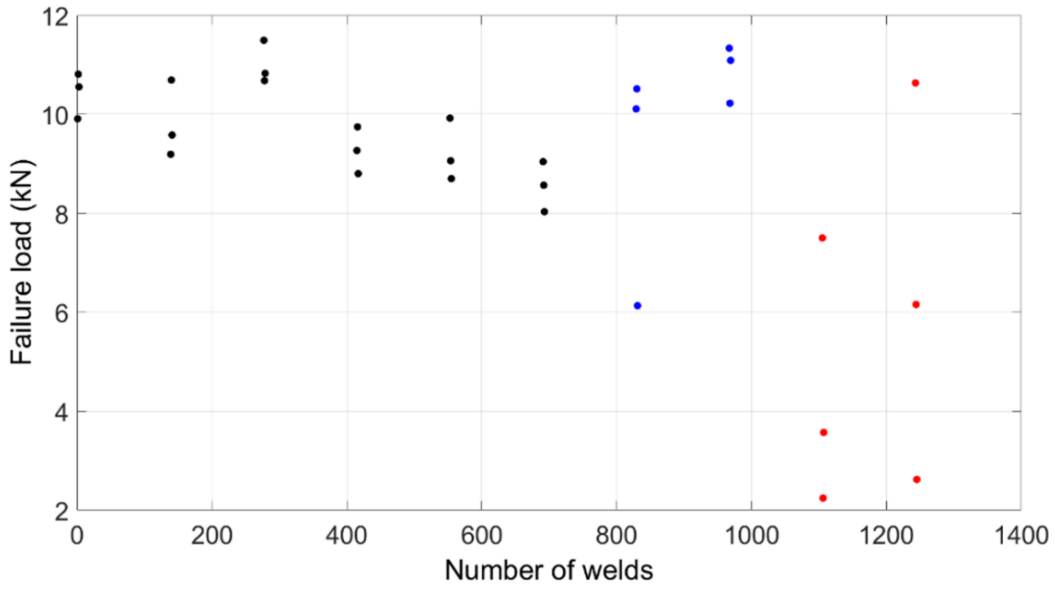


Figure 39: Shear tension strength of the welded spots at varying number of welds.

The observed trend in the strength data aligns with findings from previous studies in the literature that have examined the impact of electrode wear on the mechanical properties of spot welds [155], [154], [171].

5.4.2 Target variable definition

Geometrical features representing electrode degradation were derived from the carbon imprint tests using image processing techniques. Initially, the electrode imprints were scanned to convert them into image format. As shown in Figure 40, the carbon imprint test revealed electrode degradation through an increase in the contact area (depicted in black) resulting from plastic deformation at elevated temperatures, which also led to a reduction in electrode length. Furthermore, pitting damage (displayed in white) initially occurred at the edges of the electrodes before spreading to the central zone. The MATLAB Image Processing Toolbox was employed to extract various geometrical features from the scanned images, which could serve as potential health indicators of electrode [172].

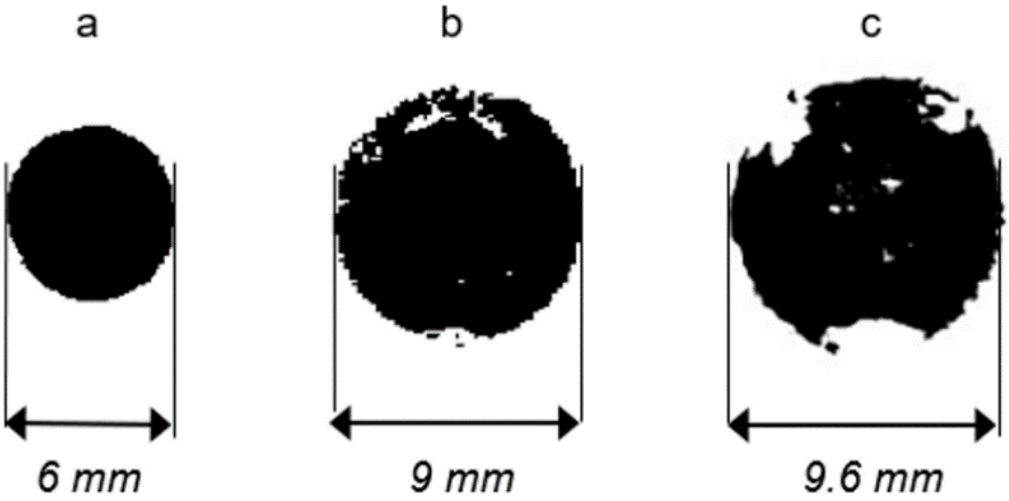


Figure 40: Electrode tip shape as obtained from the carbon imprint tests at a) 0 welds, b) 600 welds, c) 1200 welds.

The following geometrical features were calculated from the imprint images:

- Contact area: the number of pixels encompassed by the black region (contact zone) within the analyzed imprint.
- Equivalent diameter: the diameter of a circle with an area equal to that of the electrode's contact area.
- Major contact length: the number of pixels along the major axis of the ellipse that encloses the imprint.
- Minor contact length: the number of pixels along the minor axis of the ellipse that encloses the imprint.
- Perimeter: a linear measure of the pixels along the boundary of the imprint.

In order to identify the most suitable health indicator for describing electrode wear, the aforementioned geometrical features were graphed in relation to the

number of welds and failure load, as illustrated in Figure 41 to Figure 43.

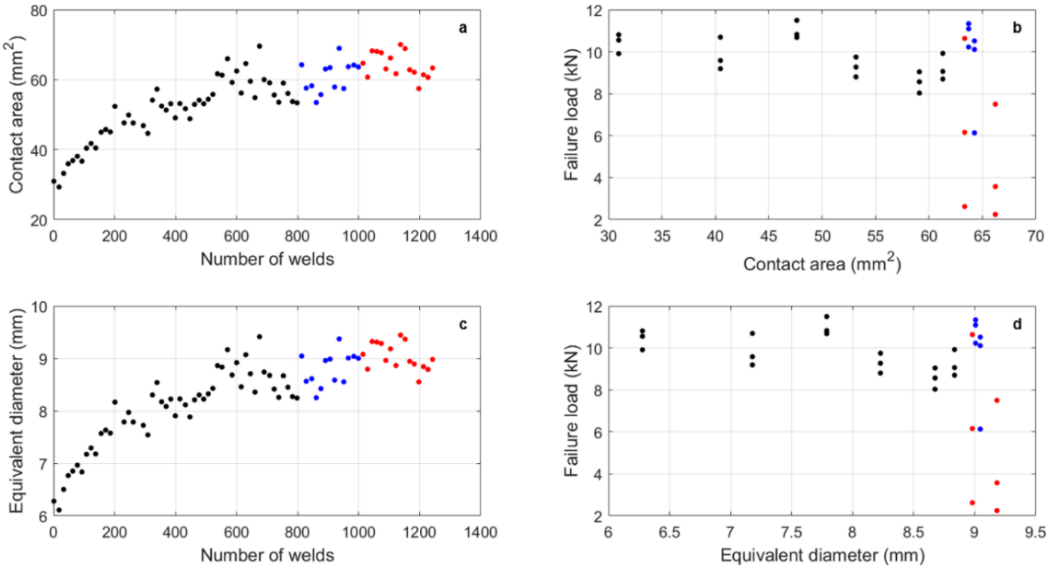


Figure 41: Contact area and equivalent diameter vs. number of welds and failure load

The contact area increases over time due to the plastic deformation of the electrode face at elevated temperatures, as seen in Figure 41a. Initially, this increase is characterized by low variability and a steep rate. However, as the pitting zones begin to form and expand, the variability becomes greater, and the rate of increase decreases. In Figure 41b, the failure load of the spot welds is plotted against the contact area. Initially, the mechanical strength of the spot welds remains relatively constant despite the increasing contact area. At this stage, the widening of the electrode's contact area is a result of the plastic deformation of the electrode tips, while the pitting zones have not yet formed. The electric current and thermal power distribution stay relatively uniform across the contact area and the sheet stack. As the number of welds continues to increase, pitting zones start to appear. Initially, this phenomenon has a positive impact. Some studies [155], [154], [171] found that the slight irregularity in thermal power distribution can encourage the formation of larger weld nuggets, leading to an increase in weld strength, as depicted in Figure 41b for a contact area of 47.5 mm^2 (approximately spot number 275 from the shear test results shown in Figure 39). However, when the pitting areas grow larger, in conjunction with oxidation and plastic deformation of the electrode tip, the uneven thermal power distribution consistently reduces the nugget size and the failure load of the spot welds. Once the electrode tip is significantly worn, typically after around 1000 weld spots, the welding process becomes highly unstable, and the weld nugget size, as well as the mechanical strength of the spot welds, cannot be effectively

controlled. This instability occurs when the contact area surpasses 62 mm^2, which is 2.2 times greater than the initial contact area. It is important to note the clear differentiation of the black dots from the others in the shear tension values displayed in Figure 41b. The equivalent diameter has been directly calculated from the contact area, resulting in a similar behavior for this feature, as shown in Figure 41c and Figure 41d.

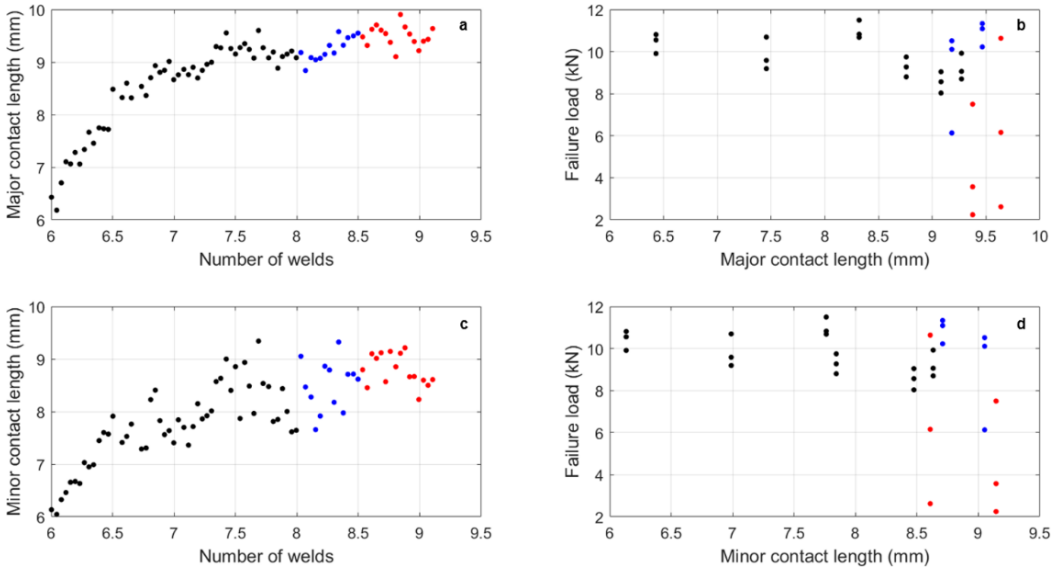


Figure 42: Major and minor contact length vs. number of welds and failure load.

The major contact length exhibits a consistent increase over time but with limited variability as the number of welds progresses (as shown in Figure 42a). However, this particular feature extracted from the electrode imprints does not effectively distinguish the different behaviors in relation to the mechanical strength of the spot welds. In the corresponding plot (Figure 42b), it is possible to observe areas with overlapped black, blue, and red dots, which indicate a lack of clear differentiation based on this feature. Instead, the minor contact length displays an increase over time with more pronounced variability (as depicted in Figure 42c). When this feature is examined in relation to the failure load of the spot welds, overlapped areas with different colored dots become apparent, highlighting the challenges in using this feature to distinguish the mechanical strength of the spot welds (as seen in Figure 42d).

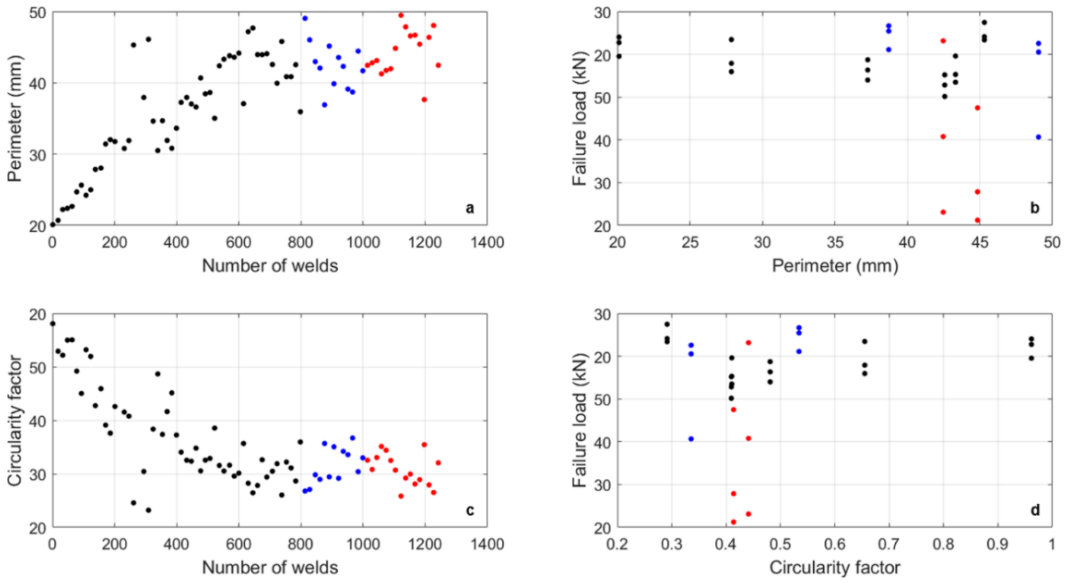


Figure 43: Perimeter and circularity factor vs. number of welds and failure load.

The perimeter of the electrode imprints exhibits a general increase, although with significant variability (as depicted in Figure 43a). The circularity factor, on the other hand, steadily decreases until approximately 700 welds and subsequently exhibits a variable trend (shown in Figure 43c). However, when both of these features are plotted against the failure load of the joint, they do not reveal a distinct transition between acceptable joints and improper spot welds. In these plots, black, blue, and red dots overlap in certain regions, as illustrated in Figure 43b and Figure 43d. Consequently, these features cannot be considered suitable health indicators for the electrode.

Of all the factors analyzed in Figure 41 to 43, the relationship between the failure load and the contact area, as shown in Figure 41b, exhibits a pattern similar to the shear test results presented in Figure 39. Furthermore, as previously discussed, the contact area allows to determine when the electrode enters in an instability state (specifically, when the contact area is 2.2 times greater than the nominal value) and, thus, it must replaced or dressed. This is emphasised in Figure 44.

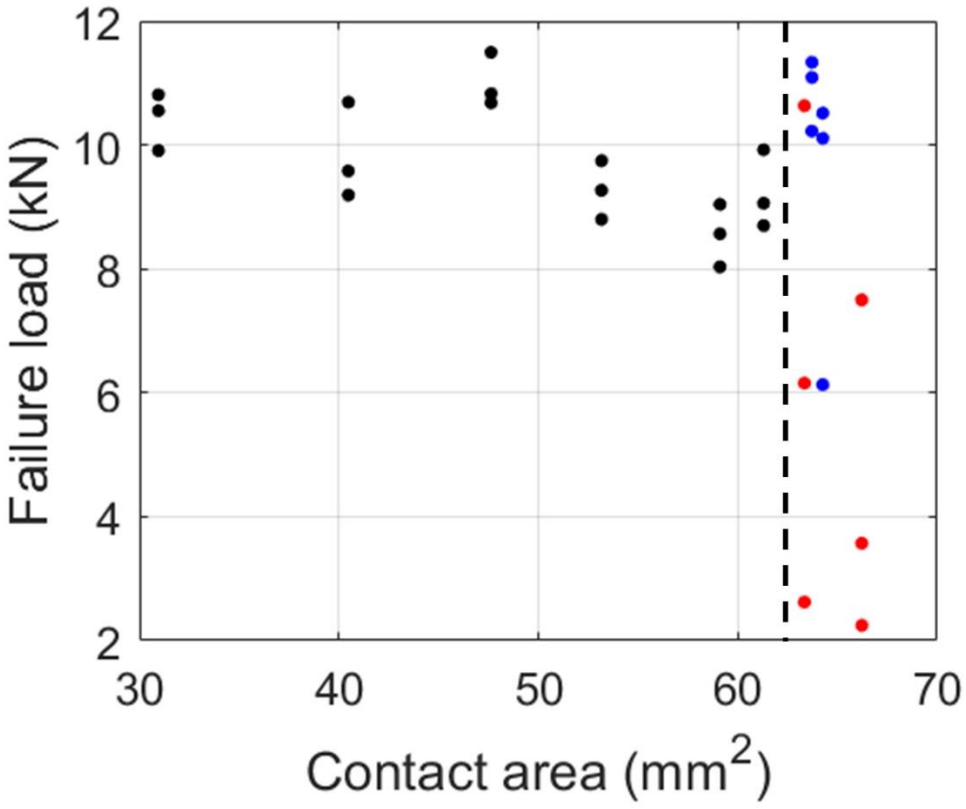


Figure 44. The contact area indicator allows to effectively discriminate the instability of RSW process due to electrode wear.

Consequently, the contact area can be considered the most suitable geometrical characteristic of the electrode imprint for describing the impact of electrode degradation on joint strength. Given that it is not feasible to measure the electrode face continuously during an operative industrial process, this geometrical feature has been predicted through predictive variables defined from the electrode displacement signal recorded during the welding process.

5.4.3 Predictive variables definition

As explained in the methodology section, a pre-processing activity of the recorded signal is needed. The validity of manufacturing operations were visually performed by expert operators that assist the welding process throughout the experiments. The electrode force signal, which begins and ends a spot weld cycle, is responsible to automatically detect the RSW machine's activity period. The

moving average method was used to smooth the time series of the electrode displacement signal with a window size equal to 2000 data points. It is worth remembering that the electrode position sensor has an acquisition frequency of 40000 Hz, i.e., it performs 40000 measurements every second. If the signal is smoothed every 2000 data points, it means that the average information is retained every 2000/40000 = 0.05 seconds.

Figure 45 presents a typical smoothed electrode displacement curve, from the beginning of the current passage to 200 ms after its shutdown (Figure 45b). The electrode displacement signal is initiated by the welding current, so it is recorded as soon as the welding current begins to flow through the electrodes and the sheet stack. By this time, the electrodes are already pressed onto the sheet stack due to the previous squeezing stage, causing the electrode displacement to begin with a negative value. As the current increases, the area of the sheet stack through which the current flows heats up and expands, resulting in an upward movement of the top electrode (the moving electrode) during the welding process until it reaches a peak, which is directly related to the nugget size [173], [149]. Subsequently, when the electric current decreases and the sheets cool down, the volumetric contraction occurs, causing a reduction in the electrode displacement during the holding stage, as illustrated in Figure 45a. Detailed descriptions of this phase can be found in [174], [175] where it is explained that the electrode position is influenced by its axial contraction due to cooling and three distinct phenomena associated with spot weld cooling, namely: liquid cooling of the nugget, solidification, and solid cooling. Initially, the liquid volumetric contraction leads to a rapid decline in electrode displacement. As solidification continues, the rate of decrease in electrode displacement lessens, occurring at around 0.7 seconds, due to the heat released by the solidification process, known as latent heat, of the nugget.

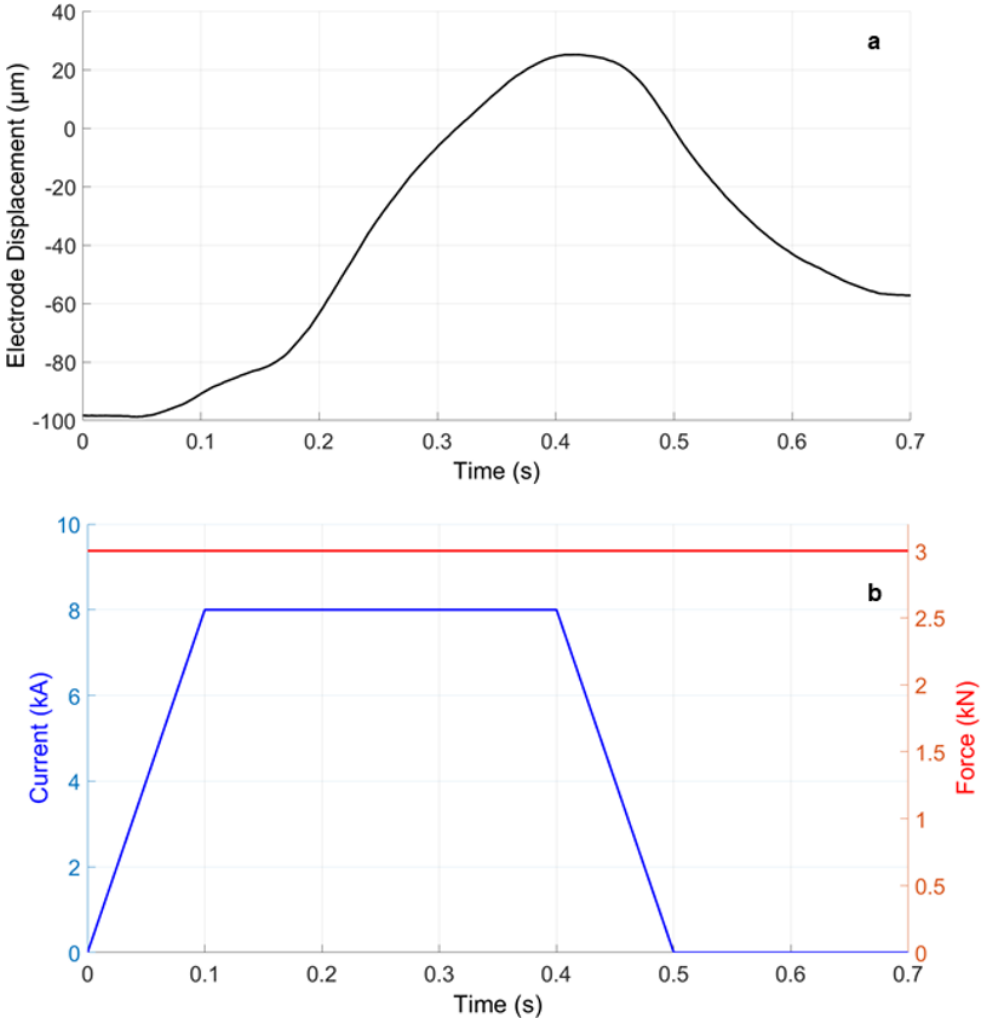


Figure 45: A typical (a) electrode displacement curve with (b) the corresponding spot weld cycle.

In Figure 46, it is possible to see the electrode displacement curves corresponding to the 1st, 600th, and 1200th welds, along with their respective electrode carbon imprint images.

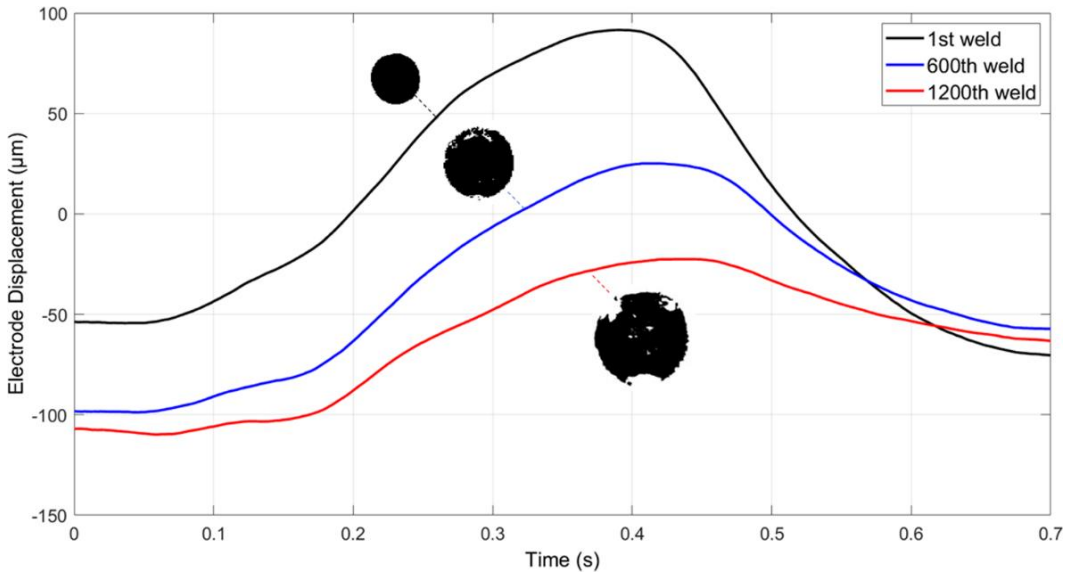


Figure 46: Different electrode displacement curves with associated electrode imprints.

As the deterioration process advances, the electrode requires a longer stroke to clamp the sheet stack due to the axial contraction of the electrode, resulting from its plastic deformation and wear. Initially, the electrode displacement ranges from approximately -50 to -100 µm from the first spot weld to the 1200th, as shown in Figure 46. The amplitude of the displacement curves decreases with the number of spot welds. The wear of the electrode tip leads to an uneven distribution of contact resistance between the electrode and the sheet. During welding, this causes localized heating on the electrode tip surface, and oxidation may occur over time. The enlargement of the contact area results in a decrease in the electric current density, while wear and oxidation of the contact surface lead to an irregular electric current distribution through the electrodes and the sheets. Consequently, the thermal power developed at the faying interface of the sheets decreases and becomes non-uniform over time [176]. As a result, less metal is melted, and the welded joint volumetrically expands less than it did at the beginning of the endurance test. Figure 46 illustrates how the amplitude of the displacement curves, measured as the distance between the start and the peak value of the electrode displacement, decreases from about 150 to 75 µm. For the same reason, the slope of the electrode displacement curve reduces, particularly in the final cooling (hold) stages.

Several statistics were derived from the electrode displacement curve to identify the relevant features associated with the electrode health indicator, which is the contact area. To assess the relationship between variables, the Pearson coefficient, a measure of linear dependence, was employed. The analyzed weld spots corresponded to the electrode wear measurements conducted with the carbon imprint tests. All statistics were computed within a time range of 700 ms, starting from the activation of the electric current and extending up to 200 ms after its deactivation. Several features were extracted from the electrode displacement curves and plotted against the contact area. However, based on the correlation coefficient values and visual examination of scatter plots, only the significant features were kept. For each welding, the electrode displacement signal was stored in a dedicated vector, as outlined below.

$$D^i = \left[d_1^i, \dots, d_j^i, \dots, d_N^i\right]^T \quad (\mu m) \tag{61}$$

D^i is the electrode displacement signal vector corresponding to the i-th welding, d_j^i is the j-th displacement value detected by the position sensor during the i-th welding, N is the number of electrode positions acquired in a welding. N can be computed multiplying the acquisition frequency of the sensor (40000 Hz) by the recorded time laps (0.7 s), i.e., 28800.

A range of features was calculated for the purpose of feature extraction in the time domain. The mathematical definitions of only the selected features are provided below.

- *maximum displacement:* peak value of the electrode displacement curve, corresponding with the greater value of the electrode displacement vector;

$$d_{max}^i = \max\left(D^i\right) \quad (\mu m) \tag{62}$$

- *mean displacement:* average value of the electrode displacement vector;

$$d_{mean}^i = \frac{1}{N}\sum_{j=1}^{N} d_j^i \quad (\mu m) \tag{63}$$

- *standard deviation:* variability of the electrode displacement data around its mean;

$$d_{std}^i = \sqrt{\frac{1}{N-1}\sum_{j=1}^{N}(d_j^i - d_{max}^i)^2} \quad (\mu m) \tag{64}$$

- *Euclidean distance from the 1st weld:* square root of the sum of squared differences between the data obtained from the first electrode displacement curve and the following curves. It is a measure of how the displacement curve changes with the electrode degradation as compared to that obtained from unused electrodes;

$$d_{eucl}^{i} = \sqrt{\sum_{j=1}^{N}\left(d_j^i - d_j^1\right)^2} \quad (\mu m) \tag{65}$$

- *average decreasing slope during the hold time stage:* assessed in the first 100 ms of the hold time, ranging from 500 ms to 600 ms after the start of the sensor acquisition. Such temporal instants corresponding to the 20000th (acquisition frequency multiplied by 0.5 s) and 24000th (acquisition frequency multiplied by 0.6 s) elements of the electrode displacement vector.

$$d_{slope,hold}^{i} = \frac{d_{24000}^{i} - d_{20000}^{i}}{0.1} \quad (\mu m/s) \tag{66}$$

- *skewness:* asymmetry of electrode displacement data around its mean.

$$d_{skewness}^{i} = \frac{\frac{1}{N}\sum_{j=1}^{N}\left(d_j^i - d_{mean}^i\right)^3}{\left(\sqrt{\frac{1}{N}\sum_{j=1}^{N}\left(d_j^i - d_{mean}^i\right)^2}\right)^3} \tag{67}$$

The evolution of these features over the number of welds is displayed in Figure 47.

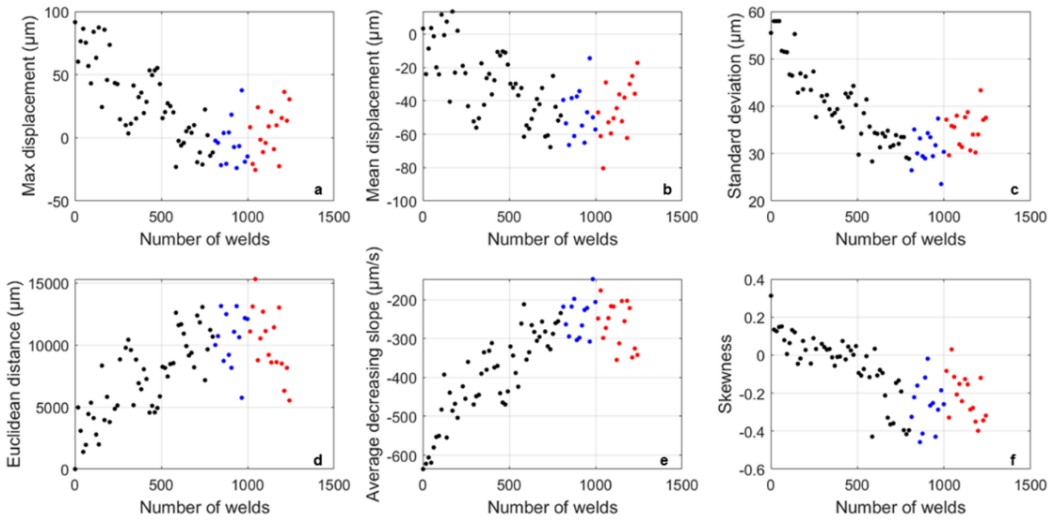


Figure 47: Geometrical features extracted from the electrode displacement curve vs. the number of welds.

As mentioned earlier, the maximum displacement exhibits a continuous decline as the electrode degrades due to the decreasing thermal power at the faying surface. It becomes more variable when the electrode reaches its critical condition, corresponding to an electrode contact area 2.2 times greater than the nominal value, due to instability of the wear process (Figure 47a). A similar pattern is observed for the mean displacement and standard deviation, displayed in Figure 47b and Figure 47c, respectively. The mean displacement has a more variable trend as it averages all the values of the displacement curve, encompassing various phenomena such as different initial values, peak values, slope changes, and so on. In contrast, the standard deviation is more closely related to thermal power density, reflecting the variability of displacement values from their average. As expected, the Euclidean distance increases with electrode degradation, albeit with considerable variability (Figure 47d). During the hold stage, electrode movement slows down (Figure 47e) in line with the minor volumetric changes occurring in the weld region due to reduced thermal input for joint formation. The different initial values of the electrode displacement curve and the slower electrode displacements lead to a decrease in skewness over the course of welds, as depicted in Figure 47f.

Figure 48 illustrates scatter plots of the chosen features extracted and selected from the electrode displacement signal and the contact area obtained from the electrode imprints. It also presents the Pearson correlation coefficient for each pair of variables.

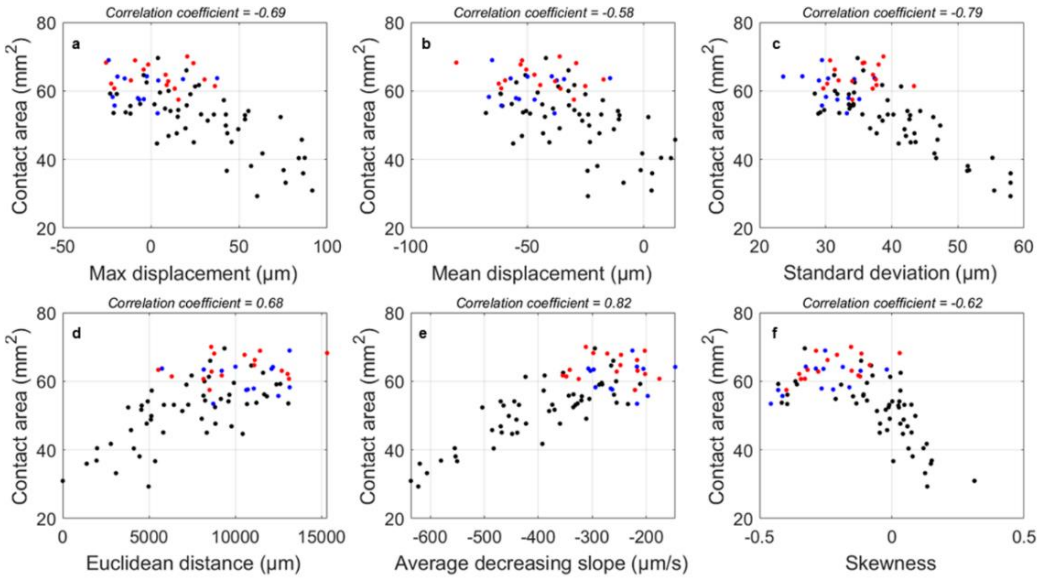


Figure 48: Scatter plots of the electrode wear indicator, i.e., the contact area, vs. the predictive variables.

The scatter plots in Figure 48 confirm the connection between the chosen features extracted from the electrode displacement and the contact area. An increase in the contact area corresponds to a decrease in the maximum displacement and standard deviation. On the other hand, the distance between the electrode displacement curves and the initial one increases, as indicated in the scatter plot of the Euclidean distance in Figure 48d. Both the average decreasing slope and skewness exhibit a clear relationship with the contact area. The standard deviation and the average decreasing slope are the electrode displacement features most strongly correlated with the contact area, with Pearson correlation coefficients of -0.79 and 0.82, respectively.

A regression analysis has been employed to deduce a relationship between the electrode health indicator (i.e., contact area) and the predictive variables defined from the electrode displacement curves. Furthermore, a NN algorithm has been applied to accurately predict the evolution of the electrode contact area with the number of spot welds, based on the predictive variables selected from the electrode displacement curve. These analysis are presented in the following sections.

5.4.4 Inferential analysis

As explained in the methodology section, an inferential analysis based on linear regression has been conducted to find a mathematical model that explain the relationship between the most explanatory predictive variables and the target variable, i.e. the electrode contact area. As described, before to formulate the linear regression model is necessary to analyse the multicollinearity problem among the predictive variables. Thus, the correlation involving the correlation coefficient computed for each pair of predictive variables is reported in Table 9.

Table 9*:* Correlation matrix between the predictive and response variables obtained from the welding experiments.

	Contact area	**Max displacement**	**Mean displacement**	**Standard deviation**	**Euclidean distance**	**Decreasing slope**	**Skewness**
Contact area	1	-0.69	-0.58	-0.79	0.68	**0.82**	-0.62
Max displacement	-0.69	1	0.96	0.88	-0.97	-0.85	0.71
Mean displacement	-0.58	0.96	1	0.73	-0.97	-0.70	0.54
Standard deviation	-0.79	0.88	0.73	1	-0.83	-0.94	0.76
Euclidean distance	0.68	-0.97	-0.97	-0.83	1	0.80	-0.63
Decreasing slope	**0.82**	-0.85	-0.70	-0.94	0.80	1	-0.82
Skewness	-0.62	0.71	0.54	0.76	-0.63	-0.82	1

The correlation matrix reveals strong correlations among the predictive variables, indicating that they are not independent, violating one of the fundamental assumptions of linear regression. Among the predictive variables, the average decreasing slope stands out as the most influential factor in explaining the variation in contact area during the electrode degradation process. Thus, only the average

decreasing slope has been selected for the inferential analysis. To ensure consistent scaling, the average decreasing slope has been normalized using standardization.

Then, a 2nd-degree polynomial function has been defined as a regression model:

$$Y = b_o + b_1 x_1 + b_2 x_1^2 + \varepsilon \quad (68)$$

where Y is the contact area, x_1 is the normalized average of the decreasing slope of the electrode, b_0, b_1, and b_2 are the coefficient estimates of the model, and ε is the residual between the observed value and the predicted one. The coefficient estimates of the regression model performed with the OLS method are reported in Table 10.

Table 10: Coefficient estimates of the regression model displayed in Eq. 68.

Coefficient	p-value	Estimate	95 % Confidence interval
b_0	<0.00001	57.03	[55.49, 58.56]
b_1	<0.00001	6.58	[5.23, 7.94]
b_2	0.00061	-1.86	[-2.90, -0.82]

The coefficient estimates exhibit low p-values (<0.05), indicating their high statistical significance in explaining the target variable. Additionally, the 95% confidence intervals are notably narrow. The polynomial regression model is visualized in Figure 49. The coefficient of determination, denoted as R^2, amounts to 0.72. This implies that the electrode descent speed after the current switch-off can explain nearly 75% of the total variation in the contact area during the electrode degradation process. This level of explanatory power is reasonably acceptable for characterizing electrode degradation using a single process signal.

While the polynomial regression model successfully captures the influence of electrode descent speed on contact area, it is important to note that RSW process involves several physical mechanisms, including mechanical, electrical, thermal, and metallurgical factors. To gain deeper insights into the electrode degradation process, multi-fusion sensor techniques that integrate multiple welding signals, such as electrical power, electrode voltages, and dynamic resistance, as recommended by [177] and [178] could be employed. Such an approach might lead

to a higher coefficient of determination (R^2) for explaining the variation in contact area during electrode deterioration.

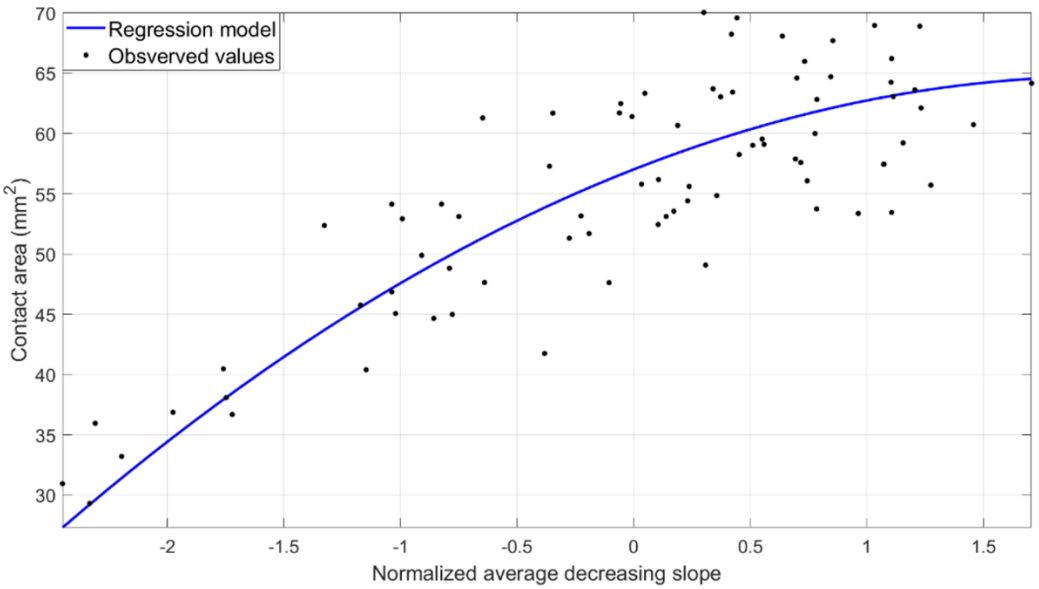


Figure 49: Fitting of the contact area vs. normalized decreasing speed with the polynomial regression model.

Figure 50 illustrates the graphical residual analysis, which is essential for verifying whether the underlying assumptions of the linear regression are met. As explained earlier, two critical assumptions are the normal distribution of residuals and homoscedasticity. In Figure 50a, the residuals are plotted against the number of observations, while Figure 50b depicts the residuals against the fitted values generated by the regression model. These scatter plots indicate no apparent issues concerning the homogeneity of variance.

Figure 50c presents a histogram of the residuals, and Figure 50d display the normal probability plot of the residuals. From these visualizations, it is evident that the distribution of the residuals closely resembles a normal distribution, with the exception of the extreme regions.

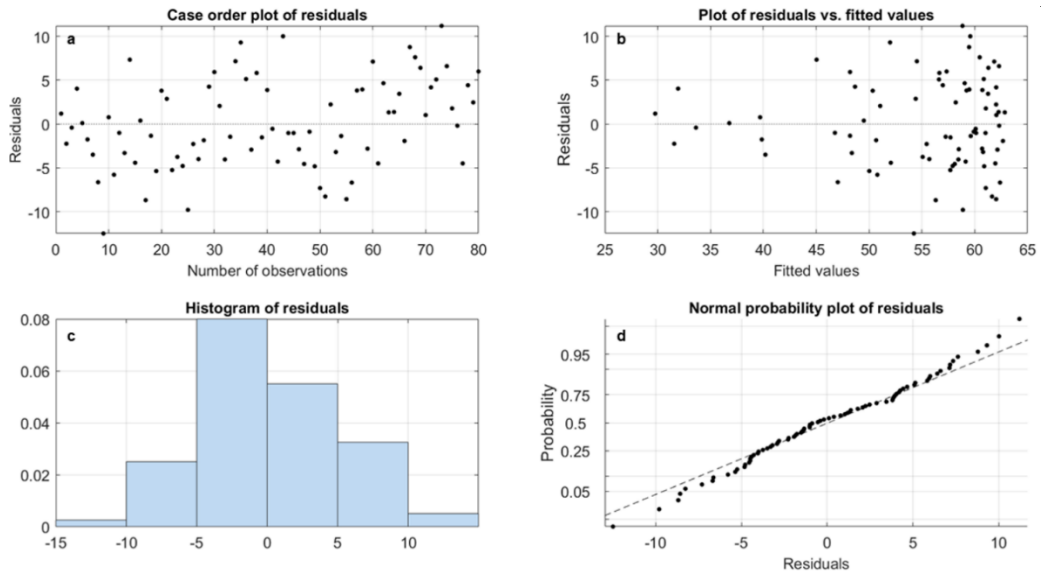


Figure 50: Graphical residual analysis.

5.4.5 Predictive analysis

The goal of the predictive analysis is to develop an algorithm that can accurately forecast the electrode health indicator using the predictive variables defined with the electrode displacement signal. Over the last years, Artificial Intelligence and Machine Learning algorithms have garnered significant attention in both industrial and academic sectors [136]. This is primarily due to their remarkable predictive capabilities. Consequently, a NN has been applied to predict the health indicator, i.e. the electrode contact area. This model leverages all the selected features extracted from the electrode displacement signal, as discussed previously.

Given the relatively limited number of predictive variables and observations available, employing a large number of neurons per layer and numerous layers might result in overfitting. As a result, an optimal architecture was determined through a trial-and-error process, starting with a shallow NN featuring one hidden layer with ten neurons. After experimentation, the final NN architecture was established with two fully connected hidden layers, each consisting of five neurons. Sigmoid activation functions were applied to the hidden layers, while a linear activation function was utilized for the output layer. A Bayesian regularization

training function was employed to minimize the combination of squared errors and weights, ensuring strong generalization properties in the test set. The dataset was partitioned into a training set (75%) and a test set (25%) containing the inspected weld spots. The NN architecture is illustrated in Figure 51.

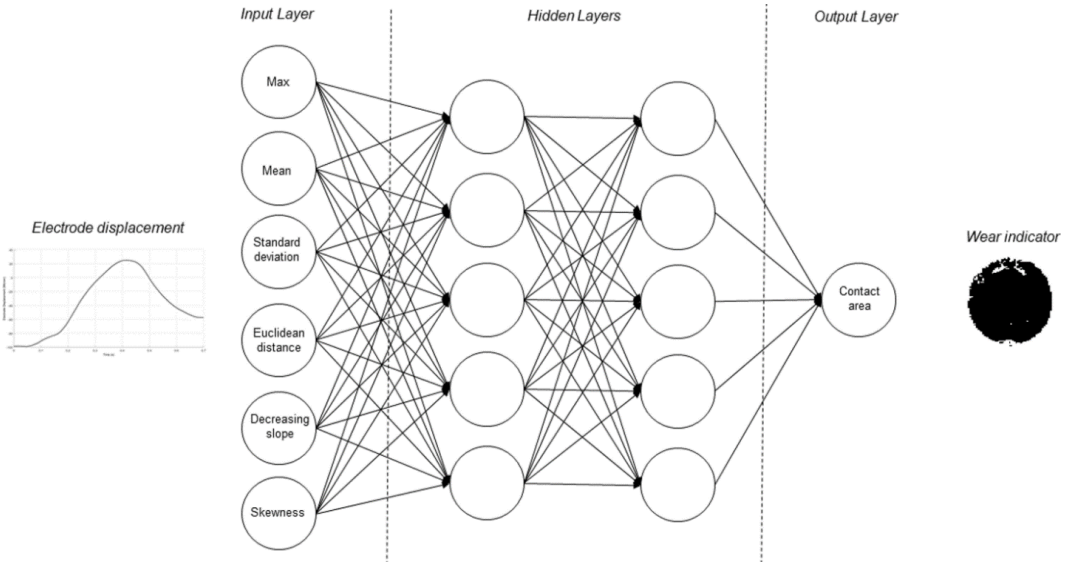


Figure 51: Neural Network architecture.

The performance of the NN is depicted in Figure 52 and summarized in Table 11. The error is determined as the difference between the observed value (i.e., electrode contact area) and the predicted value, while the relative error is calculated as the ratio of the error to the observed value.

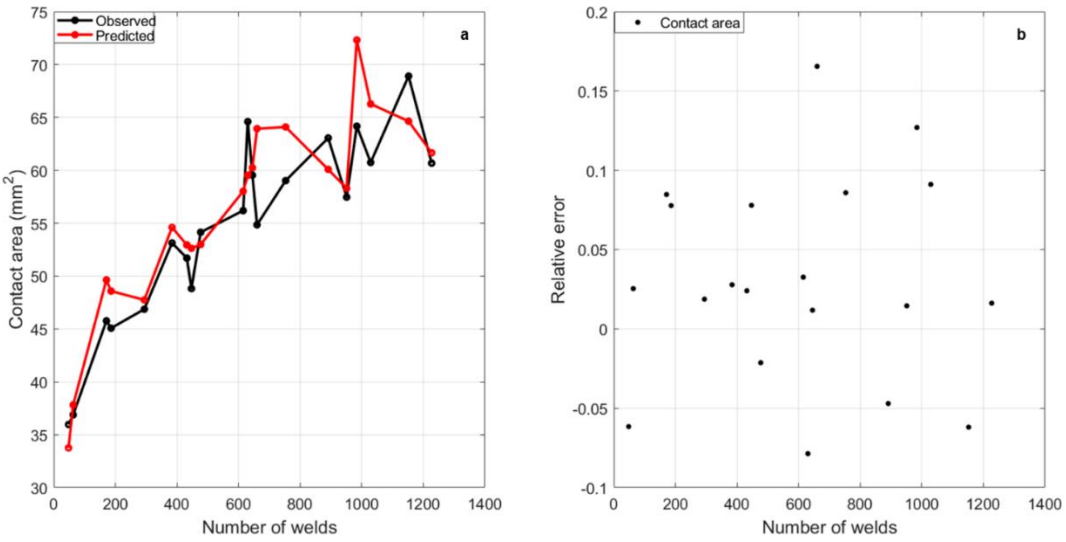


Figure 52: Neural Network performances for the prediction of the electrode contact area and relative error.

Table 11: Neural Network performance metrics obtained from the data of Figure 49a.

Mean error	Median error	Standard deviation	Mean relative error	Median relative error	Relative standard deviation
1.61 mm^2	1.11mm^2	3.73 mm^2	0.03	0.02	0.06

Both the median error and the mean error are less than 2 mm^2, and the standard deviation is quite limited. The variability of the relative error, as estimated by its variance, is about 6%, with both the median value and the mean value within 3%. The scatter plot shows that the relative error is generally within 10%

Machine Learning algorithms continue to enhance predictive capabilities, enabling real-time prediction of electrode degradation through welding signals. This facilitates the timely replacement of electrodes as soon as the most significant geometrical feature, representing electrode wear, reaches a critical value. Consequently, electrodes could be replaced based on predictive contact area analysis derived from electrode displacement during the welding process.

5.5 Main contributions and limitations

This research introduces a novel approach for the indirect prediction of electrode degradation in RSW. It combines the analysis of electrode displacement, evaluation of electrode face damage using a carbon imprint test, and the mechanical strength of spot welds. A regression analysis has been employed to establish a relationship between the electrode contact area, which is representative of the electrode degradation, and the electrode descent speed during the hold stage. In contrast to previous studies that overlooked the impact of electrode wear, this research utilizes a NN to predict the contact area, thereby providing a quantitative assessment of electrode degradation that is currently missing in the literature. The main conclusions are summarized in the following.

- The contact area proves to be the most suitable feature for characterizing electrode degradation due to its capacity to identify the reduction in joint mechanical strength during welding. As such, it is considered the electrode health indicator (target variable) of this study.
- The contact area provides a means to differentiate the welding process's stability based on the mechanical strength of the spot welds. More precisely, as long as the contact area remains below 2.2 times the nominal value, the process can be considered stable, and the produced joints are of acceptable quality. However, once this threshold is exceeded, the RSW process becomes unstable, resulting in an increased number of low-quality joints.
- The regression analysis has demonstrated a strong relationship between the electrode descent speed during the hold stage and the contact area, accounting for more than 70% of the variation in contact area during the electrode degradation process.
- A NN was applied using selected predictive features defined from the electrode displacement signal to achieve an accurate prediction of the electrode contact area, thereby estimating electrode degradation. The predictive accuracy is satisfactory, with a mean relative error of 0.03 and a relative standard deviation of 0.06.

Therefore, according with the main results of this research, when the predictive tool indicates that the electrode contact area is approaching 2.2 times the nominal value, it is an indication that the electrode needs to be replaced or dressed. This predictive threshold serves as a warning sign that the electrode is reaching a critical condition, and the welding process is likely to become unstable, as observed in this

study. Replacing or dressing the electrode at this point can help maintain the stability and quality of the RSW process, preventing the execution of redundant welds. In fact, as already discussed, currently manufacturers perform extra welds (1000-1200 more than necessary) to compensate for uncertainty related to electrode degradation. With an accurate predictive tool, these redundant welds can be avoided because there is a better understanding of when the electrode is nearing the critical condition. This enables the possibility to replace or dress the electrode at the right time, preventing the welding process from becoming unstable. By avoiding these unnecessary extra welds, manufacturers can save time, energy, and resources. This reduces operational costs and it is a more sustainable and cost-effective approach that optimizes resource usage and minimizes waste in the manufacturing process.

This study represents an example of sustainability-oriented process innovation where incremental improvements can be achieved by developing tools capable of enhancing the resource efficiency of the process and, in turn, of the product.

Moreover, this study can be a key element for the development of digital twin of RSW process. In fact, the ML tool developed in this research can be integrated into a broader digital twin framework and be used to guide decisions whether to replace/redress or not the electrode. Information collected from sensors can be used in a digital space to perform the electrode degradation assessment. The latter can then be used to inform decision makers and guide maintenance operations.

It is important to acknowledge the limitations of this research. The analysis was conducted using a specific material and geometry of electrode, as well as a specific material and geometry of the sheets to be welded. For the sake of generalizability and wider applicability, future research should aim to validate these findings with other types of electrodes and materials commonly used in RSW processes. Variations in electrode materials, coatings, and workpiece materials can introduce unique characteristics and behaviors that may affect the predictive model's performance. Therefore, expanding the study to encompass a broader range of materials and electrode types would provide a more comprehensive understanding of how electrode wear indicators relate to the RSW process across different manufacturing contexts. Such research would contribute to the robustness and versatility of the predictive tool, making it even more valuable for industrial applications.

Chapter 6

Conclusions

6.1 Summary of the work

The extensive utilization of Earth's resources by human activities over the years is significantly disrupting the natural state of our planet. This alteration has led to the identification of a new geological epoch, named Anthropocene. Notably, the Planetary Boundaries (PBs) framework can be used to quantify the limits of the Earth’s carrying capacity. Nowadays, it turns out that six out of the nine PBs have already been transgressed, highlighting the urgent need to shift towards a responsible and sustainable human development.

In this context, the manufacturing sector plays a critical role. In the second quarter of 2022, it was responsible for 23% of the European Union's CO_2 equivalent emissions, a key indicator of the PB for climate change. Consequently, there is a pressing requirement for the generation sustainable value. In response to this challenge, the Circular Economy (CE) model has gained significant attention in recent years. This model is considered effective because it seeks to decouple economic growth from its environmental impact through a continuous reintegration of used products, components, and materials into value chains.

However, implementing CE principles within the manufacturing context necessitates significant technological innovations across product, process, and system levels. At the same time, it is fundamental to consider the lifecycle of a technology when these innovations are delivered into the economy. In fact, the lifecycle of a technology is characterized by different phases that require different types of innovations. Hence, the first goal of this doctoral thesis is to present a sustainability-oriented technological innovation framework that effectively connects the innovation levels - namely, product, process, and system - with distinct phases in the technology lifecycle. This framework can serve as a valuable reference to determine the most appropriate timing for specific sustainability-oriented innovations. Consequently, it allows for the assessment of the suitability

of the methods and tools put forth for the implementation of sustainability-oriented innovations in accordance with the technology lifecycle.

In line with this reference framework, three distinct sustainability-oriented technological innovation activities were developed to target a specific innovation level in each technology lifecycle phase. Consequently, a research focused on sustainability-oriented product innovation was done, primarily applicable during the initial phase of the technology lifecycle, where early product design and development hold greater significance. This effort lays the foundation for the first set of research questions addressed in this doctoral thesis:

1.1 What are the product requirements for a CE?

1.2 What is the minimum carbon tax value that causes at least one environmental parameter to be included in the product requirements?

Subsequently, a second sustainability-oriented technological innovation activity was conducted, focused on the second phase of the technology lifecycle. This phase occurs when the dominant design of a technology has emerged, and its architecture is well-established. During this phase, sustainability-oriented technological innovations at system level are suitable, allowing for the improvement of the value chain system. In this context, the implementation of a digital product passport within a product value chain can result in substantial sustainability improvements because it would increase transparency and traceability. As a result, a second set of research questions has been formulated:

2.1 What are the sustainability-oriented data requirements for the digital product passport ?

2.2 How can these data automatically collect and store in the DPP?

Lastly, the third sustainability-oriented technological innovation activity of this doctoral thesis focuses on the final phase of a technology lifecycle, during which sustainability improvements can be attained through process innovations. In this context, a case study was undertaken concerning a manufacturing process that hold great opportunities for sustainability enhancements. Specifically, the Resistance Spot Welding (RSW) process, widely employed in the automotive sector, was investigated. This process serves as the primary joining method in car-body assembly lines. It is characterized by significant uncertainty related to the health of the electrodes, as the degradation process encompasses various distinct phenomena,

including mechanical, thermal, metallurgical, and more. Typically, car manufacturers perform 1000-1200 welds more than necessary to account for the uncertainty associated with electrode wear. If these redundant welds could be eliminated, it would result in significant resource savings, encompassing energy, time, and costs. Therefore, the third set of research questions, aimed at addressing sustainability-oriented process innovation, has been defined as follows:

3.1 In Resistance Spot Welding, when the electrode starts to produce low-quality quality welds?

3.2 Is it possible to quantitatively predict this condition in real-time?

The following sections reassumes the answers of the research questions, the conclusive remarks, the limitations and future developments of the research.

6.2 Discussion of research questions

Regarding the first research question of the first set (RQ 1.1), this is addressed through the creation of a decision-making tool in the form of a decision tree. This decision tree illustrates when a CE business model outperforms a LE model considering both economic and environmental criteria. Moreover, if the CE is the selected business model, it further delineates whether the product components should be recycled, remanufactured, or reused. Specifically, the economic criterion is represented by the economic costs of the different phases involved, and the environmental criterion is represented by the $CO_{2,eq}$ emissions of the different activities involved. The environmental criterion is then monetized through the application of a carbon tax so that the two criteria can be integrated into a single metric, called total cost. The decision tree provides clear and transparent guidance on the decision rules that must be followed to make the most performing decision. Consequently, the decision rules within the tree can serve as a foundation for establishing product requirements for a CE model. It turns out that, with the current level of carbon tax, only the cost of product disassembly, the cost of product disposal, and the product quality are part of the product requirements for a CE. This is an interesting conclusions because, even if the developed model considers 18 parameters, only three of them influences the convenience of adopting a CE and, thus, are part of the product requirements for a CE. When the economic cost of product disassembly is medium/low, and when the economic costs of product disposal are not very low, or when the quality of the component is high, the CE is always the preferable business model. When, instead, the economic cost of product

disassembly $rc_{disassembly}$ is high, the CE is the preferable business model only when the costs of product disposal $rc_{disposal}$ are high and the quality of the components is not low. Quantitative requirements can be established by reading the decision tree in Figure 13. When it comes to the CE strategy selection, the quality component mainly determines the convenience of pursuing a specific CE strategy, followed by a slight importance of the multiplicative factor of the remanufacturing economic cost. Quantitative requirements can be established by referring to the decision tree displayed in Figure 18.

Regarding the second research question of the first set (RQ 1.2), the impact of carbon tax on the decision-making process is investigated in order to ascertain whether environmental parameters, in addition to economic ones, really influence the choice between a CE or LE business model. This allows to understand when the environmental parameters starts to appear in the decision tree and, thus, become part of the product requirements for a CE. However, a unique value cannot be established because it depends by the values assumed by the cost and carbon footprint of product manufacturing. Hence, carbon tax level curves are created with the aim of identifying the minimum carbon tax value that render the environmental criterion impactful in the decision-making process. As demonstrated in the thesis, this allows to achieve greater $CO_{2,eq}$ savings than the situations when the environmental criterion does not affect the adoption of a CE. It turns out that with the highest carbon tax value today adopted (140€/ton$CO_{2,eq}$ in Uruguay), only a small portion of products, characterized by low economic cost and high carbon footprint of product manufacturing, is influenced by environmental parameters. This means that the achievable carbon footprint savings are today limited. The whole situation is depicted in the carbon tax level curves in Figure 21. The decision-making tools developed to answer the RQ 1.1 are then re-created under a new carbon tax regime, based on the carbon tax level curves, to demonstrate the emergence of environmental parameters in the decision rules of the trees and, hence, in the product requirements for a CE.

Regarding the first research question of the second set (RQ 2.1), sustainability-oriented data requirements for the digital product passport are proposed aimed at conducting a comprehensive evaluation of absolute environmental sustainability that aligns with the Earth's ecological limits. These requirements are established by referring to the well-established Life Cycle Assessment (LCA) and the Planetary Boundaries (PBs) frameworks. Specifically, the Environmental Footprint (EF) methodology is adopted within the LCA framework because it is used as a reference

inside the European Union. For each environmental impact category provided by the EF methodology, threshold values are reported based on the PBs framework. Such threshold values serve as ecological limits that should be written inside the digital product passport to understand whether a product is sustainable in absolute terms or not. Moreover, technical data to insert in the digital product passport are proposed with the aim of fostering the application of CE principles throughout the value chain. In fact, as discussed in the thesis, for an effective implementations of CE principles the stakeholders of a value chain need data relating conditions of the resources connected with the product.

The second research question of the second set (RQ 2.2), instead, aims to propose a conceptual framework for the establishment of a digital product passport. Specifically, a framework based on Cyber-Physical Systems (CPSs) is proposed to facilitate the automated collection of both technical and environmental data previously identified. This framework is constructed based on the well-established 5C architecture, a widely recognized architecture in the existing literature, and it adopted only the first three layers, namely, Connection, Conversion, and Cyber. Every stakeholder can utilize the Connection Level of their CPS to collect the necessary technical and environmental attributes for the digital product passport. The Conversion Level is tasked with processing this data and transmitting it to the Cyber Level, where technical parameters, environmental impact indicators based on the EF methodology, and the corresponding thresholds based on the PBs are made accessible. Consequently, each stakeholder's Cyber level will contain relevant product technical parameters and environmental impact indicators along with associated PBs thresholds, which can then be forwarded to the DPP.

The research question 3.1, then, is addressed performing a huge experiment involving more than 1200 resistance spot welds. These welds were performed with the aim of inducing the electrode degradation and inspect its effect on the weld quality. The electrode degradation was induced through the repetition of the same welding cycle throughout the experiment so that the only phenomenon that could systematically change was the electrode degradation. The latter was measured through carbon imprint tests, whereas the weld quality was assessed through shear-tension tests. The image obtained from carbon imprint tests were digitized and Image Processing techniques were applied in order to extract several geometrical features to relate with the weld quality. It turns out that the electrode contact area is the health indicator that better represents the weld quality, quantified by the peak load of the shear-tension tests. In fact, the contact area value allows to detect when the resistance spot welding process starts to produce low-quality welds. According

to the literature, a low-quality weld due to electrode degradation is defined as when the peak load drops below 80% of the peak load associated with a new electrode. This situation starts to occur when the contact area becomes 2.2 times greater than its nominal value, i.e., when the electrode is new.

Finally, the last research question (RQ 3.2) is addressed by developing a data-driven predictive tool. The aim is to quantitatively compute the electrode contact area in real-time in order to understand when the electrode starts to produce low-quality welds because of its degradation process. This is accomplished by exploiting data recorded during the experiments performed to address the RQ 3.1. Specifically, a sensor capable of measuring the electrode displacement signals was adopted and used to define the predictive variables of the contact area. Then, a neural network was employed to establish the real-time predictive tool. This shows satisfactory predictive performances, with a mean relative error of 0.03, and relative standard deviation of 0.06.

6.3 Conclusive remarks

The research developed in this doctoral thesis offer several contributions from different perspectives. First, the developed sustainability-oriented technological innovation framework provides a reference for researchers and practitioners, assisting them in contextualizing the optimal timing for specific sustainability-oriented innovations. It, in turn, aids in evaluating the adequacy of methods and tools for executing sustainability-oriented technological innovations aligned with the stages of the technology lifecycle.

The first research carried out in this thesis provides a practical contribution for the development of sustainability-oriented product innovation. In fact, it presents a practical and actionable decision-making tool in form of a decision tree, a valuable tool for practitioners and decision-makers. Such a tool facilitates the most suitable choice of business model between the CE and LE by leveraging the advantages of a user-friendly decision tree, enhancing transparency and interpretability and ensuring the objectiveness and reliability of the decision since it relies on a data-driven approach. Thus, it is expected to empower manufacturing organizations to make informed choices to set product requirements for a CE that align with sustainability goals. Then, this research makes also a significant theoretical contribution by introducing carbon tax level curves. These curves highlight the minimum carbon tax values necessary to render the influence of environmental criteria in the decision-making process relevant. This theoretical aspect of the

research enhances the understanding of how carbon taxes shape sustainable business strategies. It offers valuable insights into the relationship between carbon tax, the carbon footprint of product manufacturing, and the cost of product manufacturing. These practical and theoretical contributions support the development of sustainability-oriented product innovations.

The second research carried out in this thesis provides a theoretical contribution for the development of sustainability-oriented process innovation Specifically, the suggested sustainability-oriented data requirements for the digital product passport, coupled with the conceptual framework for their acquisition, enhance the sustainability aspects of this tool. For the first time in the literature, in fact, it is discussed the need to assume an absolute perspective of sustainability that consider the natural limits of our planet. As a result, the digital product passport becomes a more sustainability-oriented tool, capable of aiding the decision-making process of the stakeholders of a value chain.

The third and last research carried out in this thesis provides provides a practical contribution to sustainability-oriented process innovation, and two main theoretical contributions focused on the analyzed manufacturing process. Starting from the theoretical contributions, first, the contact area is a suitable indicator of the electrode's health state. In fact, it allows to detect when the electrode starts to produce low-quality welds and entering in a instability phase because of its degradation. Second, the electrode displacement during welding provides valuable information correlated with the degradation process. In fact, the average electrode descent speed during welding is highly correlated with the electrode contact area. Regarding the practical contribution, a predictive tool of the contact area based on neural networks is developed. This tool allows to automatically assess the contact area value based on the electrode displacement signal acquired during welding. This allows for the automatic detection of the moment when the electrode begins to generate low-quality welds, offering crucial insights for maintenance operations. By proactively replacing or dressing the electrode before it starts producing low-quality welds, redundant welds (which make up 20% of total spot welds in a car body) can be avoided. Eliminating these unnecessary additional welds results in time, energy, and resource savings for manufacturers, thereby contributing to a substantial enhancement in the sustainability of the manufacturing process.

6.4 Limitations and future developments

The research developed in this doctoral thesis presents also some limitations that needs to be recognized and addressed in the future.

Regarding the first research focused on supporting sustainability-oriented product innovation, it is worth noting that for the development of a holistic decision-making tool that support the establishment of product requirements for a circular economy, it is essential to include also the social criterion in the decision-making process. Unfortunately, the lack of objective methodologies in the field of social sustainability poses a challenge in incorporating such criterion into the analysis. Moreover, the scope of the environmental criterion should not be limited solely to $CO_{2,eq}$ emissions. Other essential environmental indicators, such as water consumption, resource usage, pollution emissions, and more, should also be considered in the decision-making process to obtain a more comprehensive understanding of the environmental impact. Additionally, the number of CE strategies could be expanded beyond the ones explored in this study. Options like repair, refurbishment, repurposing, and others should be considered to offer a broader range of sustainable choices for businesses and decision-makers. Furthermore, regarding the carbon tax level curves, the adoption of more stringent carbon tax regimes should take into account other factors beyond solely prioritizing environmental considerations in the transition to a circular economy. For instance, increased carbon taxes can lead to higher production costs for manufacturers, which may pass these costs onto consumers in the form of higher prices for products.

For what concerns the second research focused on supporting sustainability-oriented system innovation, the incorporation of social data within the digital product passport is crucial to have an holistic comprehension of value chain sustainability. Due to the subjective nature of social data and its dependence to different cultural values and perceptions, currently a standardized methodology to quantify the social impact is not available. Moreover, standardization is essential to determine the entity responsible for collecting and documenting social data in the passport. According to UNEP, social data collection often relies on licensed databases such as PSILCA. Alternatively, when primary data is necessary, it can be acquired by visiting specific production facilities or through collaboration with relevant organizations. Primary data can be obtained through direct engagement with organizations and companies, working alongside NGOs or similar entities, observing on-site business and production procedures, or conducting interviews and surveys with affected stakeholders, such as workers. Furthermore, it is imperative

to evaluate the sustainability of the digitization process itself. While digitalization holds significant promise for the CE and sustainability, it is crucial to acknowledge that Information and Communication Technology (ICT) consumes a substantial amount of energy, leading to environmental emissions. Digitization presents invaluable prospects for advancing the CE, but this transition should be coupled with an increase in the adoption of clean energy sources and enhanced energy efficiency. Therefore, efforts directed at digitalization must be accompanied by a simultaneous escalation in the utilization of clean energy sources and improved energy efficiency to counteract the environmental impact associated with ICT technologies.

Finally, the third research focused on supporting sustainability-oriented process innovation necessitates a comprehensive investigation to determine the generalizability of the obtained findings. In fact, the analysis was conducted using a specific material and geometry of electrode, as well as a specific material and geometry of the sheets to be welded. For the sake of generalizability and wider applicability, future research should aim to validate these findings with other types of electrodes and materials commonly used in resistance spot welding processes. Variations in electrode materials, coatings, and workpiece materials can introduce unique characteristics and behaviors that may affect the predictive model's performance, as well as the theoretical insights achieved. Therefore, expanding the study to encompass a broader range of materials and electrode types would provide a more comprehensive understanding of how electrode wear indicators relate to the resistance spot welding process across different manufacturing contexts. Such research would contribute to the robustness and versatility of the predictive tool, making it even more valuable for industrial applications.

References

[1] J. Rockström *et al.*, “A safe operation space for humanity,” *Nature*, vol. 461, no. September, pp. 472–475, 2009.

[2] M. Z. Hauschild, S. Kara, and I. Røpke, “Absolute sustainability: Challenges to life cycle engineering,” *CIRP Ann.*, vol. 69, no. 2, pp. 533–553, 2020, doi: 10.1016/j.cirp.2020.05.004.

[3] A. Bjørn and M. Z. Hauschild, “Introducing carrying capacity-based normalisation in LCA: framework and development of references at midpoint level,” *Int. J. Life Cycle Assess.*, vol. 20, no. 7, pp. 1005–1018, 2015, doi: 10.1007/s11367-015-0899-2.

[4] W. Steffen *et al.*, “Planetary boundaries: Guiding human development on a changing planet,” *Science (80-.).*, vol. 347, no. 6223, 2015, doi: 10.1126/science.1259855.

[5] L. Persson *et al.*, “Outside the Safe Operating Space of the Planetary Boundary for Novel Entities,” *Environ. Sci. Technol.*, vol. 56, no. 3, pp. 1510–1521, 2022, doi: 10.1021/acs.est.1c04158.

[6] K. Richardson *et al.*, “Earth beyond six of nine planetary boundaries,” *Sci. Adv.*, vol. 9, no. 37, p. eadh2458, 2023, doi: 10.1126/sciadv.adh2458.

[7] W. Steffen, W. Broadgate, L. Deutsch, O. Gaffney, and C. Ludwig, “The trajectory of the anthropocene: The great acceleration,” *Anthr. Rev.*, vol. 2, no. 1, pp. 81–98, 2015, doi: 10.1177/2053019614564785.

[8] W. Steffen, A. Sandersons, and P. Tyson, *Global Change and the Earth System: A Planet Under Pressure.* New York: Springer-Verlag, 2004.

[9] J. H. Ausubel and C. Marchetti, “Elektron: Electrical systems in retrospect and prospect,” *Daedalus*, vol. 225, no. 3, pp. 139–169, 1996.

[10] C. L. Magee and T. C. Devezas, “A simple extension of dematerialization theory: Incorporation of technical progress and the rebound effect,” *Technol. Forecast. Soc. Change*, vol. 117, pp. 196–205, 2017, doi: 10.1016/j.techfore.2016.12.001.

[11] M. F. Ashby, *Materials and the Environment*, 3rd ed. Elsevier, 2020. [Online]. Available: https://www.elsevier.com/books/materials-and-the-environment/ashby/978-0-12-821521-0

[12] World Bank, “Manufacturing, value added (% of GDP),” 2023. https://ourworldindata.org/grapher/manufacturing-value-added-to-gdp?tab=table&time=latest&region=Europe&facet=entity (accessed Oct. 10, 2023).

[13] Eurostat, “Quarterly greenhouse gas emissions in the EU,” 2022. https://ec.europa.eu/eurostat/statistics-explained/index.php?title=Quarterly_greenhouse_gas_emissions_in_the_EU#Emissions_by_economic_activity

[14] United Nations, “Manufacturing jobs as a share of total employment, 2000 to 2021,” 2022. https://ourworldindata.org/grapher/manufacturing-share-of-total-employment?tab=chart (accessed Oct. 10, 2023).

[15] H. Zhang and K. R. Haapala, “Integrating sustainable manufacturing assessment into decision making for a production work cell,” *J. Clean. Prod.*, vol. 105, pp. 52–63, 2015, doi: 10.1016/j.jclepro.2014.01.038.

[16] I. S. Jawahir and R. Bradley, “Technological Elements of Circular Economy and the Principles of 6R-Based Closed-loop Material Flow in Sustainable Manufacturing,” *Procedia CIRP*, vol. 40, pp. 103–108, 2016, doi: 10.1016/j.procir.2016.01.067.

[17] C. Enyoghasi and F. Badurdeen, “Industry 4.0 for sustainable manufacturing: Opportunities at the product, process, and system levels,” *Resour. Conserv. Recycl.*, vol. 166, no. November 2020, p. 105362, 2021, doi: 10.1016/j.resconrec.2020.105362.

[18] Y. Liu, M. Farooque, C. H. Lee, Y. Gong, and A. Zhang, “Antecedents of circular manufacturing and its effect on environmental and financial performance: A practice-based view,” *Int. J. Prod. Econ.*, vol. 260, no. March, p. 108866, 2023, doi: 10.1016/j.ijpe.2023.108866.

[19] D. Antonioli, C. Ghisetti, M. Mazzanti, and F. Nicolli, “Sustainable production: The economic returns of circular economy practices,” *Bus. Strateg. Environ.*, vol. 31, no. 5, pp. 2603–2617, 2022, doi: 10.1002/bse.3046.

[20] J. A. Garza-Reyes, A. Salomé Valls, S. Peter Nadeem, A. Anosike, and V. Kumar, “A circularity measurement toolkit for manufacturing SMEs,” *Int. J. Prod. Res.*, vol. 57, no. 23, pp. 7319–7343, 2019, doi: 10.1080/00207543.2018.1559961.

[21] CIRCLE Economy, “THE CIRCULARITY GAP REPORT 2020,” 2020. https://www.circularity-gap.world/2020

[22] CIRCLE Economy, “THE CIRCULARITY GAP REPORT 2023,” 2023, [Online]. Available: https://www.circularity-gap.world/2023#download

[23] I. S. Jawahir, F. Badurdeen, and K. E. Rouch, “Innovation in Sustainable Manufacturing Education,” *11th Glob. Conf. Sustain. Manuf.*, pp. 9–16, 2013.

[24] A. D. Jayal, F. Badurdeen, O. W. Dillon, and I. S. Jawahir, “Sustainable manufacturing: Modeling and optimization challenges at the product,

process and system levels," *CIRP J. Manuf. Sci. Technol.*, vol. 2, no. 3, pp. 144–152, 2010, doi: 10.1016/j.cirpj.2010.03.006.

[25] The National Council For Advanced Manufacturing, "NIST MEL SLIM (Sustainable & Life-cycle Information-based Manufacturing) project," 2009. https://www.nacfam.org/projects/nist-mel-slim-sustainable-life-cycle-information-based-manufacturing-project/ (accessed Oct. 10, 2023).

[26] H. Berg *et al.*, "Digital circular economy: a cornerstone of a sustainable European industry transformation," *ECERA Eur. Circ. Econ. Res. Alliance*, p. 28, 2020.

[27] M. Cantamessa and F. Montagna, *Management of Innovation and Product Development*. 2023. doi: 10.1007/978-1-4471-7531-5.

[28] K. T. Ulrich and S. D. Eppinger, *Product Design and Development*. McGraw-Hill Education, 2016.

[29] C. M. Christensen, *The innovator's dilemma: when new technologies cause great firms to fail*. Harvard Business Review Press, 2013.

[30] J. M. Utterback and W. J. Abernathy, "A Dynamic Model of Process and Product Innovation," *Omega*, vol. 3, no. 6, pp. 639–656, 1975.

[31] F. Montagna and M. Cantamessa, "Unpacking the innovation toolbox for design research and practice," *Des. Sci.*, vol. 5, 2019, doi: 10.1017/dsj.2019.3.

[32] C. Vezzoli *et al.*, *Product-Service System Design for Sustainability*, no. March. 2014.

[33] F. Ceschin and I. Gaziulusoy, *Design for sustainability*. 2020.

[34] L. M. Viespoli, L. Panza, A. Johanson, A. Alvaro, A. Somà, and F. Berto, "Tape winding angle influence on subsea cable sheathing fatigue performance," *Eng. Struct.*, vol. 229, no. January 2020, 2021, doi: 10.1016/j.engstruct.2020.111660.

[35] A. Rejeb, J. G. Keogh, S. J. Simske, T. Stafford, and H. Treiblmaier, "Potentials of blockchain technologies for supply chain collaboration: a conceptual framework," *Int. J. Logist. Manag.*, vol. 32, no. 3, pp. 973–994, 2021, doi: 10.1108/IJLM-02-2020-0098.

[36] M. Kouhizadeh, Z. Qingyun, and S. Joseph, "Blockchain and the circular economy: potential tensions and critical reflections from practice," *Prod.*

Plan. Control, pp. 950–966, 2020.

[37] I. Erol, I. Murat Ar, I. Peker, and C. Searcy, "Alleviating the Impact of the Barriers to Circular Economy Adoption Through Blockchain: An Investigation Using an Integrated MCDM-based QFD With Hesitant Fuzzy Linguistic Term Sets," *Comput. Ind. Eng.*, vol. 165, no. January, p. 107962, 2022, doi: 10.1016/j.cie.2022.107962.

[38] European Commission, "Ecodesign your future: How ecodesign can help the environment by making products smarter," pp. 1–12, 2014.

[39] M. C. den Hollander, C. A. Bakker, and E. J. Hultink, "Product Design in a Circular Economy: Development of a Typology of Key Concepts and Terms," *J. Ind. Ecol.*, vol. 21, no. 3, pp. 517–525, 2017, doi: 10.1111/jiec.12610.

[40] European Commission, "Paris Agreement," 2023. https://climate.ec.europa.eu/eu-action/international-action-climate-change/climate-negotiations/paris-agreement_en

[41] L. Haigh *et al.*, "The Circularity Gap Report 2021," *Circ. Econ.*, p. 71, 2021, [Online]. Available: https://www.circularity-gap.world/2021#downloads

[42] D. Pigosso and T. McAloone, "How can design science contribute to a circular economy? / ICED23: Design in a complex world," *Proc. 21st Int. Conf. Eng. Des. (IDED 17)*, vol. 5, no. August, pp. 299–307, 2017, [Online]. Available: https://iced.designsociety.org/publication/39752/How+can+design+science+contribute+to+a+circular+economy%3F

[43] C. Sassanelli, A. Urbinati, P. Rosa, D. Chiaroni, and S. Terzi, "Addressing circular economy through design for X approaches: A systematic literature review," *Comput. Ind.*, vol. 120, p. 103245, 2020, doi: 10.1016/j.compind.2020.103245.

[44] J. X. Wang, H. Burke, and A. Zhang, "Overcoming barriers to circular product design," *Int. J. Prod. Econ.*, vol. 243, no. July 2020, p. 108346, 2022, doi: 10.1016/j.ijpe.2021.108346.

[45] A. Zakeri, F. Dehghanian, B. Fahimnia, and J. Sarkis, "Carbon pricing versus emissions trading: A supply chain planning perspective," *Int. J. Prod. Econ.*, vol. 164, pp. 197–205, 2015, doi: 10.1016/j.ijpe.2014.11.012.

[46] I. Konstantaras, K. Skouri, and L. Benkherouf, "Optimizing inventory decisions for a closed–loop supply chain model under a carbon tax regulatory

mechanism," *Int. J. Prod. Econ.*, vol. 239, no. May 2020, p. 108185, 2021, doi: 10.1016/j.ijpe.2021.108185.

[47] R. Luo, L. Zhou, Y. Song, and T. Fan, "Evaluating the impact of carbon tax policy on manufacturing and remanufacturing decisions in a closed-loop supply chain," *Int. J. Prod. Econ.*, vol. 245, no. March 2020, p. 108408, 2022, doi: 10.1016/j.ijpe.2022.108408.

[48] Van Den Berg M.R. and Bakker C.A., "A product design framework for a circular economy," in *Product Lifetimes And The Environment*, 2015, pp. 365–379.

[49] N. Hultgren, "Guidelines and design strategies for improved product recyclability - how to increase the recyclability of consumer electronics and domestic appliances through product design," p. 100, 2012.

[50] J. Peeters, P. Vanegas, W. Dewulf, and J. Duflou, "Design for demanufacturing: a life cycle approach," 2012.

[51] T. F. Go, D. A. Wahab, and H. Hishamuddin, "Multiple generation life-cycles for product sustainability: The way forward," *J. Clean. Prod.*, vol. 95, pp. 16–29, 2015, doi: 10.1016/j.jclepro.2015.02.065.

[52] M. Moreno, C. De los Rios, Z. Rowe, and F. Charnley, "A conceptual framework for circular design," *Sustain.*, vol. 8, no. 9, 2016, doi: 10.3390/su8090937.

[53] M. E. Toxopeus, N. B. Van Den Hout, and B. G. D. Van Diepen, "Supporting Product Development with a Practical Tool for Applying the Strategy of Resource Circulation," *Procedia CIRP*, vol. 69, pp. 680–685, 2018, doi: 10.1016/j.procir.2017.11.033.

[54] B. Pozo Arcos, A. R. Balkenende, C. A. Bakker, and E. Sundin, "Product design for a circular economy: Functional recovery on focus," *Proc. Int. Des. Conf. Des.*, vol. 6, pp. 2727–2738, 2018, doi: 10.21278/idc.2018.0214.

[55] S. G. Lee, S. W. Lye, and M. K. Khoo, "A multi-objective methodology for evaluating product end-of-life options and disassembly," *Int. J. Adv. Manuf. Technol.*, vol. 18, no. 2, pp. 148–156, 2001, doi: 10.1007/s001700170086.

[56] A. Desai and A. Mital, "Incorporating work factors in design for disassembly in product design," *J. Manuf. Technol. Manag.*, vol. 16, no. 7, pp. 712–732, 2005, doi: 10.1108/17410380510619932.

[57] S. Takeuchi and S. Kazuhiro, "Design for Product-Embedded Disassembly

with Maximum Profit," *Int. Symp. Environ. Conscious Des. Inverse Manuf. IEEE, 2005.*, vol. 1, pp. 199–206, 2005.

[58] M. Sabaghi, C. Mascle, and P. Baptiste, "Evaluation of products at design phase for an efficient disassembly at end-of-life," *J. Clean. Prod.*, vol. 116, pp. 177–186, 2016, doi: 10.1016/j.jclepro.2016.01.007.

[59] P. Vanegas *et al.*, "Ease of disassembly of products to support circular economy strategies," *Resour. Conserv. Recycl.*, vol. 135, no. May 2017, pp. 323–334, 2018, doi: 10.1016/j.resconrec.2017.06.022.

[60] C. Favi, M. Marconi, M. Germani, and M. Mandolini, "A design for disassembly tool oriented to mechatronic product de-manufacturing and recycling," *Adv. Eng. Informatics*, vol. 39, no. May 2018, pp. 62–79, 2019, doi: 10.1016/j.aei.2018.11.008.

[61] C. M. Rose, "Design for Environment : a Method for Formulating Product End-of-Life Strategies," 2000.

[62] M. Remery, C. Mascle, and B. Agard, "A new method for evaluating the best product end-of-life strategy during the early design phase," vol. 4828, 2012, doi: 10.1080/09544828.2011.605061.

[63] J. Ma and G. E. Okudan, "A fuzzy logic-based approach to determine product component end-of-life option from the views of sustainability and designer ' s perception," *J. Clean. Prod.*, vol. 108, pp. 289–300, 2015, doi: 10.1016/j.jclepro.2015.08.029.

[64] C. Bakker, F. Wang, J. Huisman, and M. Den Hollander, "Products that go round: Exploring product life extension through design," *J. Clean. Prod.*, vol. 69, pp. 10–16, 2014, doi: 10.1016/j.jclepro.2014.01.028.

[65] M. D. Bovea and V. Pérez-Belis, "Identifying design guidelines to meet the circular economy principles: A case study on electric and electronic equipment," *J. Environ. Manage.*, vol. 228, no. August, pp. 483–494, 2018, doi: 10.1016/j.jenvman.2018.08.014.

[66] L. Panza, A. Faveto, G. Bruno, and F. Lombardi, "Open product development to support circular economy through a material lifecycle management framework," *Int. J. Prod. Lifecycle Manag.*, vol. 14, no. 2–3, pp. 255–281, 2022, doi: 10.1504/ijplm.2022.125826.

[67] L. Panza, G. Bruno, and F. Lombardi, "A Collaborative Architecture to support Circular Economy through Digital Material Passports and Internet of Materials," *IFAC-PapersOnLine*, vol. 55, no. 10, pp. 1491–1496, 2022,

doi: 10.1016/j.ifacol.2022.09.601.

[68] V. Delpla, J. P. Kenné, and L. A. Hof, “Circular manufacturing 4.0: towards internet of things embedded closed-loop supply chains,” *Int. J. Adv. Manuf. Technol.*, vol. 118, no. 9–10, pp. 3241–3264, 2022, doi: 10.1007/s00170-021-08058-3.

[69] K. Meng, P. Lou, X. Peng, and V. Prybutok, “Multi-objective optimization decision-making of quality dependent product recovery for sustainability,” *Int. J. Prod. Econ.*, vol. 188, no. March, pp. 72–85, 2017, doi: 10.1016/j.ijpe.2017.03.017.

[70] Y. A. Yuksek, Y. Haddad, E. Pagone, S. Jagtap, S. Haskew, and K. Salonitis, “Sustainability Assessment of Electronic Waste Remanufacturing: The Case of Laptop,” *Procedia CIRP*, vol. 116, pp. 378–383, 2023, doi: 10.1016/j.procir.2023.02.064.

[71] M. Reimann, Y. Xiong, and Y. Zhou, “Managing a closed-loop supply chain with process innovation for remanufacturing,” *Eur. J. Oper. Res.*, vol. 276, no. 2, pp. 510–518, 2019, doi: 10.1016/j.ejor.2019.01.028.

[72] Eupedia, “Carbon footprint of common consumer products,” 2021. https://www.eupedia.com/ecology/carbon_footprint_consumer_products.shtml

[73] statista, “Carbon tax rates worldwide as of March 31, 2023, by country,” 2023. https://www.statista.com/statistics/483590/prices-of-implemented-carbon-pricing-instruments-worldwide-by-select-country/

[74] WONDER, “Assembly cost,” 2019. https://start.askwonder.com/insights/assembly-cost-pylx1wu94

[75] C. Poli, *Design for manufacturing: a structured approach.* Butterworth-Heinemann, 2001. [Online]. Available: https://www.sciencedirect.com/book/9780750673419/design-for-manufacturing

[76] P. W. Kalgren, C. S. Byington, M. J. Roemer, and M. J. Watson, “Defining PHM, a lexical evolution of maintenance and logistics,” *AUTOTESTCON (Proceedings)*, pp. 353–358, 2006, doi: 10.1109/AUTEST.2006.283685.

[77] D. C. Montgomery, *Design and analysis of experiments*. John Wiley & Sons, 2017.

[78] Wikipedia, “Triangular distribution,” 2023.

https://en.wikipedia.org/wiki/Triangular_distribution

[79] AnyLogic, "triangular distribution," 2023. https://anylogic.help/advanced/functions/triangular.html

[80] A. Cantini, M. Peron, F. De Carlo, and F. Sgarbossa, "A decision support system for configuring spare parts supply chains considering different manufacturing technologies," *Int. J. Prod. Res.*, 2022, doi: 10.1080/00207543.2022.2041757.

[81] S. Nasiriany, G. Thomas, and W. William, "A Comprehensive Guide to ML," vol. I, 2019, [Online]. Available: http://www.eecs189.org/

[82] J. Morgan, R. Daugherty, Hilchie Allan;, and B. Carey, "Sample Size and Modeling Accuracy with Decision Tree Based Data Mining Tools," *Acad. Inf. Manag. Sci. J.*, vol. 6, no. 2, pp. 71–99, 2003.

[83] F. Sgarbossa, M. Peron, F. Lolli, and E. Balugani, "Conventional or additive manufacturing for spare parts management: An extensive comparison for Poisson demand," *Int. J. Prod. Econ.*, vol. 233, no. December 2020, p. 107993, 2021, doi: 10.1016/j.ijpe.2020.107993.

[84] G. E. P. Box and R. D. Meyer, "An Analysis for Unreplicated Fractional Factorials," *Technometrics*, vol. 28, no. 1, pp. 11–18, Feb. 1986, doi: 10.1080/00401706.1986.10488093.

[85] MATLAB, "MATLAB documentation," 2023. https://se.mathworks.com/help/stats/fscmrmr.html#mw_733b9b36-11f2-4aa2-85fc-0988c425cd95_head

[86] C. Ding and P. Hanchuan, "Minimum redundancy feature selection from microarray gene expression data," *J. Bioinform. Comput. Biol.*, vol. 03, no. 2, 2005.

[87] L. Panza, G. Bruno, and F. Lombardi, "Integrating Absolute Sustainability and Social Sustainability in the Digital Product Passport to Promote Industry 5.0," *Sustainability*, 2023, doi: https://doi.org/10.3390/su151612552.

[88] J. Ehrenfeld, *Sustainability by design: A subversive strategy for transforming our consumer culture*. 2008.

[89] J. Kurilova-Palisaitiene, L. Lindkvist, and E. Sundin, "Towards facilitating circular product life-cycle information flow via remanufacturing," *Procedia CIRP*, vol. 29, pp. 780–785, 2015, doi: 10.1016/j.procir.2015.02.162.

[90] Y. F. Huang, S. G. Azevedo, T. J. Lin, C. S. Cheng, and C. T. Lin, "Exploring the decisive barriers to achieve circular economy: Strategies for the textile innovation in Taiwan," *Sustain. Prod. Consum.*, vol. 27, pp. 1406–1423, 2021, doi: 10.1016/j.spc.2021.03.007.

[91] N. Bocken and P. Ritala, "Six ways to build circular business models," *J. Bus. Strategy*, 2021, doi: 10.1108/JBS-11-2020-0258.

[92] G. M. K. Jesus and D. Jugend, "How can open innovation contribute to circular economy adoption? Insights from a literature review," *Eur. J. Innov. Manag.*, 2021, doi: 10.1108/EJIM-01-2021-0022.

[93] J. A. Mesa, I. Esparragoza, and H. Maury, "Trends and Perspectives of Sustainable Product Design for Open Architecture Products: Facing the Circular Economy Model," *Int. J. Precis. Eng. Manuf. - Green Technol.*, vol. 6, no. 2, pp. 377–391, 2019, doi: 10.1007/s40684-019-00052-1.

[94] O. Fisher, N. Watson, L. Porcu, D. Bacon, M. Rigley, and R. L. Gomes, "Cloud manufacturing as a sustainable process manufacturing route," *J. Manuf. Syst.*, vol. 47, pp. 53–68, 2018, doi: 10.1016/j.jmsy.2018.03.005.

[95] T. Heikkilä and J. Kääriäinen, "Digital product passport promotes sustainable manufacturing Digital Product Passport promotes sustainable manufac- turing Antti Pulkkinen and Tuija Rantala," 2022.

[96] European Commission, "establishing a framework for setting ecodesign requirements for sustainable products and repealing Directive 2009/125/EC," *Eur. Comm.*, 2022.

[97] C. Plociennik *et al.*, "Towards a Digital Lifecycle Passport for the Circular Economy," *Procedia CIRP*, vol. 105, pp. 122–127, 2022, doi: 10.1016/j.procir.2022.02.021.

[98] S. Guth-Orlowski, "The digital product passport and its technical implementation," *Medium*, 2021, [Online]. Available: https://medium.com/@susi.guth/the-digital-product-passport-and-its-technical-implementation-efdd09a4ed75

[99] S. F. Jensen, J. H. Kristensen, S. Adamsen, A. Christensen, and B. V. Waehrens, "Digital product passports for a circular economy: Data needs for product life cycle decision-making," *Sustain. Prod. Consum.*, vol. 37, pp. 242–255, 2023, doi: 10.1016/j.spc.2023.02.021.

[100] J. Lee, B. Bagheri, and H. A. Kao, "A Cyber-Physical Systems architecture for Industry 4.0-based manufacturing systems," *Manuf. Lett.*, vol. 3, pp. 18–

23, 2015, doi: 10.1016/j.mfglet.2014.12.001.

[101] L. Stratmann, G. Hoeborn, C. Pahl, and G. Schuh, “Classification of Product Data for a Digital Product Passport in the Manufacturing Industry,” pp. 448–458, 2023.

[102] M. Jansen, T. Meisen, C. Plociennik, H. Berg, A. Pomp, and W. Windholz, “Stop Guessing in the Dark: Identified Requirements for Digital Product Passport Systems,” *Systems*, vol. 11, no. 3, p. 123, 2023, doi: 10.3390/systems11030123.

[103] M. R. N. King, P. D. Timms, and S. Mountney, “A proposed universal definition of a Digital Product Passport Ecosystem (DPPE): Worldviews , discrete capabilities , stakeholder requirements and concerns,” *J. Clean. Prod.*, vol. 384, no. December 2022, p. 135538, 2023, doi: 10.1016/j.jclepro.2022.135538.

[104] R. H. E. M. Koppelaar *et al.*, “A Digital Product Passport for Critical Raw Materials Reuse and Recycling,” *Sustain.*, vol. 15, no. 2, 2023, doi: 10.3390/su15021405.

[105] K. Berger, J. P. Schöggl, and R. J. Baumgartner, “Digital battery passports to enable circular and sustainable value chains: Conceptualization and use cases,” *J. Clean. Prod.*, vol. 353, no. July 2021, 2022, doi: 10.1016/j.jclepro.2022.131492.

[106] T. Adirson, L. Tholen, and T. Götz, “Towards a Digital Product Passport Fit for Contributing to a Circular Economy,” *Energies*, 2021.

[107] ISO, “ISO/IEC 15459-2:2015 Information technology — Automatic identification and data capture techniques — Unique identification — Part 2: Registration procedures.” p. 4, 2015.

[108] Ä. Boukhatmi, R. Nyffenegger, and S. N. Grösser, “Designing a digital platform to foster data-enhanced circular practices in the European solar industry,” *J. Clean. Prod.*, vol. 418, no. June, 2023, doi: 10.1016/j.jclepro.2023.137992.

[109] D. Piétron, P. Staab, and F. Hofmann, “Digital circular ecosystems: A data governance approach,” *GAIA - Ecol. Perspect. Sci. Soc.*, vol. 32, pp. 40–46, 2023, doi: 10.14512/gaia.32.S1.7.

[110] C. Ducuing and R. H. Reich, “Data governance: Digital product passports as a case study,” *Compet. Regul. Netw. Ind.*, vol. 24, no. 1, pp. 3–23, 2023, doi: 10.1177/17835917231152799.

[111] H. Treiblmaier, “The impact of the blockchain on the supply chain: a theory-based research framework and a call for action,” *Supply Chain Manag.*, vol. 23, no. 6, pp. 545–559, 2018, doi: 10.1108/SCM-01-2018-0029.

[112] M. Rusch, J. P. Schöggl, and R. J. Baumgartner, “Application of digital technologies for sustainable product management in a circular economy: A review,” *Bus. Strateg. Environ.*, vol. 32, no. 3, pp. 1159–1174, 2023, doi: 10.1002/bse.3099.

[113] A. Rejeb, S. Zailani, K. Rejeb, H. Treiblmaier, and J. G. Keogh, “Modeling enablers for blockchain adoption in the circular economy,” *Sustain. Futur.*, vol. 4, no. August, p. 100095, 2022, doi: 10.1016/j.sftr.2022.100095.

[114] S. Khadke *et al.*, “Efficient plastic recycling and remolding circular economy using the technology of trust–blockchain,” *Sustain.*, vol. 13, no. 16, pp. 1–15, 2021, doi: 10.3390/su13169142.

[115] Y. Gong, Y. Wang, R. Frei, B. Wang, and C. Zhao, “Blockchain application in circular marine plastic debris management,” *Ind. Mark. Manag.*, vol. 102, no. January, pp. 164–176, 2022, doi: 10.1016/j.indmarman.2022.01.010.

[116] I. Erol, I. Murat Ar, I. Peker, and C. Searcy, “Alleviating the Impact of the Barriers to Circular Economy Adoption Through Blockchain: An Investigation Using an Integrated MCDM-based QFD With Hesitant Fuzzy Linguistic Term Sets,” *Comput. Ind. Eng.*, vol. 165, no. August 2021, p. 107962, 2022, doi: 10.1016/j.cie.2022.107962.

[117] Y. Kayikci, N. Gozacan-Chase, A. Rejeb, and K. Mathiyazhagan, “Critical success factors for implementing blockchain-based circular supply chain,” *Bus. Strateg. Environ.*, vol. 31, no. 7, pp. 3595–3615, 2022, doi: 10.1002/bse.3110.

[118] A. Chaudhuri, N. Subramanian, and M. Dora, “Circular economy and digital capabilities of SMEs for providing value to customers: Combined resource-based view and ambidexterity perspective,” *J. Bus. Res.*, vol. 142, no. December 2020, pp. 32–44, 2022, doi: 10.1016/j.jbusres.2021.12.039.

[119] M. Hrouga, A. Sbihi, and M. Chavallard, “The potentials of combining Blockchain technology and Internet of Things for digital reverse supply chain: A case study,” *J. Clean. Prod.*, vol. 337, no. January, p. 130609, 2022, doi: 10.1016/j.jclepro.2022.130609.

[120] A. D. Joshi and S. M. Gupta, “Evaluation of design alternatives of End-Of-Life products using internet of things,” *Int. J. Prod. Econ.*, vol. 208, no. May 2018, pp. 281–293, 2019, doi: 10.1016/j.ijpe.2018.12.010.

[121] C. Magrini *et al.*, "Using internet of things and distributed ledger technology for digital circular economy enablement: The case of electronic equipment," *Sustain.*, vol. 13, no. 9, 2021, doi: 10.3390/su13094982.

[122] N. Gupta and P. Bedi, "E-waste Management Using Blockchain based Smart Contracts," *2018 Int. Conf. Adv. Comput. Commun. Informatics, ICACCI 2018*, pp. 915–921, 2018, doi: 10.1109/ICACCI.2018.8554912.

[123] P. Centobelli, R. Cerchione, P. Del Vecchio, E. Oropallo, and G. Secundo, "Blockchain technology for bridging trust, traceability and transparency in circular supply chain," *Inf. Manag.*, vol. 59, no. 7, p. 103508, 2022, doi: 10.1016/j.im.2021.103508.

[124] ISO, "ISO 14044:2006 Environmental management — Life cycle assessment — Requirements and guidelines." p. 46, 2006.

[125] S. Sala, E. Crenna, M. Secchi, and E. Sanyé-Mengual, "Environmental sustainability of European production and consumption assessed against planetary boundaries," *J. Environ. Manage.*, vol. 269, no. April, 2020, doi: 10.1016/j.jenvman.2020.110686.

[126] M. Z. Hauschild, "Better - but is it good enough? On the need to consider both eco-efficiency and eco-effectiveness to gauge industrial sustainability," *Procedia CIRP*, vol. 29, pp. 1–7, 2015, doi: 10.1016/j.procir.2015.02.126.

[127] A. Bjørn, M. Diamond, M. Owsianiak, B. Verzat, and M. Z. Hauschild, "Strengthening the link between life cycle assessment and indicators for absolute sustainability to support development within planetary boundaries," *Environ. Sci. Technol.*, vol. 49, no. 11, pp. 6370–6371, 2015, doi: 10.1021/acs.est.5b02106.

[128] J. Lee, J. Ni, J. Singh, B. Jiang, M. Azamfar, and J. Feng, "Intelligent Maintenance Systems and Predictive Manufacturing," *J. Manuf. Sci. Eng. Trans. ASME*, vol. 142, no. 11, 2020, doi: 10.1115/1.4047856.

[129] D. G. S. Pivoto, L. F. F. de Almeida, R. da Rosa Righi, J. J. P. C. Rodrigues, A. B. Lugli, and A. M. Alberti, "Cyber-physical systems architectures for industrial internet of things applications in Industry 4.0: A literature review," *J. Manuf. Syst.*, vol. 58, no. PA, pp. 176–192, 2021, doi: 10.1016/j.jmsy.2020.11.017.

[130] E. Oztemel and S. Gursev, "Literature review of Industry 4.0 and related technologies," *J. Intell. Manuf.*, vol. 31, no. 1, pp. 127–182, 2020, doi: 10.1007/s10845-018-1433-8.

[131] T. Zheng, M. Ardolino, A. Bacchetti, and M. Perona, “The applications of Industry 4.0 technologies in manufacturing context: a systematic literature review,” *Int. J. Prod. Res.*, vol. 59, no. 6, pp. 1922–1954, 2021, doi: 10.1080/00207543.2020.1824085.

[132] A. A. Ahmed, M. A. Nazzal, and B. M. Darras, “Cyber-Physical Systems as an Enabler of Circular Economy to Achieve Sustainable Development Goals: A Comprehensive Review,” *Int. J. Precis. Eng. Manuf. - Green Technol.*, no. 0123456789, 2021, doi: 10.1007/s40684-021-00398-5.

[133] UNEP Life Cycle Initiative and Social LC Alliance, “Guidelines for Social Life Cycle Assessment of Products and Organizations 2020,” *UNEP*, no. 2, 2020, [Online]. Available: https://www.lifecycleinitiative.org/wp-content/uploads/2021/01/Guidelines-for-Social-Life-Cycle-Assessment-of-Products-and-Organizations-2020-22.1.21sml.pdf

[134] L. Panza, M. De Maddis, and P. Russo Spena, “Use of electrode displacement signals for electrode degradation assessment in resistance spot welding,” *J. Manuf. Process.*, vol. 76, no. October 2021, pp. 93–105, 2022, doi: 10.1016/j.jmapro.2022.01.060.

[135] T. Zonta, C. A. da Costa, R. da Rosa Righi, M. J. de Lima, E. S. da Trindade, and G. P. Li, “Predictive maintenance in the Industry 4.0: A systematic literature review,” *Comput. Ind. Eng.*, vol. 150, no. August, p. 106889, 2020, doi: 10.1016/j.cie.2020.106889.

[136] L. Biggio and I. Kastanis, “Prognostics and Health Management of Industrial Assets: Current Progress and Road Ahead,” *Front. Artif. Intell.*, vol. 3, no. November, pp. 1–24, 2020, doi: 10.3389/frai.2020.578613.

[137] S. Chen, T. Sun, X. Jiang, J. Qi, and R. Zeng, “Online monitoring and evaluation of the weld quality of resistance spot welded titanium alloy,” *J. Manuf. Process.*, vol. 23, pp. 183–191, 2016, doi: 10.1016/j.jmapro.2016.06.003.

[138] D. Zhao, Y. Wang, D. Liang, and M. Ivanov, “Performances of regression model and artificial neural network in monitoring welding quality based on power signal,” *J. Mater. Res. Technol.*, vol. 9, no. 2, pp. 1231–1240, 2020, doi: 10.1016/j.jmrt.2019.11.050.

[139] L. Zhou *et al.*, “Comparative study on resistance and displacement based adaptive output tracking control strategies for resistance spot welding,” *J. Manuf. Process.*, no. December 2019, 2020, doi: 10.1016/j.jmapro.2020.03.061.

[140] L. Zhou *et al.*, "Online monitoring of resistance spot welding electrode wear state based on dynamic resistance," *J. Intell. Manuf.*, no. 2016, 2020, doi: 10.1007/s10845-020-01650-6.

[141] K. Zhou and P. Yao, "Overview of recent advances of process analysis and quality control in resistance spot welding," *Mech. Syst. Signal Process.*, vol. 124, pp. 170–198, 2019, doi: 10.1016/j.ymssp.2019.01.041.

[142] A. S. Kiselev and M. S. Slobodyan, "Effects of electrode degradation on properties of small-scale resistance spot welded joints of e110 alloy," *Mater. Sci. Forum*, vol. 970, no. September, pp. 227–235, 2019, doi: 10.4028/www.scientific.net/MSF.970.227.

[143] M. El-Banna, D. Filev, and R. B. Chinnam, *Automotive Manufacturing: Intelligent Resistance Welding*. 2008.

[144] R. Spitsen, D. Kim, B. Flinn, M. Ramulu, and E. T. Easterbrook, "The effects of post-weld cold working processes on the fatigue strength of low carbon steel resistance spot welds," *J. Manuf. Sci. Eng.*, vol. 127, no. 4, pp. 718–723, 2005, doi: 10.1115/1.2034514.

[145] J. Sheppard, M. Kaufman, and T. Wilmer, "IEEE standards for prognostics and health management," *IEEE Aerosp. Electron. Syst. Mag.*, vol. 24, no. 9, pp. 34–41, 2009, doi: 10.1109/MAES.2009.5282287.

[146] X. Wan, Y. Wang, and D. Zhao, "Quality evaluation in small-scale resistance spot welding by electrode voltage recognition," *Sci. Technol. Weld. Join.*, vol. 21, no. 5, pp. 358–365, 2016, doi: 10.1080/13621718.2015.1115161.

[147] X. Wan, Y. Wang, D. Zhao, Y. A. Huang, and Z. Yin, "Weld quality monitoring research in small scale resistance spot welding by dynamic resistance and neural network," *Meas. J. Int. Meas. Confed.*, vol. 99, pp. 120–127, 2017, doi: 10.1016/j.measurement.2016.12.010.

[148] N. Haghshenas and H. Moshayedi, "Monitoring of Resistance Spot Welding Process," *Exp. Tech.*, vol. 44, no. 1, pp. 99–112, 2020, doi: 10.1007/s40799-019-00341-z.

[149] Y. J. Xia *et al.*, "Online measurement of weld penetration in robotic resistance spot welding using electrode displacement signals," *Meas. J. Int. Meas. Confed.*, vol. 168, no. August 2020, p. 108397, 2021, doi: 10.1016/j.measurement.2020.108397.

[150] Y. J. Xia, Z. W. Su, Y. B. Li, L. Zhou, and Y. Shen, "Online quantitative evaluation of expulsion in resistance spot welding," *J. Manuf. Process.*, vol.

46, no. June, pp. 34–43, 2019, doi: 10.1016/j.jmapro.2019.08.004.

[151] D. Zhao, M. Ivanov, Y. Wang, D. Liang, and W. Du, "Multi-objective optimization of the resistance spot welding process using a hybrid approach," *J. Intell. Manuf.*, 2020, doi: 10.1007/s10845-020-01638-2.

[152] K. Mahmud, S. P. Murugan, Y. Cho, C. Ji, D. Nam, and Y. Do Park, "Geometrical degradation of electrode and liquid metal embrittlement cracking in resistance spot welding," *J. Manuf. Process.*, vol. 61, no. July 2020, pp. 334–348, 2021, doi: 10.1016/j.jmapro.2020.11.025.

[153] X. Q. Zhang, G. L. Chen, and Y. S. Zhang, "Characteristics of electrode wear in resistance spot welding dual-phase steels," *Mater. Des.*, vol. 29, no. 1, pp. 279–283, 2008, doi: 10.1016/j.matdes.2006.10.025.

[154] I. Lum, S. Fukumoto, E. Biro, D. R. Boomer, and Y. Zhou, "Electrode Pitting in Resistance Spot Welding of Aluminum Alloy 5182," *Metall. Mater. Trans. A Phys. Metall. Mater. Sci.*, vol. 35 A, no. 1, pp. 217–226, 2004, doi: 10.1007/s11661-004-0122-8.

[155] J. Peng, S. Fukumoto, L. Brown, and N. Zhou, "Image analysis of electrode degradation in resistance spot welding of aluminium," *Sci. Technol. Weld. Join.*, vol. 9, no. 4, pp. 331–336, 2004, doi: 10.1179/136217104225012256.

[156] Y. S. Zhang, H. Wang, G. L. Chen, and X. Q. Zhang, "Monitoring and intelligent control of electrode wear based on a measured electrode displacement curve in resistance spot welding," *Meas. Sci. Technol.*, vol. 18, no. 3, pp. 867–876, 2007, doi: 10.1088/0957-0233/18/3/040.

[157] H. Wang, Y. Zhang, and G. Chen, "Resistance spot welding processing monitoring based on electrode displacement curve using moving range chart," *Meas. J. Int. Meas. Confed.*, vol. 42, no. 7, pp. 1032–1038, 2009, doi: 10.1016/j.measurement.2009.03.005.

[158] Q. Fan, G. Xu, and T. Wang, "The influence of electrode tip radius on dynamic resistance in spot welding," *Int. J. Adv. Manuf. Technol.*, vol. 95, no. 9–12, pp. 3899–3904, 2018, doi: 10.1007/s00170-017-1513-5.

[159] C. Mathiszik, D. Köberlin, S. Heilmann, J. Zschetzsche, and U. Füssel, "General approach for inline electrode wear monitoring at resistance spot welding," *Processes*, vol. 9, no. 4, 2021, doi: 10.3390/pr9040685.

[160] Y. Xiao-Jie, W. Bin, S. Xiao-Yan, and L. Yu-Xin, "Research on adaptive control of medium frequency DC resistance spot welding," *Proc. - 2021 Int. Conf. Artif. Intell. Electromechanical Autom. AIEA 2021*, pp. 30–34, 2021,

doi: 10.1109/AIEA53260.2021.00014.

[161] J. Zeng, B. Cao, and R. Tian, "Heat generation and transfer in micro resistance spot welding of enameled wire to pad," *J. Manuf. Process.*, vol. 82, no. July, pp. 113–123, 2022, doi: 10.1016/j.jmapro.2022.07.046.

[162] S. Heilmann, M. Baumgarten, J. Koal, J. Zschetzsche, and U. Füssel, "Electrode wear investigation of aluminium spot welding by motion overlay," *Int. J. Adv. Manuf. Technol.*, vol. 123, no. 3–4, pp. 749–760, 2022, doi: 10.1007/s00170-022-10157-8.

[163] D. Zhao, N. Vdonin, Y. Bezgans, L. Radionova, and L. Glebov, "Correlating Electrode Degradation with Weldability of Galvanized BH 220 Steel during the Electrode Failure Process of Resistance Spot Welding," *Crystals*, vol. 13, no. 1, 2023, doi: 10.3390/cryst13010039.

[164] E. Traini, G. Bruno, and F. Lombardi, "Tool condition monitoring framework for predictive maintenance: a case study on milling process," *Int. J. Prod. Res.*, no. Ml, 2020, doi: 10.1080/00207543.2020.1836419.

[165] L. Panza, G. Bruno, M. De Maddis, F. Lombardi, P. Russo Spena, and E. Traini, "Data-Driven Framework for Electrode Wear Prediction in Resistance Spot Welding," *Prod. Lifecycle Manag. Green Blue Technol. to Support Smart Sustain. Organ.*, p. 14, 2021, doi: 10.1007/978-3-030-94335-6_17.

[166] J. Grus, *Data Science from Scratch: First Principles with Python*. O'Reilly Media, 2015.

[167] M. G. Kendall, *The Advanced Theory of Statistics*, 4th ed. Macmillan, 1979.

[168] P. R. Spena, M. De Maddis, and F. Lombardi, "Mechanical Strength and Fracture of Resistance Spot Welded Advanced High Strength Steels," *Procedia Eng.*, vol. 109, pp. 450–456, 2015, doi: 10.1016/j.proeng.2015.06.262.

[169] American Welding Society, "Test Methods for Evaluating the Resistance Spot Welding Behavior of Automotive Sheet Steel (AWS D8.9M:2012)," *Ansi*, p. 7, 2012.

[170] Japanese Standard Association, *JIS Z 3136 Specimen Dimensions and Procedure for Shear Testing Resistance Spot and Embossed Projection Welded Joints*. 2018.

[171] S. Fukumoto, I. Lum, E. Biro, D. R. Boomer, and Y. Zhou, "Effects of

electrode degradation on electrode life in resistance spot welding of aluminum alloy 5182," *Weld. J. (Miami, Fla)*, vol. 82, no. 11, 2003.

[172] MATLAB, "Image Processing Toolbox," 2023. https://se.mathworks.com/products/image.html

[173] B. Xing, Y. Xiao, and Q. H. Qin, "Characteristics of shunting effect in resistance spot welding in mild steel based on electrode displacement," *Meas. J. Int. Meas. Confed.*, vol. 115, no. June 2017, pp. 233–242, 2018, doi: 10.1016/j.measurement.2017.10.049.

[174] P. Podržaj and S. Simončič, "A machine vision-based electrode displacement measurement," *Weld. World*, vol. 58, no. 1, pp. 93–99, 2014, doi: 10.1007/s40194-013-0086-7.

[175] Y. J. Xia, Z. W. Su, M. Lou, Y. B. Li, and B. E. Carlson, "Online precision measurement of weld indentation in resistance spot welding using servo gun," *IEEE Trans. Instrum. Meas.*, vol. 69, no. 7, pp. 4465–4475, 2020, doi: 10.1109/TIM.2019.2943981.

[176] H. Zhang and J. Senkara, *RESISTANCE WELDING Fundamentals and Applications*. Taylor & Francis Group, 2011.

[177] Y. Ma, P. Wu, C. Xuan, Y. Zhang, and H. Su, "Review on techniques for on-line monitoring of resistance spot welding process," *Adv. Mater. Sci. Eng.*, vol. 2013, 2013, doi: 10.1155/2013/630984.

[178] P. Russo Spena, M. De Maddis, G. D'Antonio, and F. Lombardi, "Weldability and monitoring of resistance spot welding of Q&P and TRIP steels," *Metals (Basel).*, vol. 6, no. 11, 2016, doi: 10.3390/met6110270.